



Identification and characterisation of new potential antigens involved in GAP-mediated immunity



Dissertation
Eva Hippler

Dissertation
submitted to the
Combined Faculties for the Natural Sciences and for Mathematics
of the Ruperto-Carola University of Heidelberg, Germany
for the degree of
Doctor of Natural Sciences

presented by

Eva Hippler

Diploma-Biologist
born in Schweinfurt

Oral examination:

Identification and characterisation of new potential antigens involved in GAP-mediated immunity

Referees: Prof. Dr. Michael Lanzer
Dr. Ann-Kristin Müller

Hiermit erkläre ich, dass ich die vorliegende Arbeit von Oktober 2007 bis Dezember 2010 unter Anleitung von Dr. Ann-Kristin Müller selbst durchgeführt habe und bis September 2012 schriftlich ausgearbeitet habe. Ich habe mich keiner anderen Hilfsmittel und Quellen bedient als die hier ausdrücklich erwähnten.

.....
Datum

.....
Eva Hippler

Index

List of figures and tables.....	VI
Summary.....	IX
Zusammenfassung	XI
Abbreviations	XIII
1. Introduction	1
1.1 Malaria.....	1
1.2 <i>Plasmodium</i> life cycle	2
1.3 Vaccination strategies against malaria.....	5
1.3.1 Anti-disease vaccines	6
1.3.2 Anti-transmission vaccines	7
1.3.3 Anti-infective vaccines	7
1.4 Natural vaccination models	9
1.5 Live sporozoite vaccination models.....	10
1.6 Pre-erythrocytic antigens.....	11
1.7 Malaria liver-stage immunology.....	13
1.8 Aim of this study.....	16
2. Materials and methods.....	18
2.1 Laboratory equipment	18
2.2 Consumables	19
2.3 Strains	20
2.3.1 Bacteria strains	20
2.3.2 Cell lines	20
2.3.3 Parasite strains.....	20
2.3.4 Mosquito strains	21
2.3.5 Mouse strains	21
2.4 Chemicals and reagents	21
2.5 Peptides.....	22
2.6 Oligonucleotides	22
2.7 Media, buffer and solutions	22
2.7.1 Media and buffer for molecular biological methods	22
2.7.2 Media and solutions for cell culture.....	23
2.7.3 Media, buffer and solutions for parasitological methods	24
2.7.4 Buffer for immunological methods	24

2.7.5 Buffer and solutions for biochemical methods	24
2.8 Molecular biological methods	25
2.8.1 Cloning of the targeting constructs for parasite transfection.....	25
2.8.1.1 Amplification of the specific DNA fragments by Polymerase chain reaction (PCR).....	26
2.8.1.2 Analysis of DNA fragments by agarose gel electrophoresis	26
2.8.1.3 Purification of DNA with Qiaquick PCR purification Kit.....	26
2.8.1.4 Digestion of double-stranded DNA	26
2.8.1.5 Ligation of DNA.....	27
2.8.1.6 Preparation of transformation competent <i>E. coli</i> XL1 blue	27
2.8.1.7 Transformation of competent <i>E. coli</i> XL1 blue.....	27
2.8.1.8 Plasmid isolation with Qiaprep Spin Miniprep Kit	28
2.8.1.9 Preparation of bacteria-glycerine stocks	28
2.8.1.10 Determination of DNA concentration by photometric measurement.....	28
2.8.1.11 Ethanol precipitation of DNA	28
2.8.1.12 Site-directed mutagenesis of the <i>P. yoelii</i> circumsporozoite CD8 ⁺ T cell epitope	29
2.8.2 Stage specific RNA isolation and cDNA synthesis for RT and qRT PCR.....	29
2.8.2.1 Isolation of total RNA with RNeasy Mini Kit (Qiagen).....	30
2.8.2.2 Trizol extraction of total RNA	30
2.8.2.3 DNase treatment of total RNA	30
2.8.2.4 First strand cDNA synthesis.....	30
2.8.2.5 Reverse transcriptase PCR (RT PCR)	31
2.8.2.6 Quantitative Real-time PCR (qRT PCR)	31
2.8.3 Generation of subtraction libraries for Suppression Subtractive Hybridisation (SSH).....	31
2.8.3.1 RNA sample preparation.....	32
2.8.3.2 cDNA synthesis with SMART™ method.....	32
2.8.3.3 PCR-Select™ cDNA subtraction	32
2.8.3.4 T/A cloning	32
2.8.3.5 Sequencing	33
2.8.3.6 Bioinformatical analysis	33
2.9 Cell culture.....	33
2.9.1 Cultivation of human hepatoma cells Huh7.....	33

2.9.2 <i>In vitro</i> liver-stage development	34
2.9.3 Isolation and cultivation of bone marrow dendritic cells (BMDCs).....	34
2.10 Parasitological methods.....	35
2.10.1 <i>Plasmodium</i> methods.....	35
2.10.1.1 Determination of parasitemia in giemsa stained blood smears.....	35
2.10.1.2 Examination of exflagellating gametocytes	35
2.10.1.3 Cryopreservation of <i>Plasmodium</i> parasites.....	35
2.10.1.4 Parasite transfection.....	36
2.10.1.4.1 Overnight culture and merozoite purification.....	36
2.10.1.4.2 AMAXA transfection and selection for transformants	37
2.10.1.4.3 Isolation of blood stage parasites for genomic DNA purification.....	37
2.10.1.4.4 Genotyping PCR of transfected parasites.....	38
2.10.1.5 Parasite cloning.....	38
2.10.2 <i>Anopheles</i> mosquito methods.....	39
2.10.2.1 Mosquito breeding	39
2.10.2.2 Parasite transmission.....	39
2.10.2.3 Mosquito dissection	39
2.10.2.4 Sporozoite extraction from midguts and salivary glands.....	40
2.11 Animal experimental methods	40
2.11.1 Administration of anaesthesia	40
2.11.2 Infection of rodents with <i>Plasmodium</i> parasites	40
2.11.3 Blood withdrawal by heart puncture	41
2.11.4 Liver perfusion	41
2.12 Immunological methods	41
2.12.1 Immunisation and parasite challenge experiments.....	41
2.12.2 Cell isolation and purification from spleens, livers and lymph nodes	42
2.12.3 <i>In vivo</i> cytotoxicity assay.....	43
2.12.4 Restimulation of lymphocytes from immunised animals <i>in vitro</i>	43
2.12.5 Flow cytometry.....	43
2.12.6 Cytokine ELISpot.....	44
2.13 Biochemical methods	45
2.13.1 Recombinant overexpression of the <i>P. berghei</i> ferlin-like protein as His-tag fusionprotein	45
2.13.2 SDS polyacrylamide gel electrophoresis (SDS-PAGE)	45

2.13.3 Coomassie staining of SDS polyacrylamide gels.....	46
2.13.4 Western Blot analysis	47
2.13.5 Purification of His-tag fusionproteins by nickel-ion affinity chromatography....	47
3. Results	49
3.1 <i>P. yoelii</i> circumsporozoite (CSP) epitope mutant - an elegant tool to study the role of CSP in pre-erythrocytic immunity.....	49
3.1.1 Insertion of mutations by a complementation strategy results in repaired epitope sequence and an exflagellation defect phenotype.....	49
3.1.2 A short gene (PY07369) annotated upstream of <i>P. yoelii csp</i> might also be affected when gene-targeting <i>csp</i>	53
3.1.3 Replacement of the <i>P. yoelii</i> wild-type <i>csp</i> sequence by a mutated sequence should prevent repair mechanisms	55
3.2 Comparative analysis of early <i>Plasmodium</i> liver-stages identifies potential targets of protective immunity	59
3.2.1 Suppression subtractive hybridisation results in a set of specifically up-regulated transcripts in attenuated parasites	59
3.2.2 The <i>Plasmodium</i> ferlin protein family.....	67
3.2.3 <i>P. berghei</i> ferlins are essential during blood-stage development.....	69
3.2.4 Immunological characterisation of <i>P. berghei</i> C2 domain-containing protein (C2CP) reveals specific immune responses in immunised animals.....	72
3.2.5 First immunisation studies with <i>P. berghei</i> C2CP-derived peptide T9L	80
3.2.6 Recombinant expression of <i>P. berghei</i> C2 domain-containing protein (C2CP)....	82
4. Discussion	87
5. References	108
6. Appendix	120
6.1 Oligonucleotide sequences	120
6.1.1 <i>PyCSP</i> complementation	120
6.1.2 <i>PyCSP</i> epitope mutagenesis.....	120
6.1.3 <i>PyCSprae</i> knock-out.....	120
6.1.4 <i>PyCSP</i> replacement	120
6.1.5 <i>PbFER</i> knock-out and complementation.....	121
6.1.6 <i>PbC2CP</i> knock-out and complementation.....	121
6.1.7 Reverse transcriptase PCR.....	122
6.1.8 Quantitative RT PCR.....	122

6.1.9 Sequencing.....	123
6.1.10 <i>PbC2CP</i> overexpression	123
6.2 Vector maps	123
6.3 Sequence analysis of the <i>Py</i> CSP mutant clone I-2.....	129
Danksagung.....	130

List of figures and tables

Figure 1. Global malaria distribution.....	1
Figure 2. <i>Plasmodium</i> life cycle.....	3
Figure 3. Vaccination strategies against malaria and their targets throughout the parasite's life cycle	5
Figure 4. Schematic primary structure of the <i>Plasmodium</i> circumsporozoite protein (CSP)..	12
Figure 5. Knock-in/complementation strategy inserts a mutated CD8 ⁺ T-cell epitope in the <i>P. yoelii</i> circumsporozoite protein (CSP) genomic sequence.....	50
Figure 6. Genotyping PCR of <i>P. yoelii</i> circumsporozoite protein (CSP) epitope mutant me01 after transfection with the complementation construct	51
Figure 7. Genomic locus of the <i>P. yoelii</i> <i>csp</i> gene and its neighbouring genomic sequence information	53
Figure 8. Genetic strategy to functionally knock-out the <i>P. yoelii</i> <i>csprae</i> gene	54
Figure 9. Genotyping PCR of the Δ <i>csprae</i> transfecant.....	55
Figure 10. Replacement strategy inserts a mutated CD8 ⁺ T-cell epitope in the <i>P. yoelii</i> circumsporozoite protein (CSP) genomic sequence	56
Figure 11. Genotyping PCR of <i>P. yoelii</i> circumsporozoite protein (CSP) epitope mutants me01 and me03 after transfection with the replacement constructs.....	56
Figure 12. Genes differentially expressed in attenuated parasites in comparison to wild-type (WT) parasites during early liver-stage development (20h).....	63
Figure 13. Quantitative real-time PCR of transcripts up-regulated in attenuated parasites (UAP)	66
Figure 14. Primary structures of annotated Apicomplexan C2 domain-containing proteins (C2CP) and related ferlins	68
Figure 15. Reverse transcriptase PCR detects transcripts of <i>P. berghei</i> ferlin (<i>fer</i>) and C2 domain-containing protein (<i>c2cp</i>) in different parasite stages	68
Figure 16. Knock-out (A) and complementation (B) strategy of the <i>P. berghei</i> ferlin (FER) and C2 domain-containing protein (C2CP)	70
Figure 17. Genotyping PCR of <i>P. berghei</i> ferlin (<i>fer</i>) and C2 domain-containing protein (<i>c2cp</i>) knock-out (A) or complementation (B) transfecants.....	71
Figure 18. Schematic diagram of the prime-two-boost immunisation protocol.....	73
Figure 19. Effector memory T-cell population (CD8 ⁺ CD44 ^{high} CD62L ^{low}) in the liver increases after GAP and RAS immunisation.....	75

Figure 20. <i>In vivo</i> cytotoxicity assay shows lysis of target cells pulsed with the <i>Pb</i> C2CP-derived peptides A9I, S8V and A8I.....	76
Figure 21. <i>In vivo</i> cytotoxicity assay shows lysis of target cells pulsed with a pool of all four <i>Pb</i> C2CP-derived peptides in immunised animals.....	77
Figure 22. Interferon- γ (IFN- γ) responses of effector T-cells measured by cytokine-based ELISpot after restimulation with the <i>Pb</i> C2CP-derived peptides A9I, S8V, A8I	78
Figure 23. Cytokine-based ELISpot measures Interferon- γ (IFN- γ) responses of effector T-cells from RAS and GAP immunised mice.....	79
Figure 24. Cytokine-based ELISpot to measure Interferon- γ (IFN- γ) responses of activated T-cells from RBT06.01 TS immunised mice	82
Figure 25. Recombinant overexpression of the <i>P. berghei</i> C2CPI-His fusion protein in <i>E. coli</i> BL21.....	84
Figure 26. Purification of the C2CPI-His fusion protein by nickel ion affinity chromatography	85
Figure 27. Coomassie stained SDS gel (A) and Western Blot (B) of purified C2CPI-His after dialysis against PBS	85
Figure 28. Vector map of the cloning vector b3D.....	123
Figure 29. Vector map of the cloning vector b3D+.....	124
Figure 30. Vector map of the targeting construct pcsp Δ epi	124
Figure 31. Vector map of the targeting construct p Δ csprae	125
Figure 32. Vector map of the targeting construct pcsp Δ repl Δ epi.....	125
Figure 33. Vector map of the targeting construct p Δ fer	126
Figure 34. Vector map of the targeting construct pferCONT	126
Figure 35. Vector map of the targeting construct p Δ c2cp	127
Figure 36. Vector map of the targeting construct pc2cpCONT	127
Figure 37. Vector map of the expression vector pETc2cpI	128
Figure 38. Sequence of the CD8 $^+$ T-cell epitope mutant <i>Py</i> CSP me01 clone I-2	129
Table 1. Amino acid sequences of the different mutations inserted in the <i>P. yoelii</i> circumsporozoite protein (CSP) by site-directed mutagenesis.....	50
Table 2. Genes up-regulated in genetically-attenuated parasites (GAP) in comparison to wild-type (WT) parasites during early liver-stage development (20h).....	61
Table 3. Genes up-regulated in radiation-attenuated sporozoites (RAS) in comparison to wild-type (WT) parasites during early liver-stage development (20h).....	62

Table 4. Genes down-regulated in genetically-attenuated parasites (GAP) in comparison to wild-type (WT) parasites during early liver-stage development (20h).....	65
Table 5. Genes down-regulated in radiation-attenuated sporozoites (RAS) in comparison to wild-type (WT) parasites during early liver-stage development (20h).....	65
Table 6. Predicted CD8 ⁺ T-cell epitopes of the <i>P. berghei</i> C2 domain-containing protein (C2CP).....	73
Table 7. Pre-patency of mice immunised with nanocarrier RBT06.01 TS packed with <i>P. berghei</i> C2CP-derived peptide T9L	81
Table 8. Division of the <i>P. berghei</i> C2 domain-containing protein (C2CP) for recombinant expression	83

Summary

Malaria kills hundreds of thousands of people each year and is a major impediment to social and economic development in endemic areas. An effective vaccine is widely regarded as an essential tool for sustainable malaria control. Stage-specific sterile protection can be achieved in rodents and human volunteers by administration of *Plasmodium* parasites that attenuate during liver-stage development by either radiation (RAS), genetic modification (GAP) or by chemical treatment (administration of antibiotics or drug cure). These live-attenuated whole-organism vaccination models are commonly used as a tool to study pre-erythrocytic immune responses. Dissecting the underlying effector mechanisms and antigen specificities would help to develop a safe subunit vaccine that induces similar levels of protection as the attenuated parasite vaccine. In this study we, hence, focussed on the identification and characterisation of potential antigens involved in GAP-mediated immunity.

First we addressed the role of the circumsporozoite protein (CSP) in GAP-induced protection. CSP is considered the immunodominant antigen in RAS-mediated immunity and a reasonable amount of data from the last decades argue for this. Nevertheless, recently several studies revealed that protection can also be achieved despite the absence of immune responses specific to CSP. Our goal was to generate a *P. yoelii* CSP-mutant that is no longer recognised by the immune system without affecting CSP function. Therefore we successfully inserted different point mutations into the gene sequence coding for the CD8⁺ T cell epitope of CSP. Transfection of wild-type *P. yoelii* parasites resulted in integration of the targeting constructs into the genomic locus. A stable CSP-mutant clone, however, was not achieved in spite of several applied genetic strategies. Furthermore we identified within this study novel potential antigens involved in GAP-mediated immunity. We compared the transcript repertoire expressed of *Plasmodium* liver-stage parasites from GAP and RAS versus wild-type in an attempt to detect antigens that are uniquely or differentially expressed in GAP and which may represent important targets of GAP-induced protective immunity. Using suppression subtractive hybridisation (SSH) we obtained a set of differentially expressed transcripts in attenuated parasites. Some transcripts were specific for RAS or GAP, respectively, others are shared between both attenuated parasites. One of the most abundant shared transcript that appeared during sequence analysis coded for a *P. berghei* C2-containing protein (C2CP). C2 domains are generally involved in Ca²⁺-sensing and -signalling and proteins containing C2 domains are described to mediate Ca²⁺-dependent vesicular fusion events. The *C. elegans* and human ferlins are well characterised proteins with characteristic cytosolic C2 domains.

Database search revealed beside the *Pb* C2CP one annotated *Pb* ferlin (FER) and a ferlin-like protein (FLP). The cellular functions of Plasmodial ferlins, however, are unknown. We therefore also aimed at the cellbiological characterisation of the identified protein family. Targeted gene disruption experiments revealed an essential role of *Pb* C2CP and *Pb* FER during blood-stage development. The main objective of this study, however, focussed on the investigation of the antigenic potential of this novel pre-erythrocytic antigen from the protection-inducing attenuated malarial parasites. Interestingly epitope prediction identified several high-binding *Pb* C2CP-specific H2^b-restricted CD8⁺ T-cell epitopes. Indeed, we could show that *Pb* C2CP-specific cells are recognised and lysed in immunised C57BL/6 mice. Moreover, we were able to specifically restimulate T cells in the livers of immunised animals with the *Pb* C2CP-derived peptide T9L. Altogether, both the dissection of novel antigens from the protection-inducing attenuated parasites and the immunogenic capacity as shown by a selected critical target antigen *Pb* C2CP for the first time allows specific restimulation of T cells in the experimental GAP vaccination model. Therefore this work clears the way for studying effector mechanisms underlying GAP-induced immunity. This work is of fundamental importance to understanding the mechanisms of pre-erythrocytic immunity to malaria and may further pave the way for the composition of an anti-infective multi-component subunit malarial vaccine.

Zusammenfassung

Nach aktuellen Schätzungen der Weltgesundheitsorganisation WHO sterben jährlich über einer halben Millionen Menschen an Malaria. Die Hauptübertragungsgebiete erstrecken sich über weite Teile der Tropen und Subtropen. Dort behindert die Krankheit die soziale und wirtschaftliche Entwicklung. Ein effektiver Impfstoff gegen Malaria wird dringend benötigt um die Ausbreitung der Erkrankung nachhaltig kontrollieren zu können. Abgeschwächte Malariaerreger vermitteln bereits sterilen Schutz gegen Malaria im Nagetiermodell und in Probanden. Die Abschwächung des Parasiten kann dabei entweder durch Bestrahlung (radiation-attenuated sporozoites; RAS), genetische Manipulation (genetically-attenuated parasites; GAP) oder chemische Behandlung (zeitgleiche Gabe von Antibiotika oder Chloroquin) erfolgen. Dies führt zu einer Unterbrechung der Leberstadien Entwicklung. Das Verständnis der zugrunde liegenden Immunmechanismen und präsentierten Antigene, würde die Entwicklung eines sicheren Subunit-Impfstoffes ermöglichen, der ähnlichen Schutz vermittelt, wie die abgeschwächten Parasiten selbst. In dieser Arbeit sollten daher spezifische Immunantworten untersucht werden, die dem GAP induzierten Schutz zugrunde liegen.

Dazu sollte als erstes die Rolle des Sporoziten Hauptoberflächenproteins CSP (circumsporozoite protein) im GAP vermittelten Schutz analysiert werden. Viele wissenschaftliche Daten aus den letzten Jahrzehnten sprechen dafür, dass CSP das immunodominante Antigen im RAS induzierten Impfschutz ist. Dennoch zeigen einige neuere Ergebnisse, dass ein vollständiger Schutz auch ohne CSP-spezifische Immunantworten erreicht werden kann. Das Ziel dieser Arbeit war es daher, eine *Plasmodium yoelii* CSP-Mutante zu generieren, die nicht mehr vom Immunsystem erkannt wird. Dazu wurden verschiedene Punktmutationen in die DNA Sequenz des beschriebenen CD8⁺ T-Zell Epitops SYVPSAEQI eingefügt. Die erfolgreiche Integration der dazu verwendeten Vektorkonstrukte in das *P. yoelii* Genom konnte gezeigt werden. Wir konnten jedoch trotz verschiedener Strategien keine stabile Mutante herstellen. Das Hauptziel dieser Arbeit war die Identifizierung und Charakterisierung neuer möglicher Antigene, die an der GAP induzierten Immunantwort beteiligt sind. Dazu verglichen wir das exprimierte Transkriptrepertoire von GAP, RAS und Wildtyp *Plasmodium* Leberstadien. Auf diese Weise wurden Transkripte identifiziert, die in GAP differentiell exprimiert werden und so möglicherweise als Zielantigene des GAP induzierten Impfschutzes dienen könnten. Ein Transkript das während der Sequenzanalyse am häufigsten auftauchte, kodierte für das *P. berghei* C2 Domänen Protein (C2 domain-containing protein; C2CP). C2 Domänen sind allgemein an Ca²⁺-

abhängigen zellulären Prozessen, wie Membranfusion oder vesikulärem Transport, beteiligt. Bekannte Vertreter mit charakteristischen C2 Domänen sind die sogenannten Ferline, die zum Beispiel für den Nematoden *C. elegans* oder den Menschen gut beschrieben sind. In Datenbank Analysen fanden wir neben dem *P. berghei* C2CP ein annotiertes Ferlin und ein Ferlin-ähnliches Protein. Die zellbiologische Funktion dieser Ferlin Proteininfamilie ist in *Plasmodium* nicht bekannt. Gezielte Gen-Knockouts zeigten jedoch, dass das *P. berghei* C2CP und das verwandte Ferlin essentiell während der Blutstadienentwicklung sind. Außerdem wurde die Immunogenität der identifizierten Antigen-Kandidaten untersucht. Interessanterweise konnten in der Sequenz des *Pb* C2CP mehrere H2^b-spezifische CD8⁺ T-Zell Epitope identifiziert werden. Tatsächlich wurden Zellen, die C2CP-spezifische Peptide auf der Oberfläche tragen, in RAS und GAP immunisierten C57BL/6 Mäusen erkannt und gezielt getötet. Außerdem konnte gezeigt werden, dass in der Leber von immunisierten Mäusen T-Zellen spezifisch mit dem C2CP-Peptid T9L restimuliert werden können. Diese Ergebnisse zeigen, dass in RAS und in GAP immunisierten Mäusen in der Tat Immunantworten induziert werden, die spezifisch gegen das identifizierte Antigen C2CP gerichtet sind.

Zusammenfassend wird in dieser Arbeit das erste mal eine antigenspezifische Immunantwort im GAP Vakzinierungsmodell beschrieben. Die spezifische Restimulation von T-Lymphozyten, eröffnet nun die Möglichkeit die spezifischen Immunmechanismen untersuchen zu können, die dem GAP induzierten Impfschutz zugrunde liegen. Diese Arbeit trägt damit zum Verständnis der Leberstadien Immunologie bei und könnte weiterhin dazu beitragen in Zukunft einen sicheren und effektiven Subunit-Impfstoff gegen Malaria zu entwickeln.

Abbreviations

aa	amino acids
Amp	ampicillin
APS	ammonium persulphate
bp	base pair
BMDC	bone marrow dendritic cells
BSA	bovine serum albumin
cDNA	complementary DNA
gDNA	genomic DNA
C2CP	C2 domain-containing protein
CSP	circumsporozoite protein
C-terminus	carboxy-terminus
Da	dalton
ddH ₂ O	double distilled water (Millipore)
DEPC	dliethylpyrocarbonate
DHFR	dihydrofolate reductase
DHFR/TS	dihydrofolate reductase-thymidylate synthase
DMEM	Dulbecco's Modified Eagle Medium
DMSO	dimethylsulfoxid
DNA	deoxyribonucleic acid
dNTP	desoxyribonucleosid-triphosphat
<i>E. coli</i>	Escherichia coli
EDTA	ethylenediaminetetra acetic acid
ELISPOT	enzyme-linked immunosorbent spot
FACS	fluorescence-activated cell sorting
FCS	fetal calf serum
FER	Ferlin
FLP	Ferlin-like protein
for	forward
g	gram or gravitational acceleration
G	gauge
GAP	genetically-attenuated parasites
GPI	glycophosphatidylinositol

h	hours
HRP	horseradish peroxidase
IMDM	Iscove's Modified Dulbecco's Medium
<i>i.p.</i>	intraperitoneal
<i>i.v.</i>	intravenous
k	kilo
kb	kilobase
K/X	Ketamin/ Xylalzin
l	liter
LB	Luria broth
LS	liver stage
m	milli
M	molar
mA	milli Ampere
MACS	magnetic-activated cell sorting
min	minute
ml	millilitre
MOPS	3-(N-morpholino)propanesulfonic acid
n	nano
N-terminus	amino-terminus
°C	degree Celsius
OD	optical density
PABA	<i>para</i> -Aminobenzoic acid
PAGE	polyacrylamide gel electrophoresis
PBS	phosphate buffered saline
PCR	polymerase chain reaction
PEXEL	Plasmodium Export Element
<i>Pb</i>	<i>Plasmodium berghei</i>
<i>Pf</i>	<i>Plasmodium falciparum</i>
<i>Pf</i> EMP1	<i>Plasmodium falciparum</i> Erythrocyte Membrane Protein 1
pH	potential hydrogenii
P/S	penicillin and streptomycin
PV	parasitophorous vacuole
PVM	parasitophorous vacuolar membrane

<i>Py</i>	<i>Plasmodium yoelii</i>
RAS	radiation-attenuated sporozoites
rev	reverse
RNA	ribonucleic acid
rpm	revolutions per minute
RT	room temperature or reverse transcriptase
-RT	without reverse transcriptase
+RT	with reverse transcriptase
s	second
SDS	sodium dodecylsulphate
SG	salivary glands
SP	signal peptide
spz	sporozoite/s
T4	bacteriophage T4
TAE	Tris/acetic acid/EDTA
Taq	<i>Thermus aquaticus</i>
TBS	tris-buffered saline
TBST	tris-buffered saline/tween
TE	Tris/ EDTA
TEMED	triethylmethylethyldiamine
TM	transmembrane domain
TRIS	tris (hydroxymethyl)-aminomethane
U	units
UAP	upregulated in attenuated parasites
UIS	upregulated in infective sporozoites
UTR	untranslated region
UV	ultra violet
qRT PCR	quantitative real time PCR
V	Volt
vol	volume
w/o	without
WHO	World Health Organization
WT	wildtype
μ	micro

1. Introduction

1.1 Malaria

Malaria is the world's third leading infectious killer, following HIV and tuberculosis, and around half of the world's population live at risk of malaria transmission (figure 1). According to recent estimates 1,238,000 people died from malaria in 2010 worldwide of which more than 56 % (699,000 cases) were children under the age of five from Sub-Saharan Africa (Murray et al. 2012). In endemic countries malaria has a major impact on social and economic development, so reduction of malaria burden remains an important challenge and is still a focus of extensive research.

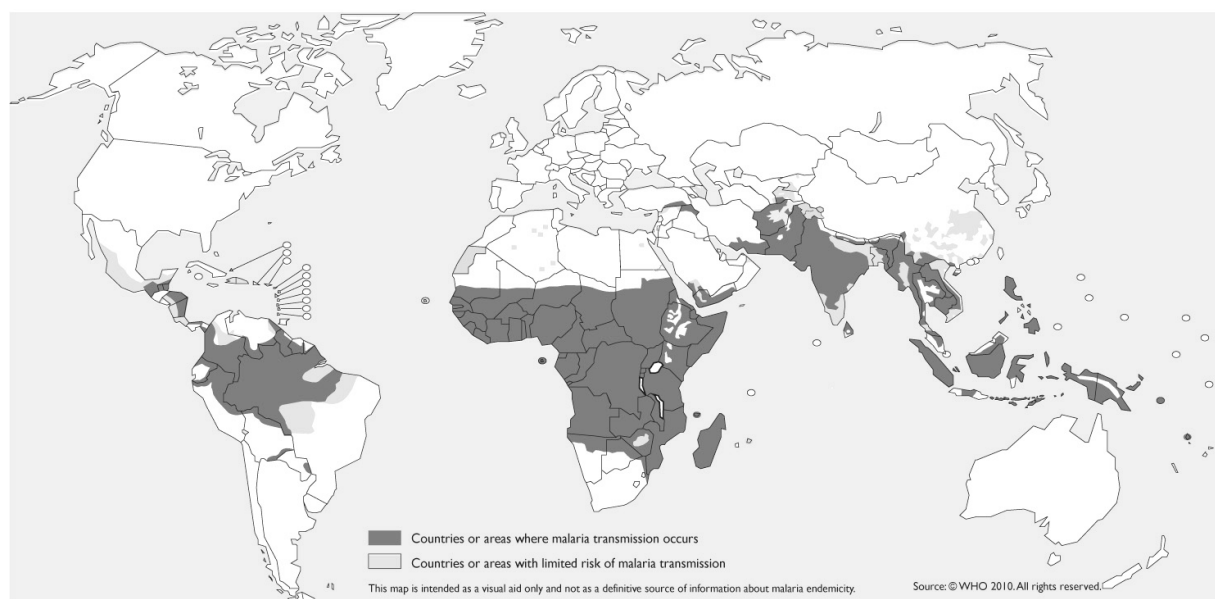


Figure 1. Global malaria distribution. Malaria transmission is mainly restricted to the world's tropical and subtropical regions. Around 3.2 billion people live at risk of malaria. The highest mortality occurs in sub-Saharan Africa. However, Asia, Latin America, and to a lesser extent the Middle East and parts of Europe are also affected (source: <http://www.who.int/ith/en/>).

Adults living in endemic areas develop a degree of immunity against malaria, due to repeated exposure to the malaria parasite [reviewed in (Artavanis-Tsakonas et al. 2003)]. This naturally acquired immunity is based on invasion-inhibitory antibodies directed against blood-stage antigens, like merozoite surface protein-1 (MSP1) or apical membrane antigen-1 (AMA1), and protects against severe symptoms and death (Riley et al. 1992) (Hodder et al. 2001). Sterilising immunity, however, is not achieved. Two high-risk groups suffering from severe symptoms of the disease and associated deaths are children and women in their first

pregnancy (primagravidae). Malaria symptoms reach from fever, headache and nausea to severe illness with anaemia, respiratory distress and cerebral malaria often leading to death. With an early diagnosis and appropriate treatment malaria disease can be reduced and death can be prevented. To date the most successful treatment is achieved with an artemisinin-based combination therapy (ACT). Together with the use of insecticide-treated bed nets and other vector control strategies [reviewed in (Ramirez et al. 2009)], these are the current interventions to handle malaria infection and transmission. Efforts to control malaria are hampered by growing resistances to anti-malarial drugs, like chloroquine and sulfadoxine-pyrimethamine (Barnes et al. 2008). Also spreading insecticide resistance display a major problem [reviewed in (van den Berg 2009)]. New strategies to prevent and eliminate malaria infection are urgently needed. New vector control strategies, like the development of new insecticides or transgenic mosquitoes refractory to malaria, as well as the development of new effective anti-malarial drugs and ultimately the development of an effective anti-infective malaria vaccine are focus of intense research [reviewed in (Enayati and Hemingway 2010)].

1.2 *Plasmodium* life cycle

The protozoan parasite *Plasmodium spp.*, the causative agent of malaria, is a member of the clade Apicomplexa. *Plasmodium* has a complex life cycle, where the parasite not only has to switch between an invertebrate and a vertebrate host, but also between extracellular/invasive and intracellular/replicative forms (figure 2). Female *Anopheles spp.* mosquitoes transmit and receive different forms of the parasite during a blood meal on a variety of vertebrate hosts. There are four human *Plasmodium* species. *P. falciparum* is the most widespread and most fatal species often causing severe symptoms leading to death. *P. vivax*, *P. ovale* and *P. malariae* cause milder disease symptoms in humans. Recently, a fifth one, *P. knowlesi*, whose natural hosts are macaques, is also transmitted by humans, especially in Malaysia (Singh B. et al. 2004). The rodent *Plasmodium* species, *P. berghei* and *P. yoelii*, share major similarities to the human species and depending on the mouse strain used, they can mimic different facets of the disease outcome, reaching from mild symptoms to cerebral malaria, which is then considered experimental cerebral malaria (ECM). Therefore these strains are used as model systems in the laboratory.

Malaria infection starts with the inoculation of infectious salivary-gland sporozoites into the skin of the vertebrate host during blood meal of female *Anopheles* mosquitoes. Typically, only a several hundred sporozoites are injected per infectious bite (Jin et al. 2007) (Vanderberg 1977). Sporozoites depart from the site of injection within minutes and reach a

blood vessel. With the blood stream sporozoites are rapidly transported to the liver, where an initial replication phase occurs (pre-erythrocytic cycle). In the liver sinusoid sporozoite invasion is activated by the highly sulfated heparan sulfate proteoglycans (HSPGs) of hepatocytes (Coppi et al. 2007). Sporozoites adhere to the endothelium cells by exposure of the C-terminal thrombospondin repeat (TSR) domain of the circumsporozoite protein (CSP) (Coppi et al. 2011). Subsequently sporozoites enter the space of Disse through Kupffer cells and transmigrate several hepatocytes before they settle down in their final host-cell (Frevert 2004) (Mota and Rodriguez 2001).

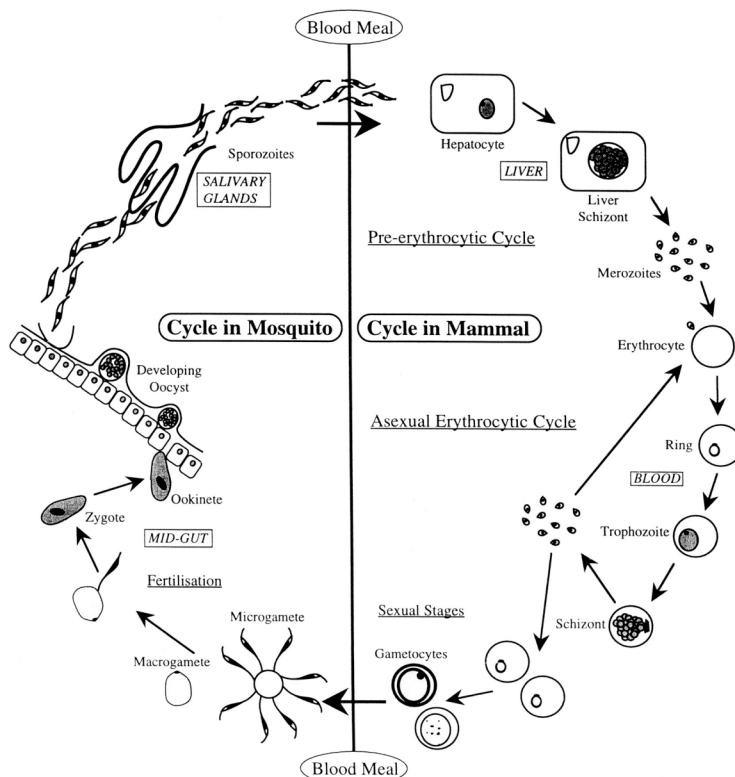


Figure 2. *Plasmodium* life cycle. The single developmental stages are underlined and explained in the text. Briefly, infectious sporozoites are transmitted during blood meal and initially invade hepatocytes where they undergo massive replication (pre-erythrocytic cycle). Merozoites are released and invade erythrocytes. The asexual erythrocytic cycle starts. Some parasites differentiate into sexual stages, which are taken up by a mosquito during blood meal. Fertilisation occurs in the mosquito's midgut and oocysts develop inside the midgut's epithelium. Midgut sporozoites travel through the hemocoel to the salivary glands, where they mature. Infectious sporozoites are then again transmitted to the vertebrate host. (from Phillips, R. S. 2001. Clin. Microbiol. Rev. 14(1):208-226)

Besides the above mentioned CSP, several other parasite proteins are described to be involved in this invasion process. Amongst them the thrombospondin-related anonymous protein (TRAP) is essential for parasite gliding motility and host-cell invasion (Sultan et al. 1997)

(Matuschewski et al. 2002). Furthermore the sporozoite microneme protein essential for cell-traversal 2 (SPECT2) is involved in breaching the sinusoidal cell layer prior to hepatocyte invasion (Ishino et al. 2005). Additionally the cell-traversal protein for ookinetes and sporozoites (CeltOS) is necessary for passage of the sporozoite through the liver endothelium (Kariu et al. 2006). During invasion of the final hepatocyte the host-cell membrane is invaginated building the parasitophorous vacuole, whose membrane is then modified by the intracellular residing parasite. Inside the hepatocyte the parasite replicates asexually, a phase known as pre-erythrocytic or exoerythrocytic schizogony. This replication lasts, depending on the *Plasmodium* species, 2-15 days and ends with the release of thousands of first-generation merozoites. These infective merozoites are packed in host-cell derived vesicles, called merosomes, that bud from the detached host-cell and reach the liver sinusoid (Sturm et al. 2006). These merosomes accumulate subsequently in the pulmonary capillaries, where merozoites are released and infect erythrocytes (Baer et al. 2007). This is the initiation of the disease-causing blood-stage malaria infection (asexual erythrocytic cycle). Liver-derived merozoites invade erythrocytes under formation of a parasitophorous vacuole. Inside the erythrocyte asexual replication, also called erythrocytic schizogony, starts from the ring stage and proceeds via the trophozoite stage to schizonts. Erythrocytes with mature schizonts rupture, which is associated with fever, and released merozoites invade new erythrocytes. Some parasites differentiate to sexual stages, the gametocytes. Sexual reproduction occurs in the mosquito's midgut, after the uptake of gametocytes during a blood meal. The female macrogamete and the male microgametes emerge from the erythrocyte inside the mosquito's midgut and fertilisation of the two results in a diploid zygote. Subsequently followed by differentiation to a motile ookinete, which actively traverses the mosquito's midgut epithelium and forms a so-called oocyst. Inside these oocysts the parasite undergoes meiosis and replicates subsequently asexual and mitotic. Mature midgut sporozoites are released into the hemocoel and travel to the mosquito's salivary glands. The invasion of the salivary glands is an active process involving also some of the afore mentioned proteins, important for hepatocyte invasion, like CSP and TRAP [reviewed in (Mueller et al. 2010)]. Inside the salivary glands sporozoites mature and infectious sporozoites are again transmitted during an infectious blood meal.

1.3 Vaccination strategies against malaria

There are several vaccination strategies against malaria under investigation, reaching from the research stage to clinical trials in phase III. A variety of approaches attack different parasite-specific targets throughout the complex life cycle and thereby might either inhibit or reduce clinical malaria disease (anti-disease), block malaria transmission (anti-transmission) or completely prevent malaria infection (anti-infective).

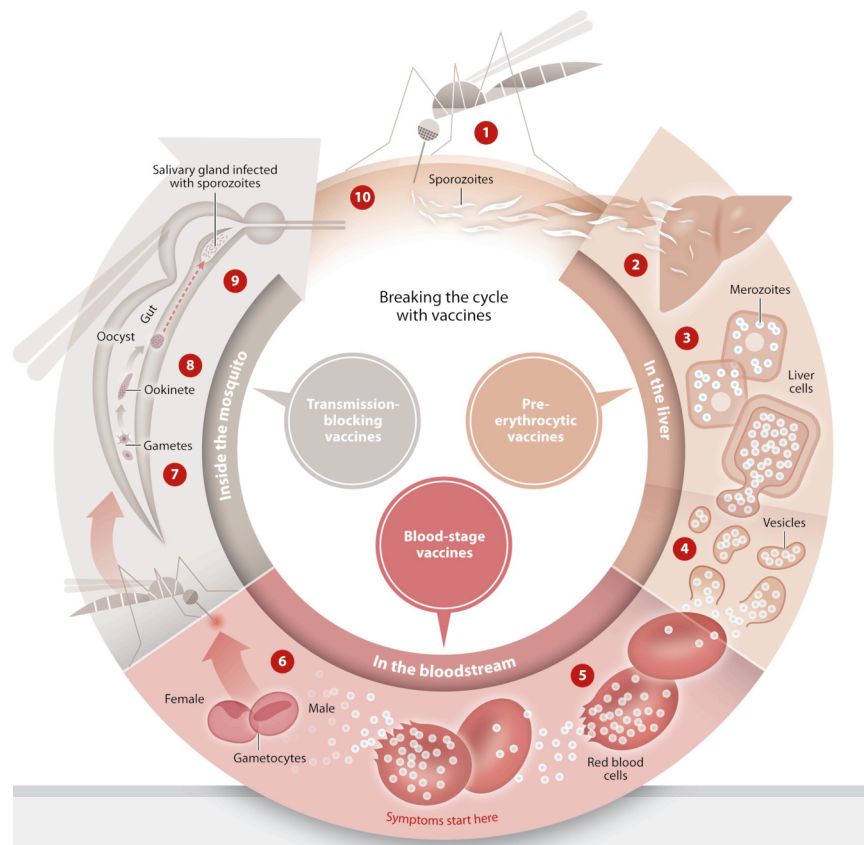


Figure 3. Vaccination strategies against malaria and their targets throughout the parasite's life cycle.
 Sporozoites injected by female mosquitoes (1) invade hepatocytes (2) and replicate inside the cell (3). Budding vesicles filled with merozoites, called merosomes, are released into the blood (4). Pre-erythrocytic vaccines (anti-infective vaccines) target this initial liver-phase and completely prevent infection. In the bloodstream merozoites invade erythrocytes and replicate. Mature schizonts rupture and release new merozoites (5). This is when malaria symptoms start. Blood-stage vaccines (anti-disease vaccines) target mainly erythrocyte invasion and ease malaria symptoms. Some parasites differentiate into sexual gametocyte stages that are taken up by a mosquito during blood meal (6). Inside the mosquito's midgut gametes fertilise (7) and transform into a motile ookinete (8). Midgut sporozoites develop inside oocysts and travel through the hemocoel to the salivary glands, where they mature to infectious sporozoites (9). Targeting the parasite stages in the mosquito prevents transmission, these vaccines are therefore called transmission-blocking vaccines (anti-transmission vaccines). (from Thera and Plowe 2012. Annu. Rev. Med. 63:345–57; adapted from PATH Malaria Vaccine Initiative)

1.3.1 Anti-disease vaccines

The disease-causing blood-stages, replicating inside erythrocytes, are hardly attacked by cellular responses as red blood cells do not express major histocompatibility complex (MHC) molecules. But vaccination strategies are pursued that target merozoite invasion and cytoadhesion of the infected erythrocyte by humoral responses. Inhibitory antibodies against merozoite surface protein-1 (MSP1), for example, reduce blood-stage parasitemia and ease malaria symptoms (Siddiqui et al. 1987) (O'Donnell et al. 2001). More recent data show, that these specific antibodies interfere with shedding of MSP1 and thereby inhibit erythrocyte invasion (Woehlbier et al. 2010). A MSP1-based vaccine formulated with the adjuvant AS02 (see below) induced high specific antibody titres in Malian adults and children Western Kenya (Thera et al. 2006). Protection, however, was not achieved with this vaccine candidate (Ogutu et al. 2009). Another merozoite protein, the apical membrane antigen-1 (AMA1), became a promising vaccine candidate as antibodies against AMA1 are associated with a degree of protection in naturally acquired immunity (Polley et al. 2004). Initial efficacy trials with AMA1-based vaccines failed to induce any protection (Sagara et al. 2009) (Ouattara et al. 2010). An AMA1 vaccine, however, also formulated with the AS02 adjuvant was highly immunogenic in a phase I trial in Malian children (Thera et al. 2010). Protection was also not achieved with this AMA1 vaccine candidate after experimental sporozoite challenge (Spring et al. 2009), but the efficacy against clinical malaria was more than 60 % when caused by the homologous strain used in the vaccine (Thera et al. 2011). Currently, this protection against clinical malaria was also observed with the merozoite surface protein-3 (MSP3) blood-stage vaccine candidate (Sirima et al. 2011). Interestingly, AMA1 is not only necessary for erythrocyte invasion, it may also play a similar role in hepatocyte invasion and might therefore even serve as a multi-stage vaccine candidate (Mitchell et al. 2004) (Florens et al. 2002). Furthermore antibodies against parasite-derived erythrocyte surface proteins, the variant surface antigen *PfEMP1*, block sequestration of infected erythrocytes and therefore prevent severe symptoms (Kyes et al. 2001). These *PfEMP1* proteins are encoded by a large family of *var* genes and therefore these highly polymorphic proteins are hardly to combine in an efficient vaccine (Smith et al. 1995). Nevertheless, one variant, the VAR2CSA, that mediates cytoadherence in placental malaria, is less polymorphic and development of such a placental malaria vaccine is ongoing (Avril et al. 2010). Beside the administration of subunit blood-stage vaccines formulated with strong adjuvants the described blood-stage antigens were also applied as viral vector vaccines. For example, vaccination with the human adenovirus AdHu5 and the modified vaccinia virus Ankara (MVA), expressing MSP1 and

administered in an approved prime-boost immunisation regime, induced high antigen-specific antibody titres and conferred protection in mice (Draper et al. 2008). In a follow-up study it was shown, that these viral vaccine vectors also induced CD4⁺ T-cells providing help to the protective B-cell responses and additionally CD8⁺ T-cells mediating anti-parasitic activity against liver-stages (Draper et al. 2009). All these described anti-disease malaria vaccines, directed against blood-stages and based on invasion-inhibitory antibodies, typically reduce parasite burden rather than clearance, sterilising immunity is not achieved similar to naturally acquired immunity. Also the parasite's life cycle proceed and malaria transmission is hardly impaired.

1.3.2 Anti-transmission vaccines

Though spreading of the parasite can very efficiently be blocked by so called transmission-blocking vaccines. This strategy is generally based on inhibitory antibodies against gamete or ookinete surface proteins that are taken up by the mosquito during the blood meal and will block parasite fertilisation or further development in the mosquito. Thereby the parasite's life cycle is interrupted. Major candidates, currently under investigation as possible targets, are *Pfs28* and *Pfs25*, which are important for oocyst development (Tomas et al. 2001). One approach based on the two proteins *Pfs25* and *Pvs25* from *P. falciparum* and *P. vivax*, respectively, showed antibody-mediated transmission-blocking activity (Wu et al. 2008). Strong adverse effects, due to the used adjuvant Montanide ISA 51, however, proscribed further trials with this vaccine candidate. Recently, also mosquito midgut proteins necessary for parasite invasion were investigated with respect to their potential as transmission-blocking vaccine candidate. The midgut-specific anopheline alanyl aminopeptidase N (AnAPN1) is a promising candidate currently under investigation (Mathias et al. 2012). There is one problem with the transmission-blocking strategies namely that these altruistic vaccines do not protect the vaccinated individuals, but following individuals. Therefore it is suggested to be administered in combination with an anti-disease vaccine. Though the smarter approach would be the development of an effective anti-infective vaccine, that prevents infection and stops transmission at the same time.

1.3.3 Anti-infective vaccines

An anti-infective malaria vaccine, that prevents disease and blocks transmission at the same time, can only be achieved by targeting the pre-erythrocytic stages, this might either be the invasive sporozoites or developing liver-stages. On example is the currently most advanced vaccine candidate, called RTS,S, that contains fragments of the circumsporozoite protein (see

below) including B-cell (R) and T-cell epitopes (T), fused to the hepatitis B surface antigen (S) and formulated with the AS adjuvant system [reviewed in (Cohen et al. 2010)]. The efficacy of this subunit vaccine is around 50 % in malaria-naïve adults (Kester et al. 2009) and similar levels of efficacy were achieved in several phase IIb field trials (Guinovart et al. 2009) (Alonso et al. 2004) (Bejon et al. 2008). But importantly the vaccine reduced the occurrence of severe symptoms about almost 60 % (Bojang et al. 2001) (Alonso et al. 2004). Several attempts were made to improve the efficacy of the RTS,S/AS01 vaccine candidate, for example by adding more antigens tested with the same adjuvant system to create a multi-stage, multi-antigen RTS,S-based vaccine (Heppner et al. 2005). Additionally it was demonstrated that priming with an adenovirus serotype 35 (Ad35) vector encoding CSP (Ad35.CS) prior to RTS,S/AS01 boosting, increased specific T-cell responses (Stewart et al. 2007). Nevertheless the candidate malaria vaccine RTS,S/AS01 is currently investigated in a huge clinical phase III trial in African children. First results of this phase III trial show similar efficacies like in the previous phase II trials from around 50 % (Agnandji et al. 2011). The main protective mechanism of this vaccine candidate is based on inhibitory antibodies directed against the repeat region of CSP (see below). These CSP-specific antibodies are thought to reduce sporozoite motility and host-cell invasion (Heppner et al. 2005). In contrast several studies revealed only moderate T-cell responses induced by RTS,S (Pinder et al. 2004) (Barbosa et al. 2009). Further results also revealed primarily humoral responses and additionally, albeit to a lesser extent, CSP-specific CD4⁺ T-cells to be elicited by RTS,S (Kester et al. 2009). This was supported by a more recent dataset, where the combination of anti-CSP antibody titres and CSP-specific TNF α ⁺ CD4⁺ T-cells could account for the level of protection conferred by the RTS,S/AS01 candidate vaccine (Olotu et al. 2011). Although the results of clinical phase II and first results from phase III showed partial protection against natural malaria infection, the question remains whether RTS,S is the ultimate vaccine?

Other recombinant subunit-protein vaccines but also DNA or viral vector vaccines targeting the pre-erythrocytic stages are under investigation. The recombinant liver stage antigen-1 (LSA1) formulated with the adjuvants AS01 or AS02 induced high antibody titers and CD4⁺ T-cell responses, but failed to induce protection in a phase I/II study (Cummings et al. 2010). In contrast a DNA prime-MVA boost vaccine encoding TRAP elicited strong INF- γ producing CD8⁺ T-cell responses and partially protected from experimental *P. falciparum* challenge (Dunachie et al. 2006). Interestingly, the combination of a viral vector with a subunit protein vaccine, both based on CSP, induced high levels of protection in rodents (Hutchings et al. 2007). Thereby the subunit protein part, containing the immunodominant B-

cell epitope, induces high levels of antibodies, while the viral vector vaccine elicits potent T-cell responses against a CD8⁺ T-cell epitope (Anderson et al. 2004). Different approaches show promising results, the self-assembling polypeptide nanoparticle (SAPN) displaying the B-cell epitope of CSP, for example, induces high antibody titers and confers protection in rodents (Kaba et al. 2009). Finally, different whole-organism vaccination models based on live sporozoites (see below) showed feasibility of a protective anti-infective malaria vaccine. Strong protective T-cell responses are induced and directed against liver-stage maturation. T-cells recognise antigens presented by MHC class I molecules on the surface of infected hepatocytes and destroy the infected cell (see below). A highly effective anti-infective malaria vaccine targeting the pre-erythrocytic stages would therefore prevent not only infection but also disease and transmission.

1.4 Natural vaccination models

In endemic areas adults acquire a degree of natural immunity to malaria due to repeated exposure to wild-type (WT) *Plasmodium* sporozoites [reviewed in (Artavanis-Tsakonas et al. 2003)]. These live parasites express a pool of immunogenic antigens in its native configuration and thereby displaying multiple targets for protective immune responses. The use of WT sporozoites as a vaccine, however, is obviously proscribed because of the subsequent development of fulminant blood-stage malaria infections. But already in the 1970s it was shown that WT sporozoites, administered along with a suppressive dose of chloroquine (CQ) during immunisation and subsequent curative primaquine treatment, protect from subsequent sporozoite challenges (Beaudoin et al. 1977). Later it was shown that immunisation with sporozoites under CQ treatment induces protective T-cell responses (Roestenberg et al. 2009). Furthermore, it was described that primaquine treatment, applied concurrently with the sporozoite plus CQ immunisation, abolished protection, by that demonstrating an essential role of developing liver-stage parasites for the induction of protective immunity in this model (Belouet et al. 2004). Meanwhile this sporozoite plus CQ immunisation model has been successfully adopted to human trials (Roestenberg et al. 2009). Although the immune responses are predominantly directed against liver-stages, a slight inhibitory effect on blood-stages was shown (Belouet et al. 2004). Recently, protection has also been achieved by administration of Azithromycin during natural immunisation (Friesen et al. 2010). This causal prophylactic antibiotic treatment suppresses apicoplast replication (Shimizu et al. 2010). This natural immunisation model produces sterile merozoites unable to establish blood-stage infection and therefore serves as a experimental vaccine (Friesen et al. 2010).

Similarly, causal-prophylactic treatment with primaquine, an anti-malarial drug that exclusively acts on liver-stages, in conjunction with WT sporozoite injection resulted in induction of protective immune responses, despite the absence of persistence (Putrianti et al. 2009). This differs fundamentally from immunisations with other whole-organism vaccines where persistence is a prerequisite for protection, suggesting maybe different underlying immunity mechanisms and a variability in the host immune-status. Recently,

1.5 Live sporozoite vaccination models

The "gold standard" of attenuated whole-organism vaccines, however, remains the radiation-attenuated sporozoite model (RAS). Rodents, monkeys and human volunteers do enjoy sterile protection against sporozoite challenge by administration of γ -irradiated sporozoites (Hoffman et al. 2002, Nussenzweig et al. 1967). These irradiated sporozoites, transmitted by bite or injection to the mammalian host, are still able to invade hepatocytes and transform into liver-stages, but ultimately arrest at different time points during intrahepatic development. Irradiation is thought to induce multiple, random point mutations in the sporozoite's genome leading to a block in liver-stage development. Arresting liver-stages alert the immune system and thereby confer stage-specific sterile immunity. In the RAS model persistence seems to be important as primaquine treatment abolishes protection (Scheller and Azad 1995). Recently, it has been shown that Plasmodial antigen is presented up to 8 weeks after immunisation. The antigen is supposed to persist in lymphoid organs and is required for optimal induction and maintenance of CD8⁺ T-cell responses (Cockburn et al. 2010). The RAS induced immune response is stage-specific as there was no response detected which is directed towards blood-stages (Romero P. et al. 1989) (Rodrigues M. M. et al. 1991). The mechanisms behind the RAS induced immunity are focus of intense research, but up to now only partly understood (see below). Although RAS confers one hundred percent sterile protection in rodents and humans, such a vaccine is difficult to be licensed for human use due to several ethical and technical issues. So far an *in vitro* cultivation system is lacking for *Plasmodium* sporozoites making a large-scale production almost impossible or at least enormous laborious and expensive. The safety of this vaccine must be considered, as over-irradiated sporozoites fail to induce protection and under-irradiated sporozoites can even cause blood-stage infections (Silvie et al. 2002). Furthermore uniformity of the end-product cannot be achieved as irradiation leads to random point mutations in the genome resulting in a genetically-undefined sporozoite population. Despite all this obstacles the biotechnology company Sanaria Inc. developed the candidate vaccine *PfSPZ* based on irradiated sporozoites (Hoffman et al. 2010)

and started a first clinical trial with this candidate vaccine in January 2012 (www.niaid.nih.gov, press release).

Some of the above mentioned problems have recently been overcome by the generation of genetically-attenuated parasites (GAP). Here liver-stage arrest is achieved by depletion of single liver-stage essential genes, such as *uis3*, *uis4* or *p36p* (Mueller et al. 2005a) (Mueller et al. 2005b) (van Dijk et al. 2005). Like RAS, GAP invade hepatocytes and transform into liver-stages, but then arrest at specific time points and thereby conferring stage-specific sterile protection. The GAPs that were initially described in rodent malaria have meanwhile been translated to *P. falciparum*. It was shown that *P. falciparum p52(-)* and *p36(-)* deletion mutants arrest during liver-stage development in cultured human hepatocytes or a chimeric mouse model (van Schaijk et al. 2008, VanBuskirk et al. 2009). Persistence probably plays also a role in the GAP experimental vaccine model as protection was abolished by primaquine treatment after immunisation with *P. berghei uis3(-)* parasites (Mueller et al. 2007). No persisting parasites, however, were detectable by qRT-PCR 40 hours after immunisation with *P. yoelii uis3(-)* and *uis4(-)* (Tarun et al. 2007). The effector mechanisms and antigenic specificities of the GAP induced immunity are hardly known (see below). In summary vaccination strategies based on live sporozoites provide ideal tools to study malaria liver-stage immunology.

1.6 Pre-erythrocytic antigens

Although a number of *Plasmodium* pre-erythrocytic proteins have been studied as possible antigen candidates (Gruner et al. 2003), i.e. liver stage antigen-1 (LSA1) or thrombospondin-related-anonymous protein (TRAP), only immune responses against the circumsporozoite protein (CSP) have been extensively studied so far [reviewed in (Nardin and Nussenzweig 1993)]. It has been shown that *P. yoelii* TRAP (also known as sporozoite surface protein 2) can activate CD8⁺ T-cells and a certain CD8⁺ T-cell clone, specific for a so far uncharacterised epitope, can protect naïve mice if adoptively transferred (Khusmith et al. 1994). Another *P. yoelii* antigen, Py-Hep17, also known as Exp1, seems to be able to stimulate protective CD8⁺ T-cells, too, but specific epitopes for this protein are also unknown (Doolan et al. 1996). Defined pre-erythrocytic epitopes have so far only been described and characterised for CSP (Romero P. et al. 1989), this built the basis for extensive investigation of specific T-cell responses and effector mechanisms in the liver.

The CS protein is, as the name already suggests, the main surface protein of sporozoites (Yoshida et al. 1981). It is expressed already early in midgut sporozoites and is essential for

sporozoite development inside the oocyst (Menard et al. 1997). In the vertebrate host CSP is important for sporozoite motility and involved in host-cell attachment and invasion (Cerami et al. 1992).

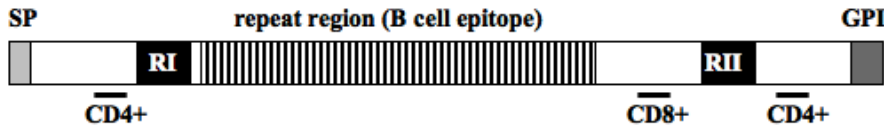


Figure 4. Schematic primary structure of the *Plasmodium* circumsporozoite protein (CSP). Localisation of the conserved regions RI and RII are shown in the amino terminus (left) and the carboxyl terminus (right), respectively. The immunogenic sections are the central amino acid repeats and CD4⁺ and CD8⁺ T-cell epitopes. SP: signal peptide; GPI: glycosylphosphatidylinositol anchor.

The CS protein can be divided into three parts, the N-terminal and the C-terminal region and the central repeat region (figure 4). The central repeats are also known as B-cell epitope-region as antibodies are directed against this part of the protein (Eichinger et al. 1986). The N-terminal and C-terminal parts contain the conserved regions RI and RII, important for host-cell binding and gliding motility (Ancsin and Kisilevsky 2004) (Tewari et al. 2002), but also a number of different T-cell epitopes. To date several CD4⁺ specific T-cell epitopes have been described in the amino as well as in the carboxy termini specific to different MHC-haplotypes (Romero P. J. et al. 1988). But so far only a single MHC class I H-2^d-restricted CD8⁺ T-cell epitope for CSP (amino acids 252-260, SYIPSAEKI for *P. berghei* and amino acids 280-288, SYVPSAEQI for *P. yoelii*) is described. Presentation and recognition of this CD8⁺ T-cell epitope is strongly correlated with protection (Romero P. et al. 1989). Because of this dominant humoral and cellular responses directed against CSP, it has been considered as the major vaccine candidate since a long time. Recently, however, a series of elegant studies revealed that protection can be achieved despite the absence of immune responses specific to CSP. In transgenic mice, that were made tolerant to CSP T-cell epitopes, protection was greatly reduced when immunised with two doses of irradiated sporozoites. But complete protection could be restored with three immunisation doses (Kumar et al. 2006). This indeed suggests an immunodominant role for CSP, but other sub-dominant responses against other, still unknown pre-erythrocytic antigens must be present. In another study the *P. berghei* CSP was complemented with the *P. falciparum* orthologue. This transgenic parasite line has been used for challenge experiments after immunisation studies with *P. berghei* RAS. Although no cross-reactivity between the two heterologous CSP proteins could be shown, *P. berghei* RAS immunised mice were protected when challenged with the parasite line expressing the

heterologous protein (Gruner et al. 2007). Furthermore CSP was ascribed only a minor role in protection achieved by immunisation with live sporozoites under chloroquine prophylaxis as protective immunity was obtained irrespective of the origin of CSP in this vaccination model (Mauduit et al. 2010). These data demonstrate that sterile protection against malaria is independent to immune responses to CSP. Finally, in the GAP vaccination model sterile protection is achieved in the C57BL/6 mouse genetic background. These mice do not recognise the CSP CD8⁺ T-cell epitope, as they do not express the H-2k^d MHC class I molecule haplotype. Altogether these findings raise the idea that other, hitherto not yet identified pre-erythrocytic antigens may exist that can be targeted in order to induce sterilising immunity to malaria infection. Searching for new immunogenic antigens that may be implicated in the acquisition of protection is necessary. Interestingly, recent transcriptome and proteomic data of liver-stage parasites aid in improving the search for new candidates (Tarun et al. 2008) (Williams and Azad 2010) (Cardoso et al. 2011).

1.7 Malaria liver-stage immunology

Immunology to malaria liver-stage infection is investigated in field studies mainly as response to pre-erythrocytic stage antigens in naturally acquired immunity. Nevertheless, these studies in endemic areas gave only little insights into liver-stage immunology of WT malaria infection (Plebanski and Hill 2000) (Offeddu et al. 2012). Antibodies directed against the sporozoite surface proteins CSP and TRAP inhibit sporozoite invasion (Hoffman and Franke 1994). However, there is no stringent correlate between high CSP-specific antibody titres and protection in malaria-exposed individuals (Riley et al. 1990) (Hoffman et al. 1987). Although parasite-specific CD8⁺ T-cells are found only rarely in humans (Plebanski et al. 1997) (Doolan et al. 1993), there is evidence that CD8⁺ T-cells execute anti-parasitic activity *in vivo* (Hill et al. 1992). Another study shows that enhanced memory T-cell responses specific to TRAP correlate with reduced malaria incidence (Todryk et al. 2008). While in the same study increased TRAP-specific CD4⁺ CD25^{high} T-cell responses were associated with higher risk of clinical malaria. The immune responses to WT liver-stage infections may also be limited due to immune evasion and modulation mechanisms driven by the parasite [reviewed in (Casares and Richie 2009)].

Therefore most research focusing on malaria liver-stage immunology utilised irradiated sporozoites to study induced protective immune responses in the liver. This RAS-mediated immunity is multi-factorial involving neutralising antibodies and interferon-gamma producing T-cells (Schofield et al. 1987b) (Tsuji et al. 1992). It has been shown already in the 1980s that antibodies against a sporozoite's surface component confer protection depending on the

number of sporozoites used for challenge and the antibody concentration in the serum (Potocnjak et al. 1980). In particular, antibodies directed against the circumsporozoite protein (CSP) neutralise sporozoites at the inoculation site and prevent their invasion into hepatocytes after RAS immunisation (Hollingdale et al. 1982). This humoral response, however, seems to be not crucial as B-cell deficient mice were still able to develop protective immunity after immunisation with RAS (Chen et al. 1977). The critical role of CD8⁺ T-cells observed for protective immunity has been shown in earlier studies where depletion of CD8⁺ T-cells reduced the immunity induced by RAS (Schofield et al. 1987b) (Weiss et al. 1988). Additionally, adoptive transfer experiments demonstrated that CSP-specific CD8⁺ T-cells conferred protection against sporozoite challenges (Rodrigues M. M. et al. 1991). These CD8⁺ T-cells are supposed to recognise major histocompatibility complex (MHC) class I presented malarial antigens and direct their cytotoxic activity against infected hepatocytes (Renia et al. 1994). How these presented antigens are processed *in vivo* was recently investigated. While CSP was cross-presented via endosomes by dendritic cells in the priming phase it had to be exported into the hepatocyte cytosol in order to be accessible to T-cells in the effector phase (Cockburn et al. 2011). The mechanisms underlying the cytotoxic activity, however, are not yet fully understood. There is a potential role for nitric oxide (NO) described as part of the downstream effector mechanism associated with protection (Nussler et al. 1993). In contrast, other effector molecules like Fas and perforin seem not to be important, as mice lacking one of these molecules can still develop protective immunity (Renggli et al. 1997) (Doolan and Hoffman 2000). Interferon-gamma (IFN- γ) produced by cytotoxic CD8⁺ T-cells seems to be the main effector cytokine in mediating anti-malarial activity. Studies in IFN- γ deficient mice or IFN- γ depletion after immunisation with irradiated sporozoites and IFN- γ treatment of infected hepatocytes *in vitro* revealed a crucial role for this regulatory cytokine for mediating the killing of intracellular parasites by CD8⁺ T-cells (Schofield et al. 1987a).

Additionally, it is suggested that other T-cell subsets are involved in pre-erythrocytic immunity in general and RAS-mediated protection in particular. There is evidence that CD4⁺ T-cells can directly mediate RAS-induced immunity, depletion of CD4⁺ T-cells in RAS immunised mice significantly reduced protective immunity (Rodrigues M. et al. 1993), as well as a certain adoptively transferred CD4⁺ T-cell clone has shown to protect naïve mice from sporozoite challenge (Tsuji et al. 1990). But in the first instance CD4⁺ T-cells provide important helper functions. Thus, it was shown that IL-4 secreting CD4⁺ T-cells are required for induction and survival of the CD8⁺ T-cell response after immunisation (Carvalho et al. 2002) (Morrot et al. 2005). In $\alpha\beta$ T-cell deficient mice, lacking CD8⁺ and CD4⁺ T-cells, it has

been shown that also $\gamma\delta$ T-cells can mediate a direct anti-malaria effect (Tsuji et al. 1994). Moreover, it was demonstrated that $\gamma\delta$ T-cell deficient mice had a higher parasite load in the liver after challenge with infectious sporozoites (McKenna et al. 2000) confirming the role of this T-cell subset in RAS-mediated pre-erythrocytic immunity. Although it was firstly described that natural killer (NK) T-cells are important for inducing high antibody responses (Schofield et al. 1999), this was negated later (Molano et al. 2000). If not important for the humoral response, NK T-cells, however, seem to act against malaria liver-stages. NK T-cells isolated from livers of malaria-infected mice, inhibited the development of liver-stages *in vitro* (Pied et al. 2000). Furthermore, the ligand α -GalCer, which stimulates NK T-cells, was successfully used as adjuvant to reduce liver infection after live sporozoite injection (Gonzalez-Aseguinolaza et al. 2000), indeed suggesting NK T-cells to act against malaria liver-stages.

Whether NK cells, which are usually associated with the innate immune system, play a role in immunity to malaria liver-stages is still under discussion. Depletion of NK cells with anti-asialoGM-1 antibodies after immunisation with irradiated sporozoites, significantly diminished protection (Doolan and Hoffman 1999). But as asialoGM-1 is also expressed by activated CD8 $^{+}$ T-cells (Slifka et al. 2000), this decrease in protection could also be due to depletion of the latter. Moreover, depletion experiments showed a role of dendritic cells for priming the CD8 $^{+}$ T-cell response (Jung et al. 2002).

Protective immune responses induced by genetically-attenuated parasites (GAP) are so far less characterised, but share at least in some aspects similarities to the RAS-induced protection. Studies in *rag1* $^{-/-}$ mice, lacking T-cells and B-cells, showed that protection is dependent on adaptive immune responses and adoptive transfer experiments demonstrated that CD8 $^{+}$ T-cells are major players. Antibodies, however, seem to be not crucial, as protection could also be achieved in B-cell deficient mice (Mueller et al. 2007). Moreover, the role of innate immune responses in the GAP induced immunity is not yet clarified, but a delay in pre-patency in *rag1* $^{-/-}$ mice might at least suggest a minor role of innate immune mechanisms (Mueller et al. 2007). Ultimately, the induced effector mechanisms and antigenic specificities induced by GAP, however, are so far not fully understood.

1.8 Aim of this study

Malaria kills nearly one million people a year and a vaccine is urgently needed. The feasibility of vaccination against malaria infection has been adequately demonstrated by the live RAS (radiation-attenuated sporozoites) vaccine that confers sterilising immunity against natural malaria infection in rodents and humans. As an alternative, recent advances in gene targeting have permitted the generation of genetically-attenuated parasites (GAP), which are unable to express essential liver stage expressed genes, thus resulting in attenuated liver stage development. These GAPs confer to a similar degree of protection as RAS, but, so far, the antigenic specificity and the effector mechanisms of this protective immune response have not been characterised. These live-attenuated parasites provide us with an ideal tool to study protective immune responses. In order to develop a safe subunit vaccine that induces similar levels of protection we need to understand how the attenuated parasite vaccine works. The aim of this research is thus to characterise antigenic specificities and effector mechanisms of immunity induced by GAP and to compare these responses to those induced by RAS and WT sporozoites.

First we wanted to create a tool to further characterise the role of the circumsporozoite protein (CSP) in pre-erythrocytic immunity. CSP has historically been considered as the major vaccine candidate, but recently several arguments revealed that protective immunity can be achieved independently of immune responses specific to main surface protein of sporozoites. Hence, we aimed at generating a *P. yoelii* parasite expressing a functional CS protein, essential for sporozoite development, that is no longer recognised by the host's immune system. For that we wanted to insert several defined point mutations in the described CD8⁺ T cell epitope, SYVPSAEQI, and subsequently subject this novel experimental genetically-engineered parasite for immunisation studies. Hypothesising that CSP cannot be a protective antigen in the GAP experimental model, we secondly wanted to isolate and characterise novel antigen candidates that might be both immunogenic and protective and expressed during liver stage development of GAP parasites. As GAP arrest early during liver stage development not all proteins that are normally expressed will be transcribed. The same accounts for RAS, irradiation, however, induces random point mutations, liver stage arrest therefore occurs at different time points, the expressed repertoire is probably more heterogeneous in comparison to GAP. We hypothesise that proteins expressed in the liver by GAP are able to initiate protective immune responses. Our hypothesis prompted us to screen for liver stage antigens that are uniquely or differentially expressed by the attenuated liver stage parasites that will ultimately allow us to narrow down antigens that may be critical for immunity. We therefore

wanted to apply differential screening methodologies and decided for a suppression subtractive hybridisation (SSH), a method that allows selective enrichment of differentially regulated cDNAs of high and low abundance. Resulting candidates should subsequently be characterised in their ability to specifically restimulate T cells from GAP and RAS immunised mice.

2. Materials and methods

2.1 Laboratory equipment

AMAXA® Nucleofector® II	
electroporation machine	Lonza, Köln
Analytical scales BL510	Sartorius GmbH, Göttingen
Autoclave	Systec GmbH, Wettenberg
Camera, DC 120 Zoom digital	Kodak, New York
Centrifuges:	
- Megafuge 1.0R	Heraeus Instruments, Hanau
- Microcentrifuges 5415 R, 5415 D	Eppendorf, Hamburg
Electrophoresis System Horizon 11.14	Whatman Inc., USA
Electrophoresis Power Supply EPS 301	Amersham Pharmacia Biotech, Freiburg
Film developer Hyperprocessor	Amersham Pharmacia Biotech, Freiburg
Film developing cassettes	Dr Goos suprema GmbH, Heidelberg
Freezer - 80 °C	Sanyo
Freezers - 20 °C	Liebherr, Biberach
Fridges	Liebherr, Biberach
Heat block thermomixer comfort	Eppendorf, Hamburg
Haemocytometer (Neubauer)	Labotec, Labor-Technik, Göttingen
Ice machine AF 30	Scotsman, Milano, Italy
Incubators:	
- Hera Cell Incubator	Heraeus Instruments, Hanau
- Shaking Incubator Innova 4000/4300	New Brunswick Scientific Co. Inc.
- Multi-gas incubator (O ₂ , CO ₂)	Mytron, Heiligenstadt
Liquid nitrogen tank	CBS, USA
Magnetic stirrer, Heidolph MR3001	NeoLab, Heidelberg
Microscopes	
- Light optical microscope, Axiostar plus	Zeiss, Jena
- Light optical microscope, Axioskop	Zeiss, Jena
- Light optical microscope, Axiovert 25	Zeiss, Jena
Microwave oven	MDA
Mosquito cages	BioQuip Products Inc, USA
PCR-machines	

- GeneAmp PCR system 9700	Applied Biosystems, CA USA
- Mastercycler Gradient	Eppendorf, Hamburg
pH-meter	Inolab, Heidelberg
Photometer	Eppendorf, Hamburg
Pipettes	
- Single channel pipettes 2 µl, 20 µl, 200 µl, 1000 µl	Abimed, Langenfeld
- 12-channel pipette 200 µl	Abimed, Langenfeld
Pipetting aid pipetus®	Hirschmann Laborgeräte, Eberstadt
Precision balance	Mettler Toledo, Switzerland
SDS-PAGE system	Amersham Pharmacia Biotech, Freiburg
Sterile work bench Gelaire X	Flow Laboratories, Meckenheim
Vortex Genie 2	Scientific Industries Roth, Karlsruhe
Water bath Julabo U3	Julabo, Seelbach
Wet blot system	Amersham Pharmacia Biotech, Freiburg

2.2 Consumables

14 ml polystyrene round bottom tubes with lid	Greiner Bio-one, Frickenhausen
15 ml polypropylene tubes with lid	Sarstedt, Nümbrecht
50 ml polypropylene tubes with lid	Sarstedt, Nümbrecht
6-well cell culture plates, Cellstar	Greiner Bio-one, Frickenhausen
8-well chamber slides	Nunc, Langenselbold
96-well round bottom plates	Greiner Bio-one, Frickenhausen
Cell culture flasks	
- Cellstar (Filter Cap, 75 cm ²)	Greiner Bio-one, Frickenhausen
- Nunc Flasks Nuclon (Filter Cap, 25 cm ²)	Nunc, Langenselbold
Cell strainer (70 µm)	BD Biosciences, Heidelberg
Cuvettes	Sarstedt, Nümbrecht
Cryovials	Greiner Bio-one, Frickenhausen
Dialysis tube membrane Nadir®	Carl Roth GmbH, Karlsruhe
ELISpot PVDF filter plates	Millipore GmbH, Schwalbach
Filter paper Whatman TM 3MM	Whatman, GE Healthcare, Dassel
Gloves, Peha-soft satin	Hartmann, Heidenheim

Immersion oil	Zeiss, Jena
Microscope cover slips	Marienfeld, Lauda-Königshofen
Needles, BD Microlance	Becton Dickinson; Heidelberg
Nitrocellulose membrane, Hybond ECL	Amersham, GE Healthcare, Freiburg
Glass slides	Marienfeld; Lauda-Königshofen
Parafilm	Pechiney Plastic Packaging; USA
Pasteur capillary pipettes	Wu; Mainz
Petri dishes (94/16 mm)	Greiner Bio-one, Frickenhausen
Pipette filter tips, Biosphere	Sarstedt, Nümbrecht
Pipette tips	Sarstedt, Nümbrecht
Reaction tubes (0.5 ml, 1.5 ml, 2.0 ml)	Sarstedt, Nümbrecht
Sterile filtration devices (500 ml)	Nalagene, Wiesbaden
Sterile pipettes (1 ml, 5 ml, 10 ml, 25 ml), Cellstar	Greiner Bio-one, Frickenhausen
Sterile syringe filter, Filtropur (0.22 µm pore size)	Sarstedt, Nümbrecht
Syringe, BD Microlance	Becton Dickinson, Heidelberg
Thermo well PCR tubes (0.2 ml)	Sarstedt, Nümbrecht

2.3 Strains

2.3.1 Bacteria strains

<i>Escherichia coli</i> XL1 blue	Stratagene; Agilent Technologies Sales & Services GmbH & Co. KG
<i>Escherichia coli</i> BL21-CodonPlus (DE3)-RIPL	Stratagene; Agilent Technologies Sales & Services GmbH & Co. KG

2.3.2 Cell lines

Huh7	human hepatoma cell line
------	--------------------------

2.3.3 Parasite strains

<i>Plasmodium yoelii</i> 17XNL	(Topley et al. 1970)
<i>Plasmodium berghei</i> ANKA GFPcon	(Franke-Fayard et al. 2004)
<i>Plasmodium berghei</i> ANKA cl15cy1	(Hall et al. 2005)
<i>Plasmodium berghei</i> NK65	(Yoeli and Most 1965)
<i>Plasmodium berghei</i> NK65 uis3(-)	(Mueller et al. 2005a)

Plasmodium berghei NK65 CS-GFP (Natarajan et al. 2001)

2.3.4 Mosquito strains

Anopheles stephensi NIJ Nijmegen, Niederlande

2.3.5 Mouse strains

Naval Medical Research Institute Charles River Laboratory, Sulzfeld,
(NMRI), outbred mice Germany

C57BL/6, inbred mice Charles River Laboratory, Sulzfeld,
Germany

2.4 Chemicals and reagents

Chemicals were typically purchased in p.a. quality from the companies Roth, Merck, Sigma, Serva and AppliChem. Chemicals and reagents from other companies are listed below.

Agarose	Invitrogen, Karlsruhe
AP Conjugate Substrate Kit	Biorad Laboratories, München
BactoTM-Agar	Difco Laboratories, Augsburg
BactoTM-Trypton	Difco Laboratories, Augsburg
BactoTM -Pepton	Difco Laboratories, Augsburg
Cellulose powder CF11 (fibrous)	Whatman, GE Healthcare, Dassel
CFSE	Invitrogen, Karlsruhe
Heparin	Braun, Melsungen
Nycodenz powder	Axis-Shield PoC, Oslo
PBS-pellets	Gibco Invitrogen, Karlsruhe
Sea salt	Alnatura
Streptavidin-ALP	Mabtech, Sweden

2.5 Peptides

Pb C2 domain-containing protein (C2CP) derived peptides were synthesised by JPT Peptide Technologies GmbH, Berlin. Peptide stock solutions with a concentration of 20 mM were dissolved in DMSO and aliquots were stored at - 80 °C.

2.6 Oligonucleotides

Oligonucleotides were ordered as custom DNA oligonucleotides in a desalted purity from Invitrogen, Karlsruhe. Lyophilised oligonucleotides were dissolved in ddH₂O in a concentration of 100 µM and stored at - 20 °C. Sequences of all used oligonucleotides are attached under 6.1.

2.7 Media, buffer and solutions

2.7.1 Media and buffer for molecular biological methods

LB (Luria Broth) Medium: 10 % trypton
5 % yeast extract
10 % NaCl
pH 7,5; autoklave

LB Agar: LB-medium; 15 g/l agar

TAE (50 x): 2 M TRIS
1M acetic acid
50mM EDTA; pH 8.0

PBS (10 x): 0.01 M KH₂PO₄
1.37 M NaCl
0.027 M KCl
pH 7.2; autoklave
or dissolve 20 PBS tablets (Gibco) in 1 l ddH₂O; autoklave

PBS (1 x): 100 ml 10 x PBS, filled up with ddH₂O to 1 l
or purchased from Invitrogen

TfB I: 30 mM potassium acetate
 50 mM MnCl₂
 100 mM KCl
 10 mM CaCl₂
 15 % glycerine

The pH was adjusted to 5.8 with acetic acid. The buffer was sterile filtered and stored at 4 °C.

TfB II: 10 mM MOPS
 75 mM CaCl₂
 10 mM KCl
 15 % glycerine

The pH was adjusted to 7.0 with NaOH. The buffer was sterile filtered and stored at 4 °C.

2.7.2 Media and solutions for cell culture

Cell culture media and supplements were purchased from Invitrogen or Gibco, Karlsruhe.

Hepatocyte culture medium:
(DMEM complete) 1 x Dulbecco's Modified Eagle Medium,
10 % FCS, 1 % penicillin/streptomycin; sterile,
stored at 4 °C

Lymphocyte culture medium:
(RPMI complete) 1 x RPMI medium 1640, 10 % FCS, 1 %
penicillin/streptomycin, 1 % glutamine,
50 µM β-mercaptoethanol; sterile, stored at 4 °C

BMDC culture medium:
(IMDM complete) 1 x Iscove's Modified Dulbecco's Medium,
10 % FCS, 1 % penicillin/streptomycin,
1 % glutamine, 50 µM β-mercaptoethanol; sterile,
store at 4 °C

prior to use 30 % GM-CSF (hybridoma supernatant, provided by Beatrix Schumack, Bonn) was added to IMDM complete and sterile filtered

Cell freezing solution: 80 % FCS, 20 % DMSO
or 90 % FCS, 10 % DMSO mixed 1 : 1 with complete culture medium

2.7.3 Media, buffer and solutions for parasitological methods

Parasite Transfection medium: (T-medium)	160 ml RPMI 1640 medium 40 ml FCS (US certified, heat inactivated for 30 minutes at 56 °C) 60 µl Gentamycin; sterile filtered
Parasite freezing solution:	10 % glycerine in Alsever's solution (Sigma)
Nycodenz stock solution:	110.4 g Nycodenz powder 5 mM TRIS/HCl; pH 7.5 3 mM KCl 0.3 mM EDTA; pH 8.0 fill up to 400 ml with ddH ₂ O; autoklave; store at 4 °C
Pyrimethamine stock solution:	7 mg/ml Pyrimethamine in DMSO, store at 4 °C

2.7.4 Buffer for immunological methods

MACS buffer:	1 x PBS, 1 % FCS, 2 mM EDTA, sterile filtered, 4 °C
FACS buffer:	1 x PBS, 1 % FCS, sterile filtered, 4 °C

Saponin buffer:	1x PBS, 2% BSA, 0.5% Saponin; prepare fresh
-----------------	---

2.7.5 Buffer and solutions for biochemical methods

Lysis buffer:	50 mM NaH ₂ PO ₄ 300 mM NaCl 0.05 % Tween 20 1 mg/ml lysozyme; adjust pH to 8.0 with NaOH
2 x SDS loading dye:	250 mM TRIS/HCl pH 6.8 6.6 % SDS 24 % glycerine 10 mM EDTA 6 % β-mercaptoethanol 0.01 % bromophenol blue

Running buffer: 250 mM glycine, 25 mM TRIS, 0,1 % SDS

10 x transfer buffer: 20 mM TRIS, 144 mM glycine, 0.01 % SDS

1 x transfer buffer: 100 ml 10 x transfer buffer, 200 ml methanol, fill up to 1 l with ddH₂O

TBST: 20 mM TRIS/HCl pH 7.6, 137 mM NaCl, 0.1 % Tween20

Coomassie staining solution: 50 % methanol, 10 % acidic acid, 0.125 % brilliant blue R-250

Coomassie destaining solution: 50 % methanol, 10 % acidic acid

2 x sodium phosphate buffer: 5.3 ml 200 mM NaH₂PO₄ stock solution

100 mM, pH 8.0 94.7 ml 200 mM Na₂HPO₄ stock solution

100 ml ddH₂O

stock solutions can be stored at 4 °C, sodium phosphate buffer is prepared fresh

Equilibration and washing buffer: 1 x sodium phosphate buffer (50 mM)
300 mM NaCl

Elution buffer: 1 x sodium phosphate buffer (50 mM)
300 mM NaCl
250 mM imidazol

2.8 Molecular biological methods

2.8.1 Cloning of the targeting constructs for parasite transfection

The targeting constructs *pcspΔepi_me01 - me04*, *pcsp*repl*Δepi_me01 - me04* and *pΔcsp*rae** for *P. yoelii* transfection and *pΔfer*, *pΔc2cp*, *pferCONT*, *pc2cpCONT* for *P. berghei* transfection were all generated using the following protocols. Vector maps of all generated targeting constructs are attached under 6.2.

2.8.1.1 Amplification of the specific DNA fragments by Polymerase chain reaction (PCR)

Specific DNA fragments were amplified by Polymerase chain reaction (PCR) (Saiki et al. 1985) using specific oligonucleotides. All used oligonucleotides and their sequences are attached under X. As templates served *P. yoelii* or *P. berghei* gDNA. For a standard PCR reaction 0.5 - 2 µl parasite gDNA was used in a reaction volume of 50 µl. Furthermore the reaction contained 50 pmol of the specific oligonucleotides (Invitrogen), 0.2 mM dNTPs, 1.5 mM MgCl₂, 1 x Taq reaction buffer (+ KCl) and 2.5 U Taq polymerase (all Fermentas) filled up to 50 µl with ddH₂O. Reaction tubes were placed into a thermal cycler running the program with an initial denaturation of the dsDNA for 5 minutes at 94 °C, followed by 30 cycles with a denaturation at 94 °C for 30 seconds, annealing of the specific oligonucleotides at 55 °C for 30 seconds and extension of the newly synthesised DNA strand at 60 °C for 1 minute per amplified kilobase plus 30 seconds. A final extension for 10 minutes at 60 °C was carried out and amplified DNA was stored at 4 °C for short-term and at - 20 °C for long-term storage.

2.8.1.2 Analysis of DNA fragments by agarose gel electrophoresis

Amplified DNA fragments were separated by size by agarose gel electrophoresis. For this 1 % agarose was dissolved in 1 x TAE buffer by heating in the microwave. Ethidium bromide (Sigma, Taufkirchen) was added to a final concentration of 50 ng/ml. Samples were mixed with 1/5 volume of 6 x Orange Loading dye (Fermentas) and loaded along with 1 µg GeneRuler™ 1 kb DNA Ladder (Fermentas) into the wells. The gel was run for 1 hour at 100 V in 1 x TAE buffer in a Whatman Horizon 11.14 electrophoresis chamber. Negatively charged DNA thereby migrates in direction of the anode. Separated DNA fragments were visualised by exposure of the DNA-intercalating ethidium bromide to UV-light and fluorescence was recorded with the Electrophoresis Documentation and Analysis System 120 (Kodak).

2.8.1.3 Purification of DNA with Qiaquick PCR purification Kit

Amplified DNA fragments were purified with Qiaquick PCR purification Kit (Qiagen, Hilden) prior to digestion with restriction endonucleases and digested DNA fragments as well as plasmid DNA also prior to ligation according to the manufacturer's manual.

2.8.1.4 Digestion of double-stranded DNA

Purified DNA fragments or plasmid DNA were digested with specific restriction endonucleases (New England Biolabs, Frankfurt) prior to ligation (preparative digest) or after

plasmid isolation (control digest). For the preparative digest the amplified and purified DNA fragments and the respective plasmid DNA were cut with the same restriction endonucleases. The complete purified DNA fragment or 1 - 3 µg plasmid DNA were mixed with 10 - 20 Units of the respective restriction enzymes, 5 µl of the matching buffer (10x) and 5 µl of BSA (10x), if necessary, and filled up to 50 µl with ddH₂O. The digest was typically incubated over night at 37 °C. For the control digest of isolated plasmids the approach was typically scaled down to 20 µl reaction volume, using only 0.5 - 1 µg DNA. The reaction was then incubated for 2 hours at 37 °C. All digested DNA was analysed by agarose gel electrophoresis as described under 2 and preparative digested DNA was purified prior to ligation as described under 3. Prior to parasite transfections 10 µg of the generated plasmids were digested completely with up to 40 Units of the respective enzymes in a volume of 100 µl over night at 37 °C. Subsequently digested plasmid DNA was ethanol precipitated as described under 2.8.1.11.

2.8.1.5 Ligation of DNA

Digested and purified DNA fragments were ligated with equally restricted plasmids in a ratio of 7:1 or 6:2 in a total reaction volume of 10 µl. 5 Units of the T4 ligase were used to catalyse the reaction in 1 x of the provided T4 ligase reaction buffer (10 x, Fermentas). The ligation reaction was incubated for 2 hours at room temperature or at 4 °C over night. Subsequently competent *E. coli* XL1 blue were directly transformed with the ligated DNA constructs.

2.8.1.6 Preparation of transformation competent *E. coli* XL1 blue

E. coli XL1 blue were cultured over night in LB medium with tetracycline (5 µg/ml). The over night culture was diluted 1 : 100 in LB medium with tetracycline (5 µg/ml) and cultivated shaking at 37 °C until it reached an OD₆₀₀ of 0.5. The culture was cooled down on ice and spun for 5 minutes at 1500 x g at 4 °C. The cell pellet of 100 ml culture was resuspended in 30 ml cold TfBI, incubated for 15 minutes on ice and spun again for 5 minutes at 1500 x g. The pellet was resuspended in 8 ml TfBII and incubated another 15 minutes on ice. 200 µl aliquots of the suspension were frozen at - 80 °C.

2.8.1.7 Transformation of competent *E. coli* XL1 blue

Transformation competent *E. coli* XL1 blue, either purchased from Stratagene or prepared as described under 6, were thaw on ice. 35 µl of the purchased cells or 200 µl of the self-made competent cells were used for one transformation. Competent cells were either treated for 10 minutes on ice with 0.68 µl β-mercaptoethanol (1.42 M; Stratagene) and subsequently mixed

with 2 µl of the ligation (Stratagene competent cells) or directly mixed with 10 µl ligation (self-made competent cells). The cells were incubated for 30 minutes on ice, followed by a heat-shock for 45 seconds at 42 °C in the water bath. Cells were incubated subsequently another 2 minutes on ice, then 1 ml pre-warmed LB medium was added and cells were incubated, shaking at 37 °C for 1 hour. The cells were spread on LB agar plates with ampicillin (100 µg/ml) and incubated over night at 37 °C.

2.8.1.8 Plasmid isolation with Qiaprep Spin Miniprep Kit

After transformation single colonies were used to inoculate 3 ml LB medium with ampicillin (100 µg/ml) each. These cultures were incubated shaking at 37 °C over night. The over night cultures were spun for 2 minutes at 16,000 x g in a table-top microcentrifuge. The plasmid isolation from the cell pellet was performed as described in the manufacturer's manual. Isolated plasmids were control digested as described under 4 and resulting DNA fragments were analysed by agarose gel electrophoresis (2.8.1.2) to confirm successful integration of the DNA fragments.

2.8.1.9 Preparation of bacteria-glycerine stocks

For conservation of transformed *E. coli* containing the generated plasmids over night cultures were prepared as described under 8. 850 µl of the over night culture were mixed with 150 µl glycerine (99.5 %, Roth) in a cryovial and stored at - 80 °C.

2.8.1.10 Determination of DNA concentration by photometric measurement

In order to determine the DNA concentration of a plasmid preparation the DNA was typically diluted 1 : 100 in ddH₂O. The absorption of the DNA at 260 nm was measured in a photometer (Eppendorf) and DNA concentration was calculated according the following relation:

$$\Delta\text{OD}_{260} \times 50 \times \text{dilution factor} = \text{concentration dsDNA } [\mu\text{g/ml}]$$

The purity of the DNA preparation was shown by the ratio of OD₂₆₀/OD₂₈₀ and typically ranged from 1.8 to 2.0.

2.8.1.11 Ethanol precipitation of DNA

Digested DNA was ethanol precipitated prior to parasite transfection. For this purpose 2.5 volumes 100 % ethanol and 1/10 volume 3 M sodium acetate, pH 5.2, were added to the DNA solution and incubated at least 30 minutes at - 80 °C. After spinning for 15 minutes at 16,000 x g the DNA pellet was washed once with ice cold 70 % ethanol and again spun for 5 minutes

at 16,000 x g. The ethanol was carefully removed and the DNA pellet was air dried. Finally the DNA was resuspended in 1 x PBS to a final DNA concentration of 1 µg/µl. Digested and precipitated DNA was once more analysed by agarose gel electrophoresis and stored at - 20 °C until parasite transfection.

2.8.1.12 Site-directed mutagenesis of the *P. yoelii* circumsporozoite CD8⁺ T cell epitope

Specific point mutations were inserted by site-directed mutagenesis into the sequences of the targeting constructs pCSPΔepi_me01 - me04 and pCSPreplΔepi_me01 - me04. For this specific complementary oligonucleotides spanning the sequence coding for the *Py* CSP CD8⁺ T cell epitope were designed to insert the four different mutations me01 - me04 into the DNA sequence. The resulting mutant sequences are shown under 3.1.1, oligonucleotide sequences are attached under X. *Py* CSP fragments were amplified by PCR as described under 1 and temporarily cloned into the pGEM®-T Easy T/A cloning vector (Promega) as described under 2.8.3.4 for mutagenesis. 20 - 50 ng of these intermediate constructs were mixed with 10 - 50 pmol of the specific oligonucleotides, 0.2 mM dNTPs, 10 µl HF buffer (5 x, containing 7.5 mM MgCl₂; Finnzymes) and 1 Unit Phusion polymerase (Finnzymes) and filled up to 50 µl with ddH₂O. The amplification was performed in a thermal cycler starting with an initial denaturation at 95 °C for 30 seconds, followed by 19 cycles with a denaturation at 95 °C for 30 seconds, annealing of the specific oligonucleotides at 55 °C for 1 minute and a DNA double-strand extension at 68 °C for 4:30 minutes. Thus the complete plasmid is amplified and mutations are inserted. The DNA was purified with Qiaquick PCR purification Kit (3). Methylated plasmid DNA that served as template was subsequently digested with DpnI. To the purified DNA 20 Units DpnI (New England Biolabs) and 5 µl supplied NEBuffer 4 (10 x) were added, filled up with ddH₂O to 50 µl and incubated for 2 hours at 37 °C. The digest was either purified with Qiaquick PCR purification Kit again or the enzyme was heat-inactivated for 5 minutes at 80 °C. *E. coli* XL1 blue were transformed with this DpnI-digest as described under 7. Mutated *Py* CSP fragments were either amplified by standard PCR conditions (2.8.1.1) or cut from the pGEMT-easy constructs and gel extracted with Qiaquick gel extraction Kit (Qiagen) and subsequently cloned into the b3D targeting vector as described (2.8.1.2 - 11).

2.8.2 Stage specific RNA isolation and cDNA synthesis for RT and qRT PCR

Different parasite stages were isolated from infected mosquitos (2.10.2.4), *in-vitro* hepatocyte cultures (2.9.2) or infected blood (2.10.1.4.3).

2.8.2.1 Isolation of total RNA with RNeasy Mini Kit (Qiagen)

Parasite cells were disrupted by addition of in 350 µl RLT buffer (supplied, Qiagen) supplemented with 1 % β-mercaptoethanol (14.3 M) and homogenised by vortexing for 1 minute. Total RNA was isolated from the cell lysate according to the "Animal Cell Spin" protocol supplied in the manufacturer's manual. Isolated RNA was stored at - 80 °C.

2.8.2.2 Trizol extraction of total RNA

Parasites were resuspended in 1 ml Trizol Reagent (Invitrogen), 200 µl chloroform was added and carefully mixed by inverting. After 3 minutes incubation at room temperature it was mixed again and subsequently spun for 15 minutes at 12,000 x g at 4 °C. The top aqueous layer, containing the RNA, was carefully transferred to a fresh RNase-free tube (Eppendorf). After addition of 500 µl isopropanol (2-propanol) the solution was incubated for 10 minutes at room temperature and spun for 10 minutes at 12,000 x g at 4 °C. The supernatant was discarded and the RNA pellet was washed with 75 % ethanol and thoroughly mixed by vortexing. After a final centrifugation for 5 minutes at 7,500 x g at 4 °C the RNA pellet was air dried, resuspended in 10 µl DEPC-treated H₂O and incubated for 10 minutes at 60 °C. Isolated RNA was stored at - 80 °C.

2.8.2.3 DNase treatment of total RNA

After RNA isolation remaining DNA contaminations were removed by digestion with DNase. The RNA was mixed with 1/10 volume of 10 x TURBO DNase buffer (Ambion) and 1 µl TURBO DNase (Ambion) and incubated for 30 - 45 minutes at 37 °C. 1/10 volume of the resuspended DNase Inactivation Reagent (Ambion) was added, mixed thoroughly and incubated for 2 minutes at room temperature. The reaction was centrifuged for 1 minute at 10,000 x g and the supernatant containing the RNA was transferred to a fresh RNase-free tube (Eppendorf). DNase treated RNA was stored at - 80 °C.

2.8.2.4 First strand cDNA synthesis

RNA was transcribed into complementary DNA (cDNA) with the Fermentas "First Strand cDNA Synthesis Kit" according to the manufacturer's manual using random hexamer oligonucleotides. The initial optional denaturation step of the total RNA for 5 minutes at 65 °C was performed. For each transcribed RNA one approach without reverse transcriptase (- RT) was run to exclude DNA contaminations. The transcribed product was directly used for reverse transcriptase PCR (2.8.2.5) or quantitative Real-time PCR (2.8.2.6) or stored at - 20 °C.

2.8.2.5 Reverse transcriptase PCR (RT PCR)

A standard PCR approach was prepared as described under 2.8.1.1. In a reaction volume of 20 µl 0.5 - 2 µl first strand cDNA (2.8.2.4) of the different parasite stages were used as template together with *P. berghei* Ferlin and Ferlin-like protein specific oligonucleotides. For each sample one tube with cDNA synthesised with reverse transcriptase (+ RT) (2.8.2.4) and one - RT control tube were prepared. Oligonucleotides specific for the *P. berghei* aldolase, expressed constantly throughout the life cycle, were used as control. All specific oligonucleotides used for RT PCR are attached under X. The amplification was performed in a thermal cycler using the standard PCR program as described under 2.8.1.1.

2.8.2.6 Quantitative Real-time PCR (qRT PCR)

Quantitive real-time RT-PCRs were performed with total RNA isolated from 20 h *P. berghei* liver-stages from either wildtype (WT), radiation-attenuated (RAS) or genetically-attenuated (GAP) as described under 2.9.2. RNA was treated with DNase I (Ambion) to remove contaminating genomic DNA. 10 - 20 ng RNA for each parasite population (WT, RAS, GAP) was used as a template in a first-strand cDNA synthesis using the TaqMan Gold reverse transcriptase kit (Invitrogen). Gene-specific oligonucleotides (designed using Primer Express software v2.0, Invitrogen) are attached under 6.1.8. PCR fragments were cloned into the T/A-cloning TOPO vector (Invitrogen). Each plasmid was used 10-fold dilution to determine the standard curve. The standard curve hence plots the threshold value (C_t), defined as the cycle number at which the reporter dye fluorescent intensity increases over the background and over plasmid copy number. Absolute transcript copy number for each gene is calculated based on the external standard curve. The Real-time RT-PCR was carried out in triplicates in a GeneAmp® PCR System 9700 thermal cycler (Applied Biosystems) using the double-stranded DNA binding probe SYBR Green (Applied Biosystems). Reactions were run to one cycle of 10 min at 95°C and 45 cycles of 15 sec at 95°C, 1 min at 60°C.

2.8.3 Generation of subtraction libraries for Suppression Subtractive Hybridisation (SSH)

Suppression Subtractive Hybridisation (SSH) is a rather fast and inexpensive method to identify differentially expressed transcripts in two cDNA populations. This *in-vitro* method was used to look for upregulated transcripts in early liver-stages of radiation-attenuated (RAS) and genetically-attenuated parasites (GAP) in comparison to wildtype (WT) liver-stages.

2.8.3.1 RNA sample preparation

For the SSH screening total RNA was isolated from RAS, GAP and WT liver-stages after 20 hours development in cultivated hepatocytes (2.9.2). For this purpose salivary gland sporozoites from *uis3(-)* and WT *P. yoelii* 17XNL strain were isolated on day 14-17 post mosquito infection (2.10.2.3). *Uis3(-)* sporozoites are, like WT sporozoites, motile, invasive and transform into liver-stages inside hepatocytes but then *uis3(-)* liver-stages arrest after around 24 hours and do not develop to mature liver schizonts. These genetically-attenuated parasites (GAP) confer to a stage specific protection against subsequent WT sporozoite challenges. Liver-stage arrestment is also achieved by γ -irradiation of WT sporozoites with a dose of 150 Gray, resulting in so called radiation-attenuated sporozoites (RAS). 25,000 - 35,000 of these RAS, GAP and WT sporozoites were incubated for 90 minutes with 25,000 cultivated Huh7 hepatocytes on 8-well chamber slides (nunc). After invasion of the sporozoites, hepatocytes were cultivated in DMEM complete/anti-contamination cocktail for 20 hours. Liver-stages were harvested as described (2.9.2) and total RNA was isolated using the Qiagen RNeasy Mini Kit (2.8.2.1).

2.8.3.2 cDNA synthesis with SMART™ method

The SMART™ technology (Clontech) is a very sensitive method to synthesise high-quality cDNA from small amounts of total RNA. For the first strand cDNA synthesis 0.4 - 0.6 μ g total liver-stage RNA (2.8.3.1) were used. The transcription to cDNA was performed according to the manufacturer's manual using the "SMART cDNA synthesis protocol for Clontech PCR-Select™ cDNA subtraction" (sections VII. - IX.).

2.8.3.3 PCR-Select™ cDNA subtraction

The cDNA subtraction was performed using the "PCR-Select™ cDNA subtraction Kit" (Clontech). The RsaI digested and purified cDNA produced with the "SMART™ PCR cDNA Synthesis Kit" (Clontech) was directly used for adaptor ligation (Clontech manual section IV.F.). All following steps were performed according to the manufacturer's manual.

2.8.3.4 T/A cloning

Resulting sequences from the cDNA subtraction were directly cloned into the T/A cloning vector pGEM®-T Easy (Promega). The thymidine(T)-overhangs of the vector can be directly ligated with the adenine(A)-overhangs of the cDNA sequences. DNA sequences were purified prior to ligation with Qiaquick PCR purification Kit (Qiagen). 50 ng of the pGEM®-T Easy vector were ligated with 3 μ l of the cDNA sequence mix using 3 Units of the supplied

T4 ligase and 2 x Rapid Ligation Buffer (Promega). The reaction was incubated for 1 hour at room temperature and subsequently *E. coli* XL1 blue were transformed with the ligation mixture as described before. The growth on LB agar plates containing ampicillin (100 µg/ml), 20 µg/ml X-Gal (bromo-chloro-indolyl-galactopyranoside) and 0.1 mM IPTG (isopropyl-β-D-thiogalactopyranosid) allowed selection for blue (no insert) and white (insert integrated) colonies. White colonies were picked for sequencing and either plasmids were isolated using the Qiaprep Spin Miniprep Kit or colonies were directly transferred to 96 well plates and sent to GATC, Konstanz.

2.8.3.5 Sequencing

Sequencing was done at a DNA sequencing facility (Institute for Virology, University of Wuerzburg) by 25 cycle sequencing with the SP6 reverse and T7 forward oligonucleotides or by GATC, Konstanz, using the same oligonucleotides.

2.8.3.6 Bioinformatical analysis

Sequences were analysed by BLAST search in the PlasmoDB database (<http://plasmodb.org>) using the blastn algorithm. Transcripts were entered as target data type to search all available target organisms. The expectation value was set at 10, maximum alignments (B) and maximum descriptions (V) were set at 50. The low complexity filter was used. Resulting coding sequences were searched using the BLAST server on the Wellcome Trust Sanger Institute homepage (www.sanger.ac.uk) to obtain full sequence information in its genomic context.

Predicted protein domains were identified with the Simple Modular Architecture Research Tool (SMART) (smart.embl-heidelberg.de).

Epitope prediction was done with help of the SYFPEITHI homepage (www.syfpeithi.de) and personal communication with T cell experts.

2.9 Cell culture

2.9.1 Cultivation of human hepatoma cells Huh7

Frozen cell stocks of the human hepatoma cell line Huh7 were kept in 80 % FCS, 20% DMSO in liquid nitrogen. Thawed cells were immediately transferred into pre-warmed DMEM culture medium containing 10 % FCS and 1 % Penicillin/Streptomycin (DMEM complete) and centrifuged for 5 minutes at 200 x g. The cell pellet was resuspended in fresh DMEM complete and transferred into a cell culture flask (25 cm² or 75 cm²). Cells were

incubated at 37 °C, 5 % CO₂ until a confluent monolayer was reached. For further cultivation medium was removed, attached cells were washed once with HBSS and detached with 0.25 % Trypsin/EDTA (Gibco) for 3 - 5 minutes at 37 °C. After addition of 10 ml DMEM complete cells were transferred to a 15 ml tube and centrifuged for 5 minutes at 200 x g. The cell pellet was washed once with HBSS and finally resuspended in 10 ml DMEM complete. Depending on the approach an aliquot of 200 µl up to 2 ml of the cell suspension were transferred to a new culture flask and filled up to 15 ml with DMEM complete.

2.9.2 *In vitro* liver-stage development

Huh7 cells cultivated to a confluent monolayer were detached with 0.25 % Trypsin/EDTA and washed as described (2.9.1). The cell pellet was resuspended in DMEM complete and counted diluted in Trypan blue (0.4 %) using a haemocytometer. Either 25,000 cells per well on a 8 well chamber slide (nunc) or 200,000 cells per well on a 6 well plate (greiner) were seeded and cultivated over night. Mature salivary gland sporozoites were purified (2.10.2.3) and 25,000 - 35,000 sporozoites or 100,000 - 200,000 sporozoites were added on the cultivated cells on the 8 well chamber slide or 6 well plate, respectively. Sporozoites were allowed to invade for at least 90 minutes, afterwards the sporozoite suspension was removed and cells were incubated in DMEM complete plus anti-contamination cocktail. Liver-stage development was stopped after different time points by harvesting the cells with 0.25 % Trypsin/EDTA as described before (2.9.1). Cells were transferred into a 1.5 ml tube and spun for 2 minutes at 4500 x g. The cell pellet was resuspended in 0.05 % digitonin in PBS and incubated for 5 minutes at room temperature. This digitonin treatment selectively permeabilised the host hepatocyte and thereby reduces RNA and DNA contaminations from the host cell in the final parasite preparation. The liver-stage parasites were centrifuged for 2 minutes at 16,000 x g and depending on the application resuspended in RLT buffer, Trizol or PBS.

2.9.3 Isolation and cultivation of bone marrow dendritic cells (BMDCs)

Dendritic cells were isolated from the bone marrow of naïve C57BL/6 mice. The femur was removed from sacrificed mice and muscles were carefully removed from the bone. The ethanol washed femur was opened sterile with a scalpel at both ends and the bone marrow was flushed using a 27 G needle and a 1 ml syringe with PBS into a petri dish. Bone marrow cells were washed with IMDM culture medium by centrifugation for 5 minutes at 400 x g and dendritic cells were cultivated in IMDM medium supplemented with 30 % GM-CSF in petri dishes (greiner). BMDCs were split once on day 4 - 5, for this non-adherent cells in the

supernatant were collected in 50 ml tubes. Adherent cells were detached with 2 mM EDTA in PBS and added to the supernatant. Cells were spun for 5 minutes at 400 x g and resuspended in fresh IMDM/30 % GM-CSF. The BMDCs were used for cultivation with lymphocytes on day 7 after isolation.

2.10 Parasitological methods

2.10.1 *Plasmodium* methods

2.10.1.1 Determination of parasitemia in giemsa stained blood smears

A small drop of blood was obtained from the tail of the infected mouse and a thin blood film was prepared on a glass slide. The blood smear was air dried and fixed for 10 seconds with methanol. The fixed blood smear was stained with giemsa, diluted 1 : 10 in deionised water, for 15 minutes. The stained blood smear was washed with water and parasites were examined under the light microscope using the 100 x objective with oil immersion.

In order to determine the parasitemia the number of all erythrocytes and the infected erythrocytes were counted in one field. Subsequently the asexual parasites were counted in typically 24 further fields. The parasitemia was calculated using the following formula:

$$\frac{\text{number of parasites in all fields}}{\text{number of erythrocytes in 1 field} \times \text{number of counted fields}} \times 100 = \text{parasitemia [%]}$$

2.10.1.2 Examination of exflagellating gametocytes

The raptures of male gametocytes from the erythrocytes is called exflagellation, this can be observed under the microscope. A high number of exflagellating parasites is important for successful transmission to the mosquito and was hence examined routinely before parasite transmission (2.10.2.2). For this a drop of tail blood was placed on a glass slide and carefully covered with a cover slip. The slide was incubated for 10 minutes at room temperature. Erupting parasites were examined under the light microscope using the 40 x objective lenses with phase contrast (Ph2). For good transmission at least 3 to 5 exflagellation centres should be observed per field.

2.10.1.3 Cryopreservation of *Plasmodium* parasites

Plasmodium parasites were conserved during blood stage development, because infected blood can be stored for long periods in liquid nitrogen. For this purpose 100 µl freshly withdrawn blood was mixed with 200 µl parasite freezing solution (10 % glycerine in

Alsever's solution) in a cryo vial and immediately frozen in liquid nitrogen. Thawed parasite stocks can be reinjected into mice to continue the parasite growth.

2.10.1.4 Parasite transfection

The rodent *Plasmodium* parasites, *P. berghei* and *P. yoelii*, are transfected with linearised DNA (2.8.1.4) using the AMAXA transfection system (Lonza). By a crossing-over event between homolog regions the targeting constructs insert into the targeted genomic loci.

2.10.1.4.1 Overnight culture and merozoite purification

For one transfection typically 2 - 3 NMRI mice with a high level parasitemia (3 - 5 % for *P. berghei* ANKA or up to 10 % for *P. yoelii* NL) were used. Mice were sacrificed and blood was collected by heart puncture (2.11.3). The blood was combined in a 50 ml tube with 10 ml T-medium containing 250 µl Heparin (200 p.i. in PBS) and centrifuged for 8 minutes at 400 x g without brake. The medium was removed and the blood pellet was resuspended in 20 ml fresh T-medium. The blood suspension was carefully dropped by gravity into a conical flask containing already 100 ml pre-warmed T-medium. The 50 ml tube was washed with 30 ml fresh T-medium and this was also dropped carefully into the flask without swirling the blood. The parasites were cultivated at 37 °C, 10 % O₂, 5 % CO₂ and 85 % N₂, shaking at 70 rpm. To enrich schizonts in the blood culture the incubation took 16 to 18 hours for *P. berghei* and 12 to 14 hours for *P. yoelii*. Mature schizonts were purified by a NycoDenz density gradient centrifugation. The NycoDenz stock solution was diluted to 55 % or 60 % working solutions in PBS for *P. berghei* or *P. yoelii* purification, respectively. The over night parasite culture was transferred into four 50 ml tubes (approximately 35 ml per tube) and each tube was under-laid with 10 ml NycoDenz solution pre-warmed to room temperature. Tubes were exactly balanced and centrifuged for 25 minutes at 200 x g at room temperature without brake. The mature schizonts appeared as a brown ring at the interface and were carefully collected to two new 50 ml tubes. Tubes were filled up to approximately 40 ml with T-medium (from top of the gradient) and centrifuged for 8 minutes at 400 x g. The schizont pellet was resuspended in fresh T-medium, the volume depended on the size of the pellet and the number of constructs the parasites should be transfected with. For one transfection 1 ml resuspended schizonts were transferred in a 1.5 ml microcentrifuge tube and spun for 15 seconds.

2.10.1.4.2 AMAXA transfection and selection for transformants

For each transfection, 100 µL of AMAXA human T cell nucleofector solution (Lonza) was added to 5 - 10 µg of digested and precipitated plasmid DNA (2.8.1.11). The DNA solution was then added to the schizont pellet (1.3.1), mixed well, transferred to the AMAXA cuvette and pulsed once using the U-033 pre-programmed setting on the AMAXA machine. After pulsing 50 µl fresh T-medium was directly added into the cuvette and transfected parasites were immediately injected *i.v.* in naïve NMRI mice. Typically 2 mice per construct were used. 24 hours post-infection a giemsa stained blood smear was prepared to record the starting parasitemia and pyrimethamine treatment of the mice was started. For this the pyrimethamine stock solution was diluted 1 : 100 in tap water (final concentration 70 µg/ml) and provided as drinking water. Parasitemia typically decreased to undetectable levels on day 2 post infection and first resistant parasites appeared in giemsa stained blood smears from day 7. When parasitemia reached at least 0.5 % mice were sacrificed and blood was withdrawn by heart puncture. Blood was transferred to new mice, cryopreserved and parasite gDNA was isolated (parental population). The transfer animals were further treated with pyrimethamine and mice were sacrificed as soon as parasitemia reached sufficient levels. The infected blood was again cryopreserved and purified for parasite DNA isolation (transfer population).

2.10.1.4.3 Isolation of blood stage parasites for genomic DNA purification

To isolate parasites from infected blood a column was made using a 5 ml syringe. The syringe was closed with cotton wool at the bottom. Thereon a 2 - 3 cm thick layer of cellulose powder CF11 (Whatman) was put and the column was completed with around 1 cm glass beads (diameter 212 - 300 µm, unwashed; Sigma). The column was equilibrated with 2 column volumes 1 x PBS and subsequently the infected blood was transferred on the column. The erythrocytes were washed off the column with 1 x PBS. Starting from the first red drop 15 ml erythrocyte suspension were collected in a respective tube. The suspension was centrifuged for 8 minutes at 400 x g, without brake, and the supernatant was carefully removed. The erythrocyte pellet was resuspended in 10 - 15 ml 0.2 % saponin in PBS to lyse the red blood cells. The suspension was again centrifuged for 8 minutes at 1500 x g and the supernatant was discarded. The parasite pellet was resuspended in 1 ml PBS and transferred to a 1.5 ml microcentrifuge tube. The isolated parasites were once more centrifuged for 2 minutes at 4500 x g and finally resuspended in 200 µl PBS. The parasite genomic DNA (gDNA) was subsequently isolated using the QIAamp Blood Mini Kit with the "Blood or Body Fluid Spin Protocol". For this 20 µl Qiagen protease and 200 µl buffer AL were added to 200 µl parasites

in PBS and thoroughly mixed by vortexing. All following steps were performed according to the manufacturer's instructions. The parasite gDNA was finally eluted in 100 - 150 µl elution buffer AE (10 mM TRIS/HCl; 0.5 mM EDTA; pH 9.0) and stored at - 20 °C.

2.10.1.4.4 Genotyping PCR of transfected parasites

The isolated gDNA of parental and transfer transfectants was tested for integration of the targeting constructs by PCR. Templates for this genotyping PCR were typically 1 - 2 µl parasite gDNA of the transfectants or wildtype (WT) parasites as control. As additional control the targeting constructs were diluted 1 : 100 in ddH₂O and also used as template for the PCR. Usually three different oligonucleotide pairs were used for genotyping PCR. The integration test oligonucleotides (test) typically bind inside the selectable marker inserted and the parasite's genome. Resulting fragments therefore verify successful integration of the targeting construct inside the targeted genomic locus. Control oligonucleotide pairs are usually WT or open-reading frame (ORF) specific oligonucleotides and vector specific oligonucleotides (epi). The PCR approach was prepared as described under 2.8.1.1 using the standard PCR program (2.8.1.1). Resulting DNA fragments were analysed by agarose gel electrophoresis (2.8.1.2).

2.10.1.5 Parasite cloning

Successfully transfected parasite populations were selected for clonal parasites by limited dilution. For this a frozen blood stock of the parental or transfer population was injected *i.p.* into a naïve NMRI mouse. Once the parasitemia ideally reached 0.3 - 0.5 % the mouse was sacrificed and blood was withdrawn by heart puncture. Parasitemia was determined very exactly by counting at least 80 fields (2.10.1.1). Assuming on average 7×10^6 erythrocytes per µl mouse blood the number of parasites was determined using the following formula:

$$7 \times 10^6 \times \text{parasitemia [\%]} \times 10^{-2} = \text{parasites}/\mu\text{l}$$

A dilution series was prepared in RPMI medium to inject theoretically one parasite per mouse. For this 100 µl blood was diluted 1 : 10 in RPMI, this dilution was again diluted 1 : 10 in RPMI and so on. Typically the 1 : 10^6 dilution contained less than one parasite per µl. The calculated amount of this dilution that theoretically held one parasite was mixed with fresh RPMI medium and 10 to 15 naïve NMRI mice were injected *i.v.* each with 100 µl medium containing one parasite. Mice usually became blood stage positive from day 7 post infection and as soon as sufficient levels of blood stage parasites were reached mice were sacrificed and blood was collected. Not all injected mice developed a blood stage parasitemia, typically mice were declared negative if there were no parasites visible in a giemsa-stained blood smear

up to 21 days post infection. Clonal parasites were isolated from infected blood as described (2.10.1.4.3) and gDNA was tested for integration of the respective targeting construct by PCR (2.8.1.1).

2.10.2 *Anopheles* mosquito methods

2.10.2.1 Mosquito breeding

Anopheles stephensi mosquitoes were bred at 28 °C, 75% humidity under a 12-h light/12-h dark cycle. Larvae were raised in 1 ‰ sea salt ddH₂O, pupae were collected and allowed to hatch in mosquito cages (BioQuip Products Inc; USA). Adult mosquitoes were fed on a 10% sucrose/PABA solution provided on cotton wool pads. In order to maintain the mosquito life cycle, female *Anopheles* mosquitoes were blood fed on naïve anaesthetized NMRI mice. Four days after the blood meal dishes with 1 ‰ sea salt ddH₂O soaked filter paper were put into the cages and female mosquitoes laid their eggs. Eggs were washed with 70 % ethanol and twice with 1 ‰ sea salt ddH₂O and again put in trays filled with 1 ‰ sea salt ddH₂O. Hatched larvae were fed on cat food (Brekkies) and split depending on the density.

2.10.2.2 Parasite transmission

For transmission of *P. berghei* or *P. yoelii* parasites 4-5 day old female mosquitoes were blood fed on anaesthetized NMRI mice that had been infected *i.p.* with parasite blood stocks. Mice were assayed for high levels of parasitemia (2.10.1.1) and the percentage of exflagellating male gametocytes was observed under the microscope (2.10.1.2). After the infective blood meal, mosquitoes were maintained at 21 °C, 80 % humidity (*P. berghei*) or 24 °C, 80% humidity (*P. yoelii*). On day 10 post feeding, mosquitoes were dissected in RPMI 1640 medium/ 3 % BSA (X), and isolated midguts were examined for the infection rate. From day 17 post infection mature *P. berghei* and already from day 14 post infection *P. yoelii* sporozoites could be isolated from the salivary glands (2.10.2.4). In order to maintain a continuous *Plasmodium* cycle naïve rodents could be exposed to bites of infected mosquitoes from day 17 or day 14 post feeding, respectively.

2.10.2.3 Mosquito dissection

Midguts of infected mosquitoes were dissected 10 days after the blood meal in order to observe oocyst formation, 12 -14 days post feeding midgut sporozoites were isolated from midgut oocysts. And 17 - 21 days post feeding for *P. bergehi* or 14- 16 days post feeding for *P. yoelii*, salivary glands were isolated and infectious sporozoites were extracted (2.10.2.4). For all dissections infected mosquitoes were anaesthetised on ice. The dissection was

performed in RPMI 1640 medium with 3 % BSA under a stereo microscope in the insectary at 15 °C using two needles (27 G and 23 G). Midguts and salivary glands were kept in RPMI 1640 medium with 3 % BSA on ice until sporozoite extraction.

2.10.2.4 Sporozoite extraction from midguts and salivary glands

Mosquito midguts or salivary glands were disrupted mechanically in RPMI 1640 medium with 3 % BSA using a pestle and spun for 3 minutes at 90 x g, 4 °C. The supernatant containing the sporozoites was transferred to a fresh tube and the pellet was again squeezed with a pestle in fresh RPMI/3 % BSA. A second centrifugation was performed for 3 minutes at 100 x g, 4 °C and the supernatant was combined with the first collected. Extracted sporozoites were subsequently count under the microscope in a haemocytometer using the 40 x objective lenses with phase contrast (Ph2). For counting the sporozoite solution was typically diluted 1/10 in RPMI/3 % BSA. The number of sporozoites was calculated with the following formula:

$$\text{number of spz in 4 large squares}/4 \times \text{dilution factor} \times 10^4 = \text{number of spz/ml}$$

The quantity of a mosquito infection was typically expressed as number of sporozoites per mosquito.

2.11 Animal experimental methods

Mice were purchased from Charles River Laboratories, Germany with a age of 18 - 20 days and animal care was done in a central facility of the University of Heidelberg (Interfakultäre Biomedizinische Forschungseinrichtung; IBF). All animal experiments were conducted according to the European regulations and approved by the state authorities (Regierungspräsidium Karlsruhe).

2.11.1 Administration of anaesthesia

Mice were anaesthetised with Ketamine/Xylazine (K/X) administered into the abdominal cavity (intraperitoneal; *i.p.*).

2.11.2 Infection of rodents with *Plasmodium* parasites

In order to transmit *Plasmodium* parasites to the rodent host the mice were either anaesthetised and exposed to bites of infected mosquitoes (2.10.2.2) or isolated salivary gland sporozoites were injected in various numbers (1,000 - 50,000 spz) into the tail veins (*i.v.*).

Furthermore blood stages injected either *i.v.* or *i.p.* established a *Plasmodium* infection, isolated schizonts, fresh isolated infected blood or frozen blood stocks were used.

2.11.3 Blood withdrawal by heart puncture

Mice were terminally anaesthetised with diethyl ether and the heart was uncovered preferably fast. Blood was withdrawn using a heparinised needle (23 G) and a 2 ml or 5 ml syringe from the right ventricle. Infected blood was immediately put on ice and processed as fast as possible. Typically 1 - 1.5 ml blood could be obtained from one mouse.

2.11.4 Liver perfusion

Livers were perfused with 0.05 % collagenase (Typ I-A; Sigma) in PBS prior to isolation of liver associated lymphocytes. Mice were either terminally anaesthetised with diethyl ether or sacrificed with CO₂ and the abdominal cavity was opened. The liver was perfused through the liver portal vein using a 25 G needle. The collagenase solution was pumped through the organ using a peristaltic pump (approximate speed 1 ml/min). Livers were perfused until the colour changed from dark red to grey beige, removed and stored on ice in PBS.

2.12 Immunological methods

2.12.1 Immunisation and parasite challenge experiments

P. berghei NK65 WT and *uis3*(-) sporozoites were isolated from salivary glands of infected mosquitoes (2.10.2.4). *Pb* NK65 WT sporozoites were γ -irradiated with a dose of 150 Gray resulting in radiation-attenuated sporozoites (RAS). Groups of 10 C57BL/6 mice were immunised with a single dose of 25,000 or 50,000 *Pb* RAS or *Pb uis3*(-) sporozoites followed by two booster dose of 20,000 or 10,000 *Pb* RAS or *Pb uis3*(-) sporozoites administered by *i.v.* injection into the tail vein. The first boost was given 7-14 days after the priming dose and a second boost 7-14 days thereafter. All animals remained blood stage negative after the immunisation as monitored by giemsa stained blood smears on days 4-7 after the sporozoite injections. Five mice per group were exposed to a challenge with 10,000 *Pb* NK65 WT parasites, injected *i.v.* into the tail vein on days 7-8 after the last boost. As a control three naïve mice were injected to verify infectivity of the sporozoite challenge. Parasitemia was monitored by giemsa stained blood smears. Naïve mice reached a parasitemia between 0.3 and 0.5 % on day 6 after challenge whereas all immunised mice remained blood stage negative. Seven days after the last boost or the WT challenge, respectively, mice were sacrificed and spleens, livers and blood serum were removed.

Besides the immunisation with RAS and GAP also an immunisation with *PbC2CP*-derived peptide T9L was performed. For this the peptide was packed in cell-specific nanocarriers called TargoSpheres® by the Rodos BioTarget GmbH (RBT). These nanocarriers provide a new adjuvant system to deliver drugs or vaccines directly to antigen-presenting cells (APCs). The packing was performed by the company. As control nanocarriers containing a FITC:Dextran solution were also provided by the RBT company. The final FITC:Dextran concentration in the targosphere solution was 172.8 µg/ml, whereas the final peptide concentration in the RBT06.01 targosphere solution was 21.277 µg/ml. Groups of three C57BL/6 mice were immunised with the targospheres (TS) using a similar prime-two-boost protocol as described before. Four groups received 1 µg or 5 µg RBT06.01 TS or FITC:Dextran TS, respectively, a fifth group remained untreated. The solutions were injected subcutaneously on day 0, day 7 and day 14. Each of the 15 animals was exposed to bites of 5 *P. berghei* NK65 infected mosquitoes 7 days after the last boost. The parasitemia was followed by daily blood smears from day 3 post infection. On day 8 post infection mice were sacrificed and organs were prepared and cultivated for cytokine ELISpot.

2.12.2 Cell isolation and purification from spleens, livers and lymph nodes

Seven days after the last immunisation boost or the WT challenge animals were sacrificed and livers were perfused with PBS including 0.05 % collagenase (2.11.4). Spleens, perfused livers and where required lymph nodes were removed and cells were isolated. Total spleen cells were obtained by passing the organs through a 70 µm nylon cell strainer (BD Biosciences) or a fine metal strainer in MACS buffer (1x PBS, 1 % FCS, 2mM EDTA) and subsequently washed with culture medium (RPMI, 10 % FCS, Pen/Strep, glutamine, β-mercaptoethanol). Lymph nodes were passed through a 70 µm nylon cell strainer in RPMI culture medium. Cells were counted in 0.4 % trypan blue in a haemocytometer. For counting total splenocytes 4% acetic acid was added to the trypan blue solution. Perfused livers were passed through a metall strainer (250 µm) and washed with culture medium. Liver lymphocytes were separated using a Percoll density gradient (stock 1.124 g/ml). The 100 % working solution was prepared by mixing 9 parts Percoll with 1 part 10 x PBS. The working solution was then diluted with 1 x PBS to 40 % and 80 %. The liver cell suspension in 4 ml 40 % Percoll was under laid with 3 ml 80 % Percoll and spun for 20 minutes, 700 x g at room temperature. The middle white layer containing the lymphocytes was carefully removed, washed with culture medium and cells were counted in a haemocytometer. Age-matched naïve and naïve/challenged mice served as controls and were treated equally.

2.12.3 *In vivo* cytotoxicity assay

Total spleen cell were isolated from naïve donors as described before and finally resuspended in 20 ml PBS. To 10 ml of this cell suspension 2 µM peptides were added and incubated for 20 minutes at 37 °C. The remaining cells were incubated without peptides. Subsequently cells were labelled with the fluorescent dye CFSE (5-(and-6)-carboxyfluorescein diacetate, succinimidyl ester, Invitrogen) in PBS. For this 10 ml 2 µM CFSE solution (CFSE^{high}) or 10 ml 0.2 µM CFSE (CFSE^{low}) were added to the cells loaded with peptides or incubated without, respectively, for further 20 minutes at 37 °C. This results in final CFSE concentrations of 1 µM and 0.1 µM. Cells were centrifuged for 7 minutes at 400 x g and washed twice with ice cold PBS. Cells were counted in Trypan blue (0.4 %) using a haemocytometer. The two cell populations were mixed in equal numbers (1 : 1) and 1 x 10⁷ cells of this mixed population were injected *i.v.* into tail veins of immunised or naïve control animals 18 hours prior cell isolation from the organs. Cell purification from spleens and livers was performed as described earlier. CFSE labelled cells were detected by Flow Cytometry. The specific lysis was calculated as ratio of CFSE^{high} cells and CFSE^{low} cells and compared to the ratio detected in naïve animals with the following formula:

$$100 - \left(\frac{\text{ratio sample}}{\text{mean ratio naive controls}} \right) \times 100 = \text{specific lysis [%]}$$

2.12.4 Restimulation of lymphocytes from immunised animals *in vitro*

1 x 10⁶ total spleen cells, 1 x 10⁵ liver lymphocytes or 1 x 10⁵ lymph node lymphocytes from immunised animals or naïve controls were cultivated with 1 x 10⁵ BMDCs per well in 96-well plates. Lymphocytes of immunised and naïve animals were restimulated by adding the specific peptides to a final concentration of 1 µM per well. As a control lymphocytes were either unspecifically restimulated with αCD3 (5 µg/ml) or Concanavalin A (1 µg/ml) or cultivated in lymphocyte culture medium without stimulus.

2.12.5 Flow cytometry

Lymphocytes of immunised or naïve control animals were cultivated and restimulated over night as described. Cell culture supernatant was removed and fresh peptide (1 µM final concentration) and Brefeldin A (10 µg/ml) were added to each well. After 5 hours incubation the cell surface was stained in a 96-well plate for 15 minutes in the dark on ice using the anti CD8a-PacBlue conjugated antibody (1:100, BD biosciences), anti CD44-FITC (1:100, BD biosciences), anti CD62L-PE (1:200, BD biosciences) and anti CD25-Alexa647 (1:50, BD biosciences) or for subsequent intracellular staining the antiCD8-PE antibody (1:300, BD

biosciences) diluted in FACS buffer. Cells were washed once with 400 µl FACS buffer per well and centrifuged for 5 minutes at 400 x g. For intracellular staining cells were fixed with 4% PFA in PBS for 7 minutes on ice and after washing once permeabilised with saponin buffer for 20 minutes at room temperature. Fixed cells were centrifuged for 5 minutes at 550 x g and washed again with FACS buffer. The intracellular staining for IFN- γ (IFN γ -APC antibody, 1:100, BD biosciences) was performed in saponin buffer for 20 minutes in the dark at room temperature. Cells were washed once with saponin buffer and subsequently twice with MACS buffer. Flow cytometry was performed in MACS buffer and analysis using FACSCanto and FACSCalibur.

2.12.6 Cytokine ELISpot

MultiScreen Filter plates (Millipore) were coated with purified IFN- γ antibody (5 or 10 µg/ml in PBS) over night at 4 °C. Plates were washed at least 4 times with PBS and subsequently blocked with medium containing 10 % FCS for 1 hour at 37 °C. Cultured lymphocytes were restimulated over night as described. Cell culture supernatant was diluted 1:1 with fresh medium and cells were transferred onto the Filter plates. After 24 hours incubation at 37 °C, 5 % CO₂, plates were washed at least 4 times with PBS to remove the cells. After incubation with the secondary biotinylated IFN- γ antibody (5 or 10 µg/ml in PBS) for 1 hour at 37 °C Streptavidin-ALP (1:1000 in PBS, Mabtech) was added and plates were incubated for another hour at room temperature in the dark. Plates were washed at least 4 times with PBS/0.05 % Tween 20 and subsequently twice with PBS. The detection of the Elispot signal was performed using the AP Conjugate Substrate Kit (Biorad). The 25 x buffer was diluted to 1 x in filtered ddH₂O and reagents A and B were added as stated by the manufacturer. Spots on the plate were developed shaking for 10 to 30 minutes at room temperature after addition of 50 µl developing solution per well. The reaction was stopped by washing the plates for 10 minutes under running deionised water. Plates were dried over night at room temperature and spot were counted by eye using a stereo microscope.

2.13 Biochemical methods

2.13.1 Recombinant overexpression of the *P. berghei* ferlin-like protein as His-tag fusionprotein

The recombinant overexpression of the *Pb* C2 domain containing protein (C2CP) as a His-tag fusionprotein was performed using the pET15-b expression vector (Novagen) in *E. coli* BL21-CodonPlus (DE3)-RIPL cells (Stratagene). For easier expression the large *Pb* C2CP was divided in three parts. These parts were defined by hydrophobic sections for better soluble expression and sequence positions suitable for oligonucleotides for successful cloning. Cloning of the expression vector was performed as described for the targeting constructs under 2.8.1 using the restriction sites NotI and XhoI on the vector. The inserted fragment was subsequently expressed under control of the T7 promotor with an N-terminal 6x Histidin-tag (His-tag). *E. coli* BL21-CodonPlus (DE3)-RIPL competent cells (Stratagene) were transformed with the expression constructs according to the manufacturer's manual. A single colony was picked for inoculating an over night culture in 3 - 5 ml LB medium supplemented with ampicillin (100 µg/ml) and chloramphenicol (50 µg/ml). The next day the culture was diluted to an OD₆₀₀ of 0.1 to 0.2 in 25 - 100 ml LB medium with ampicillin (100 µg/ml) only and cultivated shaking at 37 °C until it reached an OD₆₀₀ of 0.5. The expression was induced by the addition of 1 mM IPTG (Sigma) and the protein was expressed for 4 hours at 37 °C, 250 rpm. The culture was subsequently centrifuged for 10 minutes at 3000 x g and the cell pellet was resuspended in 10 ml lysis buffer. The bacteria suspension was incubated for 30 minutes on ice and cells were cracked by sonication for 2 x 30 seconds on ice using the Sonifier® B-12 (Branson Sonic Power Company) at an amplitude of 50 %. The cell debris was centrifuged for 10 minutes at 3000 x g, 4 °C and the soluble proteins in the supernatant was transferred to a new tube. The cell debris pellet was resuspended in 8 M urea. Pellet and supernatant were loaded on a SDS-PAGE as described in the following section.

2.13.2 SDS polyacrylamide gel electrophoresis (SDS-PAGE)

Proteins were separated according to their size by SDS polyacrylamide gel electrophoresis. For one gel with a size of 10 cm x 10 cm x 0.5 mm the following components were mixed in the indicated order:

Separating gel (12 %): 3 ml Acrylamide/Bis Solution, 29:1
 1.875 ml 1.5 M Tris/HCl, pH 8.8
 75 µl 10 % SDS

2.5 ml ddH₂O
75 µl 10 % APS
7.5 µl TEMED

Loading gel (3.6 %): 350 µl Acrylamide/Bis Solution, 29:1
 350 µl 1 M Tris/HCl, pH 6.8
 30 µl 10 % SDS
 1.75 ml ddH₂O
 20 µl 10 % APS
 20 µl TEMED

The addition of ammonium persulphate (APS) and TEMED starts the polymerisation. The anionic detergent SDS denatures the protein and applies a negative charge therefore by SDS-PAGE proteins run towards the anode. First the separating gel was poured between the two glass plates fixed in the gel caster (Amersham). The gel was overlaid with a thin layer of isopropanol and allowed to polymerise. The isopropanol was removed, the loading gel was poured on top of the separating gel and a comb was placed in order to create the wells. As soon as the loading gel is polymerised as well the comb can be removed and the gel is ready for electrophoresis. Protein samples (supernatant and pellet in 8 M urea) were mixed 1 : 1 with 2 x SDS loading dye and heated to 95 °C for 5 minutes prior to loading on the gel. Alongside 15 - 30 µl of the samples 10 µl PageRuler™ Prestained Protein Ladder (Fermentas) was loaded on the gel. The gel was fixed in the electrophoresis chamber (Amersham) and surrounded with running buffer. Electrophoresis was performed for 1 hour at 80 V, 25 mA and subsequently for further 1 - 2 hours at 100 V. The gel was then either stained with Coomassie brilliant blue to visualise the proteins or proteins were transferred to a nitrocellulose membrane and detected with specific antibodies.

2.13.3 Coomassie staining of SDS polyacrylamide gels

Proteins separated by SDS PAGE were stained with Coomassie brilliant blue R-250. The gel was incubated for 30 minutes in Coomassie staining solution and not bound stain was washed off by incubation of the gel in a destaining solution. The destaining solution was exchanged regularly until protein bands were nicely visible on the gel.

2.13.4 Western Blot analysis

For specific detection of the His-tagged fusionprotein separated proteins were transferred from the SDS gel to a nitrocellulose membrane. For this 4 x Whatman paper and 1 x nitrocellulose membrane were cut in gel size and wet together with 4 blotting sponges in 1 x transfer buffer. The Western blot sandwich was built starting with 2 blotting sponges on the cathode side of the blotting cassette (Amersham), followed by 2 x Whatman paper, the SDS gel, the nitrocellulose membrane, 2 x Whatman paper and finally 2 more blotting sponges. The cassette was closed with the anode plate and protein transfer occurred for 1 - 1.5 hours at 125 mA, approximately 20 V in 1 x transfer buffer. The membrane was subsequently blocked over night at 4 °C with 5 % milk in TBST and washed three times for 10 minutes with 1 x TBST at room temperature. The incubation with the primary mouse anti-His antibody (1 : 3000 in TBST; Novagen) was carried out for 1 hour at room temperature or again over night at 4 °C under continuous shaking. The membrane was again washed three times for 10 minutes with TBST and the secondary HRP conjugated goat anti-mouse antibody (1 : 10,000 in TBST; Sigma) was added for 1 hour at room temperature, shaking. Washing was repeated as before. The chemiluminescent detection of the labelled His-tagged protein was performed with the "ECL Western Blotting Detection Reagents" (GE Healthcare). For this the substrate solutions 1 and 2 were mixed 1 : 1 and incubated on the membrane for 1 minute. The membrane was subsequently transferred in a film cassette, a film (Kodak) was incubated in the dark for 10 seconds up to 10 minutes on the membrane and the light signal on the film was developed (Hyperprocessor Amersham Pharmacia Biotech, Freiburg).

2.13.5 Purification of His-tag fusionproteins by nickel-ion affinity chromatography

Soluble expressed His-tag fusionprotein was purified using the HIS-Select® Nickel Affinity Gel (Sigma). A column was built using a 10 ml syringe and 2 ml resuspended nickel affinity gel (in 30 % ethanol). As the gel is a 50 % suspension this results in a column of a final volume of 1 ml. The syringe was closed at the bottom with glass wool and the gel matrix was allowed to settle. The 30 % ethanol was discarded and the column was equilibrated with 10 volumes equilibration buffer (5 x 2 ml). Before loading the bacteria lysate (2.13.1) containing the His-tag fusionprotein on the column it was filtered through a 0.22 µm filter and a small aliquot was kept for following gel electrophoresis. The lysate was passed on the column and the flow-through was collected. The His-tag fusionprotein should now be bound to the column. The column was washed with 2 x 2 ml washing buffer (= equilibration buffer) and the bound protein was eluted with 5 x 1 ml elution buffer. The eluate was collected in 6

fractions at 1 ml. Aliquots of all steps were loaded on a SDS gel (2.13.2). The eluate fractions containing the purified His-tag fusionprotein were pooled and dialysed against 1 x PBS to get rid of the imidazol. For this the protein solution was pipetted into a semi permeable dialysis tube membrane with a exclusion size of 10 kDa and the tube was closed. The dialysis was performed for at least 6 hours in 2 l 1 x PBS stirring at 4 °C, the PBS was exchanged once. Dialysed protein solution in 1 x PBS was stored at 4 °C.

3. Results

3.1 *P. yoelii* circumsporozoite (CSP) epitope mutant - an elegant tool to study the role of CSP in pre-erythrocytic immunity

The circumsporozoite protein (CSP) is covering almost the entire surface of the *Plasmodium* sporozoites and has historically been considered as the major pre-erythrocytic vaccine candidate. Recently, more and more studies revealed, however, that protection could also be achieved in the absence of immune responses specific to CSP (Kumar et al. 2006) (Gruner et al. 2007). To study pre-erythrocytic immune responses independent of CSP special tools have to be designed as *csp* depletion by targeted gene disruption results in no sporozoite formation and consequently no liver-stages (Menard et al. 1997).

The goal of this work was therefore to generate a *P. yoelii* mutant parasite line that expresses a functional CSP that is no longer recognised by the host's immune system. This should be achieved by the insertion of specific point mutations into the described CD8⁺ T-cell epitope SYVPSAEQI without affecting protein function.

3.1.1 Insertion of mutations by a complementation strategy results in repaired epitope sequence and an exflagellation defect phenotype

We aimed for inserting different mutations (all based on alanisation of certain amino acids) as we were not able to predict which amino acid is important for folding and therefore for a functional CS protein. The amino acid sequences of the different mutant T-cell epitopes me01 to me04 are shown in table 1. Mutations were inserted into the gene sequence of *csp* by site-directed mutagenesis using mutation-specific oligonucleotides (for oligonucleotide sequences see appendix 6.1).

The two amino acids valine (V) and glutamine (Q) are required for anchoring the CD8⁺ T-cell epitope on the MHC I molecule. Therefore these two amino acids were exchanged by two alanine (A) to generate the mutant me01. For the mutant me02 every second amino acid within the epitope was exchanged by an alanine. The amino acids serine (S), valine (V) and isoleucine (I) that were chosen for alanisation for the mutant me03 are all neutral amino acids with rather short side chains. These properties led to the assumption that these amino acids are most probably not important for protein folding and therefore protein functionality. In addition the amino acids tyrosine (Y), proline (P), glutamic acid (E) and glutamine (Q) were exchanged by alanine, that may be more likely involved in folding and functionality, to generate the mutant me04. In what way functional importance and importance for recognition

of the immune system of certain amino acids correlate is not known. For all mutations the respective amino acid codons were exchanged by site-directed mutagenesis on DNA level as described (2.8.1.12). Mutations were verified by sequence analysis of the DNA fragments. Mutated *csp* sequences were subsequently cloned into targeting constructs containing the *TgDHFR/TS* selectable marker.

PyCSP CD8⁺ T-cell epitope SYVPSAEQI

mutant	aa sequence
mutant me01	SYAPSAEAI
mutant me02	AYAPAAAQA
mutant me03	AYAPAAEQA
mutant me04	SAVASAAAI

Table 1. Amino acid sequences of the different mutations inserted in the *P. yoelii* circumsporozoite protein (CSP) by site-directed mutagenesis. The mutations of the *Py* CSP CD8⁺ T-cell epitope were inserted on DNA level by site-directed mutagenesis. Complementary oligonucleotides spanning the epitope region and containing the mutated DNA sequence were used in a standard PCR reaction. Mutated fragments were then inserted in targeting constructs by standard cloning procedures.

The initial complementation strategy to insert the mutated *Py csp* (*Py csp**) into the parasite genome is shown in figure 5.

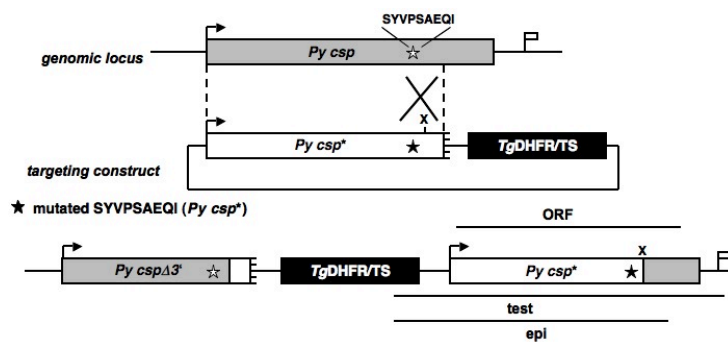


Figure 5. Knock-in/complementation strategy inserts a mutated CD8⁺ T-cell epitope in the *P. yoelii* circumsporozoite protein (CSP) genomic sequence. The Knock-in constructs *pcspΔepi_me01 - me04* contain a truncated *csp* gene that lacks the last 120 base pairs and a mutated sequence coding for the CD8⁺ T-cell epitope (*Py csp**). An additional *Xba*I restriction enzyme recognition site is inserted downstream of the CD8⁺ T-cell epitope sequence for specific linearisation prior to transfection. The *TgDHFR/TS* confers resistance to pyrimethamine and serves as a selectable marker. After homologue recombination with the *P. yoelii* genomic locus the integration construct is completely integrated into the parasite's genome. This results in a truncated *csp* gene (*Py cspΔ3'*) containing the WT epitope sequence (white star) and a complete *csp* open-reading-frame with a mutated T-cell epitope sequence (black star).

For the targeting constructs *pcspΔepi_me01 - me04* a C-terminal truncated version of the *Py csp* gene containing the mutation inside the CD8⁺ T-cell epitope was cloned into the vector b3D (for vector map see appendix 6.2) using the restriction sites *EcoRI* and *NotI*. In order to insert a unique *XbaI* restriction site for subsequent linearisation, *Py csp** was amplified in two fragments with a length of 882 bp and 96 bp.

Transfection of *P. yoelii* parasites with the *XbaI*-linearised targeting construct was performed according to the AMAXA transfection protocol as described (2.10.1.4.2) and transfected merozoites were directly injected intravenously (*i.v.*) into NMRI mice. One day after the transfection Pyrimethamine (70 µg/ml) was provided with the drinking water to select for transfected parasites. First resistant parasites were detected in giemsa-stained blood smears 6 days post transfection. Mice were sacrificed on day 8 with a parasitemia of 1.6 %. Infected blood was conserved as cryo stock and transferred intraperitoneally (*i.p.*) to naïve mice and further grown under continuous drug pressure. Parasites were isolated from the remaining blood and genomic DNA (gDNA) was extracted (parental population). The transferred parasite population was also cryo-preserved as blood stock and gDNA was prepared as soon as parasitemia reached more than 0.5 %. The integration of the targeting construct into the parasite genome was verified by genotyping PCR using test specific oligonucleotide pairs (see figure 6).

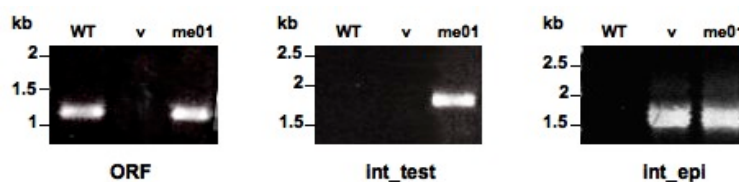


Figure 6. Genotyping PCR of *P. yoelii* circumsporozoite protein (CSP) epitope mutant me01 after transfection with the complementation construct. Standard PCRs were run with ORF, test and episomal (epi) specific oligonucleotide pairs (see figure 5). As templates served gDNA of the mutant me01 and *P. yoelii* wild-type gDNA (WT) or the complementation construct (v) as PCR controls. Specific DNA fragments were separated by agarose gel electrophoresis.

As expected the ORF specific DNA fragment was amplified with a length of 1104 bp with WT and me01 gDNA as templates, but not from the complementation construct. The episomal control (int_{epi}) fragment is amplified from the complementation construct and mutant me01 gDNA, the length of 1531 bp was verified on a agarose gel. The integration-specific DNA fragment (int_{test}) can only be amplified from mutant gDNA if the

complementation construct inserted into the parasite's genome, a respective band with a size of 1767 bp was detected on an agarose gel proving successful integration. The 1767 bp long int_test specific DNA fragment was purified and cloned into the T/A cloning vector pGEM-T Easy (Promega) for sequencing. Sequence analysis revealed the desired mutation me01 inside the *Py csp* open reading frame (ORF), including start and stop codon, and was therefore expected to be expressed.

The mutated parental parasite line *Py CSP* me01 was subsequently cloned by limited dilution in order to achieve a clonal mutant parasite line as described (2.10.1.5). The parasitemia of the parental mutant *Py CSP* me01 reached 0.67 % 3 days post injection of a respective blood stock. This mouse was sacrificed and the blood was taken by heart puncture. The infected blood was diluted 1 to 1x10⁶ in RPMI medium, 21.3 µl of this dilution was added to 78.7 µl RPMI and injected *i.v.* per mouse. In total 15 NMRI mice were injected with calculated one parasite. The parasites were grown under Pyrimethamine selection that was again provided within the drinking water. First resistant parasites were detected 7 days post infection in the blood of two mice (clones I-2 and III-3). Two more mice displayed blood-stage parasites in a giemsa-stained blood smear on day 9 post infection (clones I-5 and II-3). The remaining 11 mice remained blood-stage negative until day 16 post infection as determined by giemsa-stained blood smears. gDNA of the different clones served as template for a subsequent genotyping PCR with the integration test-specific oligonucleotides. Integration of the complementation construct could be detected for the three clones I-2, III-3 and I-5, but not for clone II-3 by genotyping PCR using the same specific oligonucleotides as in figure 6. Integration specific DNA fragments were cloned via T/A cloning into the pGEM-T Easy vector (Promega) and sequenced by conventional techniques. We used the two vector specific oligonucleotides T7 and SP6 and the *PyCSP_complIII_NotI_rev* oligonucleotide for sequencing in order to cover the whole sequence including the start and stop codon of the *csp* ORF and the epitope sequence. Integration of the vector could be observed in all cases by the presence of the selection marker and the inserted restriction sites *EcoRI*, *NotI* and *XbaI* within the *Py csp* ORF. The mutated CD8⁺ T-cell epitope sequence, however, was reverted to the WT sequence for all clones.

The combined sequence of the amplified integration specific DNA fragment of *Py CSP* me01 clone I-2 is attached under 6.3.

As the cloning of the *Py CSP* mutant me01 failed it was planned in a next step to transmit the parental mutant population to *Anopheles* mosquitoes in order to confirm its viability through

the mosquito life cycle and hence normal phenotype comparable to an unaltered CSP i.e. WT parasite.

Typically, male gametes emerge from the erythrocyte after transmission triggered by a drop of temperature, change in pH and substances in the mosquito's midgut, such as xanthurenic acid (XA). A high percentage of exflagellating gametocytes is important for reasonable mosquito infections, therefore this is routinely checked under the microscope before transmission of the parasite to the mosquito. Parasites of the *Py* CSP CD8⁺ T-cell epitope mutant line showed a defect in exflagellation as observed under the microscope. This defect cannot be explained with targeting of the *csp* gene itself, but maybe closely located genes were also impaired when targeting this genomic locus with the applied genetic strategy.

3.1.2 A short gene (PY07369) annotated upstream of *P. yoelii csp* might also be affected when gene-targeting *csp*

As the exflagellation defect we observed when integrating a targeting construct into the *P. yoelii csp* genomic locus could not be explained with described functions of CSP (Menard et al. 1997) we had a closer look at the surrounding genomic loci of *Py csp*. Sequence information and gene annotations were obtained from the PlasmoDB database (<http://plasmodb.org>). There we found a small gene annotated upstream of the *P. yoelii csp* (PlasmoDB annotation PY07368) coding for a hypothetical protein with unknown function with the annotation number PY07369. Because of its genetic localisation upstream of *csp* we preliminarily called this gene *csprae*. The stop codon of *csprae* was only 140 bp upstream of the *csp* start codon (figure 7). Hence the 5' and 3' regulatory regions of both genes most likely overlap. The coding sequence of *csprae* lies within the promotor region of *csp* and the coding sequence of *csp* in turn overlaps with the terminator region of *csprae*.

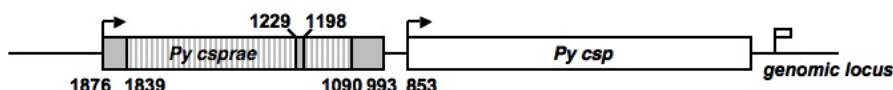


Figure 7. Genomic locus of the *P. yoelii csp* gene and its neighbouring genomic sequence information. The outline shows the PlasmoDB (<http://plasmodb.org>) genomic sequence AABL01002684 with the coding sequences for *P. yoelii* CSP and a small hypothetical protein, we for now called CSPrae (PY07369). The bold numbers indicate the annotated positions of the respective genes on the genomic sequence. The *csprae* stop codon lies at position 993, whereas the *csp* start codon is at position 853. The two coding sequences of the respective genes lie only 140 bp from each other. Large introns of *Py csprae* are marked as striped boxes.

In order to deplete the *csprae* gene the targeting construct pΔ*csprae* was generated containing a 351 bp large DNA fragment of the *csprae* 5' UTR and a second 324 bp homologue fragment

from the N-terminal coding sequence. These two fragments were cloned into the b3D cloning vector flanking the *TgDHFR/TS* selectable marker. As the *csp* promotor region should not be affected and the CSprae protein should not be expressed anymore at the same time only the first 28 bp of the *csprae* genomic sequence should be depleted during integration of this construct. As *csprae* contains two large introns (grey-striped boxes in figures 7 and 8) the depletion could be inserted more than 1 kb upstream of the *csp* start codon. Integration of the targeting construct by homologue recombination resulted in a N-terminally truncated *csprae* as shown in figure 8.

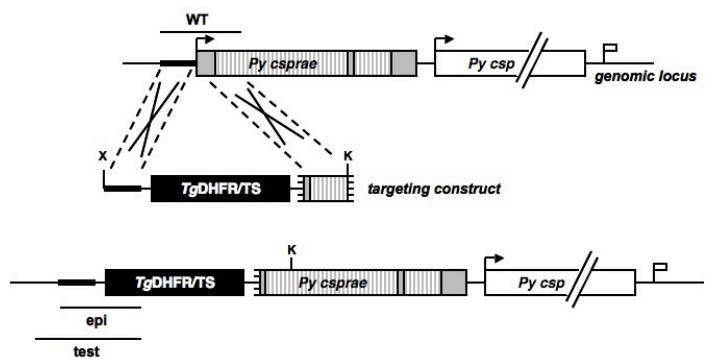


Figure 8. Genetic strategy to functionally knock-out the *P. yoelii* *csprae* gene. The targeting construct Δcsprae contains two fragments from the *P. yoelii* *csprae* (PY07369) 5' UTR and the N-terminal genomic sequence, respectively. Two large introns in the genomic sequence of *csprae* are shown as striped boxes. Integration of the constructs by a double crossing over event results in depletion of the first 28 bp of the *csprae* gene. The *TgDFRH/TS* selectable marker confers to pyrimethamine resistance.

P. yoelii parasites were transfected twice with the *XbaI/KpnI* digested Δcsprae targeting construct according to the AMAXA transfection protocol (2.10.1.4.2). The parasitemia on day one after transfection was above 0.3 % in all four NMRI mice injected in two transfection experiments. Under Pyrimethamine selection resistant transfectants were first detected in giemsa-stained blood smears on average on day 8.5. It was surprising that in both transfection experiments only one out of two injected mice became blood-stage positive under drug selection. As soon as the parasitemia reached at least 0.5 % mice were sacrificed and infected blood was collected from the heart. Blood was transferred to naïve NMRI mice and cryopreserved, parasites were isolated for gDNA extraction from the remaining blood. Transferred animals were again sacrificed when reaching a sufficient parasitemia under continuous drug cover. Genotyping of the transfectants was performed by standard PCR using integration-specific oligonucleotides (sequences attached under 6.1).

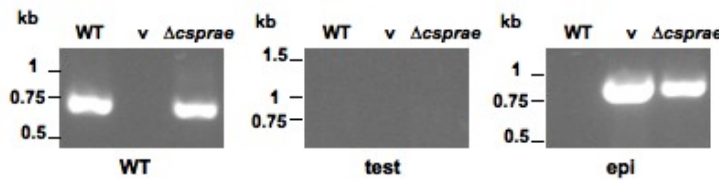


Figure 9. Genotyping PCR of the Δcsp^{rae} transfectant. Standard PCRs were run with WT, test and episomal (epi) specific oligonucleotide pairs (see figure 8). As templates served gDNA of the Δcsp^{rae} transfectant and *P. yoelii* wild-type gDNA (WT) or the targeting construct p Δcsp^{rae} (v) as PCR controls. Specific DNA fragments were separated by agarose gel electrophoresis.

The WT specific DNA fragment with a size of 706 bp was amplified from *P. yoelii* WT gDNA and also from the transfectant gDNA using the cloning oligonucleotides PyCSprae_5'UTR_XbaI_for and PyCSprae_Nterm_KpnI_rev. For episomal PCR control the 904 bp large DNA fragment was amplified from the targeting construct and the transfectant gDNA with the oligonucleotides PyCSprae_5'UTR_XbaI_for and PyCSprae_test_rev binding inside the selectable marker. The combination with the 5'test_for oligonucleotide, however, resulted in no DNA fragment with an expected size of 1013 bp as seen on the agarose gel in figure 8. This shows that the targeting construct was taken up during transfection, but did not integrate into the genomic locus. The same genotyping pattern was seen for both transfectants and their transfer populations.

3.1.3 Replacement of the *P. yoelii* wild-type *csp* sequence by a mutated sequence should prevent repair mechanisms

Targeting the *P. yoelii* *csp* genomic locus by the mutated complementation construct pcspΔepi resulted in repair mechanisms after cloning and an unexpected exflagellation phenotype of the parental mutant parasite population, therefore we changed the genetic strategy to insert the specific mutations in the endogenous CD8⁺ T-cell epitope. We focused on a replacement strategy where the endogenous *csp* ORF is exchanged by a mutated ORF (figure 9).

The replacement constructs pcsprep1Δepi_me01 - me04 contain the *Py csp* ORF starting with the ATG start codon and ending with the TAA stop codon. A respective DNA fragment with a length of 1104 bp was cloned via the *Xba*I and *Bam*HI restriction sites into the cloning vector b3D (for vector map see appendix 6.2). Before, the mutations inside the CD8⁺ T-cell epitope were again inserted by site-directed mutagenesis using the same oligonucleotides as described earlier. A second DNA fragment amplified from the 3' untranslated region (UTR) of the *Py csp* gene with a length of 732 bp was cloned into the same vector via the restriction

sites *KpnI* and *HindIII*. Hence the two homologue regions to the *P. yoelii* genome flanked the selectable marker *TgDHFR/TS* providing basis for the requested double crossing over event. Only targeting constructs with the two mutations me01 and me03 were successfully generated.

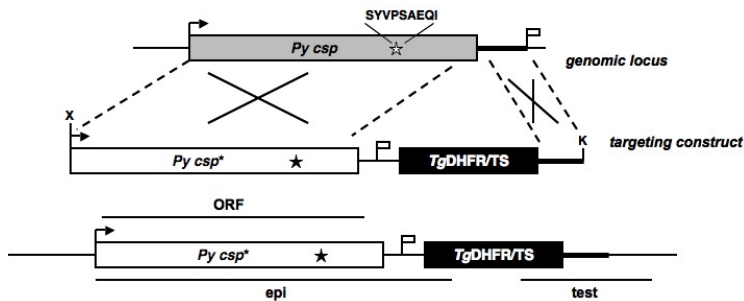


Figure 10. Replacement strategy inserts a mutated CD8⁺ T-cell epitope in the *P. yoelii* circumsporozoite protein (CSP) genomic sequence. The replacement constructs pcsprep1Δepi_me01 - me04 contain the complete *Py csp* gene, with the sequence coding for the CD8⁺ T-cell epitope mutated by site-directed mutagenesis (*Py csp**), and the 3'UTR of the *csp* open reading frame (thick black line). These homologous regions to the parasite's genome are separated by a *TgDHFR/TS* gene serving as selection marker. A double crossing-over event replaces the WT *Py csp* gene (grey) by the one with the mutated epitope sequence (white) and inserts the selection marker at the same time.

Transfection of *P. yoelii* parasites with the *XbaI/KpnI*-digested targeting constructs was performed as described before. Infected mice carrying the transfected parasites were sacrificed 7 days post transfection with parasitemias of 1.6 % and 1.1 % for the mutant me01 and 0.3 % and 0.9 % for the mutant me03. Genomic DNA isolated from transfected parasites was used as template for an integration specific PCR (figure 11).

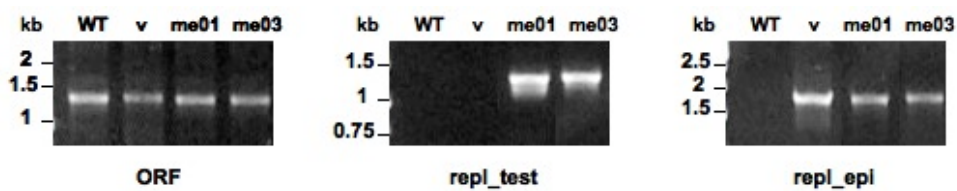


Figure 11. Genotyping PCR of *P. yoelii* circumsporozoite protein (CSP) epitope mutants me01 and me03 after transfection with the replacement constructs. Standard PCRs were run with ORF, test and episomal (epi) specific oligonucleotide pairs (see figure 9). As templates served gDNA of the mutants me01 and me03 and *P. yoelii* wild-type gDNA (WT) or the replacement construct (v) as PCR controls. Specific DNA fragments were separated by agarose gel electrophoresis.

The genotyping PCR of transfectants generated with the replacement strategy (figure 10) amplified the *Py csp* ORF with a size of 1104 bp from all shown DNA templates using the

ORF specific oligonucleotides. The episomal specific fragments with a size of 1657 bp were detected on a agarose gel when using the replacement targeting constructs or gDNA of the two mutant transfectants me01 and me03 together with the repl_епи specific oligonucleotides for PCR amplification. The repl_тест specific oligonucleotides prove integration of the replacement targeting constructs for both mutants, me01 and me03. The corresponding fragments with a size of 1310 bp were detected on an agarose gel. The mutations were again controlled by sequence analysis of the respective integration specific DNA fragments. Sequence analysis showed that both mutations, me01 and me03, were successfully inserted into the sequence coding for the *Py* CSP CD8⁺ T-cell epitope and integrated with the replacement strategy into the genome.

Cloning of the mutant parasite lines was again conducted by limiting dilution (2.10.1.5). Donor mice infected with the mutant parasites were sacrificed with a parasitemia of 0.65 % for the mutant me01 and 0.55 % for the mutant me03. The infected blood from both mice was diluted 1 to 1x10⁶, 22 µl or 26 µl, respectively, then contain one calculated mutant parasite me01 or me03. For both mutant strains 10 NMRI mice were injected *i.v.* with the indicated volumes of the diluted blood. Parasitemia was monitored by giemsa-stained blood smears. One mouse infected with the me03 mutant parasite got blood-stage positive on day 7. Integration specific PCR with isolated gDNA, however, did not show the integration specific fragment on an agarose gel. All other cloning mice remained blood-stage negative up to day 21 after the infection. The cloning procedure was repeated, but all injected mice remained blood-stage negative up to three weeks after infection. So again cloning of the mutant parasite lines failed for unknown reasons.

Again the parental mutant parasites lines were fed to mosquitoes. Exflagellation was unimpaired when mutations were inserted by the replacement strategy. However, for the mutant me01 we detected no oocysts in dissected mosquito midguts 10 days post transmission. Consequently no sporozoites were found in the salivary glands of female mosquitos 14 days post transmission. This was different for the mutant parasite line me03. Oocysts could be detected in 7 out of 9 dissected midguts 10 days post transmission. The infection was rather low with only around 20 oocysts per infected midgut. On day 14 post transmission salivary glands were dissected and around 4,200 sporozoites per mosquito were isolated. Sporozoites were also transmitted to 2 anesthetised NMRI mice by bite. Four days after the by bite infection mice reached a blood-stage parasitemia of 0.6 % and 0.37 %. Blood-stage parasites were isolated and gDNA was purified. Genotyping PCR of these blood-stage parasites, however, showed no integration of the replacement construct when using the

repl_int specific oligonucleotides. This finally suggests that only the WT parasites completed the life cycle, which were most likely left in the non-homologous parental parasite population. Mutants, however, were not able to pass through the entire life cycle as no mutated parasites could be detected in blood-stages by genotyping PCR.

In Summary targeting *csp* turned out to be a difficult project. Although we tried several mutations and integration strategies we were not able to successfully generate a *P. yoelii* CSP CD8⁺ T-cell epitope mutant. Unfortunately also the depletion of the short gene located upstream of the *Py csp* failed. The fact, however, that two genes might be located so close to each other that regulatory regions overlap should be considered for future genetic manipulations. One should definitely make sure that one is not affecting other neighbouring genes when targeting a specific gene because subsequent phenotypes could not be allocated clearly.

3.2 Comparative analysis of early *Plasmodium* liver-stages identifies potential targets of protective immunity

Genetically-attenuated parasites (GAP) and radiation-attenuated sporozoites (RAS) arrest during liver-stage (LS) development. Antigens expressed during early liver-stage development are presented to the immune system and alert protective immune responses in the liver. Wild-type (WT) sporozoites also induce immune responses in the liver but lead to disease causing blood-stage infection and at most partial protection is acquired. The antigen repertoire expressed by GAP and RAS liver-stages is probably reduced due to developmental arrest. Though these antigens can induce protection. We therefore compared the transcription profile of GAP and RAS liver-stages to that of WT LS and suggest that this method can help identifying antigens that are critical targets of pre-erythrocytic immunity.

3.2.1 Suppression subtractive hybridisation results in a set of specifically up-regulated transcripts in attenuated parasites

We utilised suppression subtractive hybridisation (SSH) to compare the transcripts of WT, GAP and RAS parasites after 20 hours LS development. This highly effective method allows the identification of differentially expressed transcripts in two different cDNA populations (Diatchenko et al. 1996). LS development of *Plasmodium* parasites was achieved in cultivated hepatocytes. It is described that *P. berghei* sporozoites enter and transform in human hepatoma cells (Hollingdale et al. 1983). Therefore the human hepatoma cell line Huh7 was used as an adequate host for LS development. This *in vitro* cultivation allowed to enhance the parasite to host-cell ratio and therefore to gain sufficient parasite RNA material for the subsequent subtraction. For one cDNA population of either GAP, RAS or WT LS, two to three 8-well chamber slides with 25,000 Huh7 cells and 25,000 to 35,000 sporozoites per well were inoculated and LS development was stopped after 20 hours. We chose this time point as *uis3(-)* parasites undergo arrested development in the liver at 24 hours and therefore already the early genes expressed during this period must be important for pre-erythrocytic immunity. Collected cells were treated with 0.05 % digitonin, this selectively permeabilised the host-cell plasma membrane without affecting the parasitophorous vacuole membrane (PVM) surrounding the intracellular parasite and thus reduced contaminations with host-cell RNA (Beckers et al. 1994). Parasite-specific RNA was subsequently isolated using the RNeasy Mini Kit (Qiagen). The achieved RNA concentrations reached from around 150 to 250 µg/ml in a volume of 40 µl, meaning final amounts of 6 to 10 µg total RNA. The cDNA synthesis with the applied SMART method (Clontech; SMART™ PCR cDNA Synthesis Kit, Protocol

No. PT3041-1) requires 0.05 to 1 µg total RNA and therefore this technique was especially useful for this approach as starting material was limited. Around 0.5 µg total RNA was used for cDNA synthesis with the SMART technology and this cDNA was subsequently used for subtraction. The subtraction procedure was performed according to the manufacturer's manual (Clontech; PCR-Select™ cDNA Subtraction Kit, Protocol No. PT1117-1). Resulting cDNA fragments were directly cloned into pGEM-T Easy T/A-cloning vector (Promega) and sequenced with conventional methods.

Sequence analysis was performed using the BLAST search tool on the PlasmoDB and GeneDB websites (<http://plasmodb.org>, <http://www.genedb.org>). The blastn algorithm was utilised to identify sequence similarities with annotated gene sequences of different *Plasmodium* species.

Although the initial screening was performed using *P. yoelii* parasites we switched during sequence analysis to *P. berghei* orthologues where possible. This was due to better sequence information and easier handling of this parasite strain under laboratory conditions.

The most abundant hits of more than 200 analysed sequences up-regulated in GAP and RAS in comparison to WT LS sequences, respectively, are shown in tables 2 and 3.

UAP 1 was identified as C2 domain-containing protein (PB402109.00.0) and contains, beside one characteristic C2 domain, one domain with predicted exonuclease activity and one predicted ATPase domain. In addition UAP 1 and also UAP 3 (PB402624.00.0) contain signal peptides (SP) predicting them as targets of the secretory pathway. The three UAPs 5, 7 and 9 (PB402174.00.0, PB403022.00.0, PB402387.00.0) contain transmembrane domains (TM) suggesting a membrane associated localisation. UAP 7 also contains a PEXEL export signal and might therefore be located beyond the parasitophorous vacuole membrane (PVM) (Martí et al. 2004). These UAPs, however, are annotated as hypothetical proteins with unknown function. UAP 6 (PB402448.00.0) was identified as a predicted serine/threonine phosphatase. More precise analysis of the sequences revealed a possible multi-gene family, located telomeric and therefore extremely difficult to study. Hence, this hit was excluded from further analysis. Several predicted domains in the identified UAPs are associated with transcriptional regulation. The krueppel-associated box (KRAB) in UAP 4 (PB402248.00.0) is a protein domain that is mainly found N-terminally in certain zinc finger proteins and acts as a transcriptional repressor (Vissing et al. 1995) (Urrutia 2003). Whereas UAP 8 (PB000424.03.0) belongs to the GTP-binding elongation factor family.

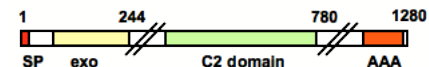
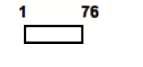
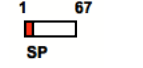
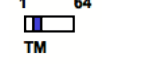
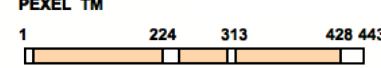
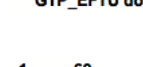
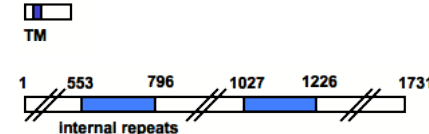
UAP	# hits	systematic name	product	primary structure	orthologs
1	5	PB402109.00.0	C2 domain-containing protein		-
2	4	PB401378.00.0	hypothetical protein		-
3	4	PB402624.00.0	hypothetical protein		-
4	3	PB402248.00.0	hypothetical protein		-
5	8	PB402174.00.0	hypothetical protein		-
6	9	PB402448.00.0	serine/threonine phosphatase	NA	-
7	4	PB403022.00.0	hypothetical protein		-
8	4	PB000424.03.0	translation elongation factor EF-1, subunit alpha		PY02338/ PY00361/2 PF13_0304/5
9	3	PB402387.00.0	hypothetical protein		-
10	1	PB301568.00.0	rhoptry protein		PY06945 PFE1045c

Table 2. Genes up-regulated in genetically-attenuated parasites (GAP) in comparison to wild-type (WT) parasites during early liver-stage development (20h). Listed are the ten most abundant genes up-regulated in GAP liver-stages as identified by suppression subtractive hybridisation (SSH). More than 200 sequences were analysed using the BLAST search tool (blastn algorithm) from the PlasmoDB and GeneDB databases (<http://plasmodb.org>, <http://www.genedb.org>). The table shows the number of hits, the systematic name, the annotated gene product, the predicted primary structure, annotated *Plasmodium* orthologues and a consecutive UAP (up-regulated in attenuated parasites) number. SP: signal peptide; exo: exonuclease domain; AAA: ATPase domain; TM: transmembrane domain; KRAB: krueppel associated box.

Even more transcription factors could be found in the list of up-regulated transcripts specific for RAS. The WW domain of PCIF1 as predicted for UAP 13 (PB000078.02.0) interacts with phosphorylated RNA polymerase II and may therefore play a role in mRNA synthesis (Fan et al. 2003). UAP 15 (PY05684) is the putative transcriptional repressor Not4hp. UAP 16 (PB000435.00.0) contains a domain specific for the transcription factor S-II. The RNA recognition motif (RRM), like predicted for UAP 11 (PB000378.03.0), obviously binds to RNA and proteins containing RRM domains are thereby involved in post-transcriptional regulation. Additionally the forkhead-associated (FHA) domain can be found in a variety of eukaryotic proteins like kinases, phosphatases, kinesins, but also transcription factors and RNA-binding proteins [reviewed in (Durocher and Jackson 2002)].

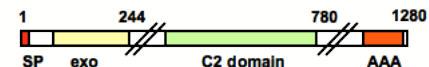
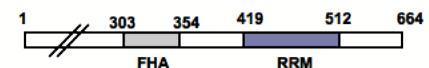
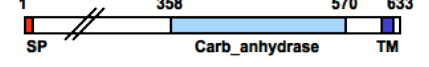
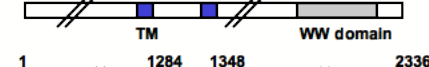
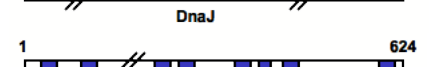
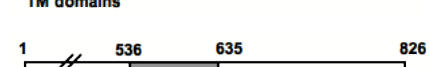
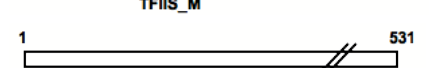
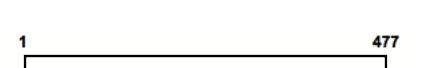
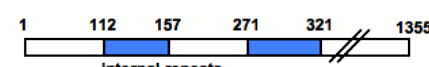
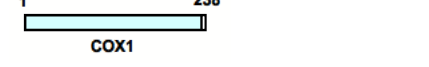
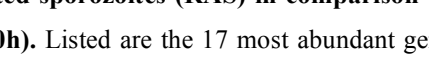
UAP	# hits	systematic name	product	primary structure	orthologs
1	14	PB402109.00.0	C2 domain-containing protein		-
2	4	PB401378.00.0	hypothetical protein		-
3	5	PB402624.00.0	hypothetical protein		-
4	2	PB402248.00.0	hypothetical protein		-
6	3	PB402448.00.0	serine/threonine phosphatase	NA	-
7	1	PB403022.00.0	hypothetical protein		-
11	6	PB000378.03.0	FHA domain		PY00240 PF11_0347
12	2	PB000654.03.0	carbonic anhydrase		PY00744 PF11_0411
13	1	PB000078.02.0	conserved protein, unknown function		PY07228 MAL8P1.49
14	3	PB108189.00.0	conserved protein, unknown function		PY03538 PF11_0433
15	8	PY05684	transcriptional repressor Not4hp		-
16	4	PB000435.00.0	MAEBL		PY3552 PF11_0289
17	3	PB001570.02.0	U1 small nuclear ribonucleoprotein C		PY00121 PF14_0026
18	3	PB001388.02.0	conserved protein, unknown function		PY07070 PFA0350c
19	2	PB402386.00.0	asparagin-rich antigen		PY05735 PF08_0060
20	2	PB300550.00.0	osmiophilic body protein		PY04958 PFL2405c
21	2	PY00149	cytochrome c oxidase subunit I-related		-

Table 3. Genes up-regulated in radiation-attenuated sporozoites (RAS) in comparison to wild-type (WT) parasites during early liver-stage development (20h). Listed are the 17 most abundant genes up-regulated in RAS liver-stages as identified by suppression subtractive hybridisation (SSH). More than 200 sequences were analysed using the BLAST search tool (blastn algorithm) from the PlasmoDB and GeneDB databases (<http://plasmodb.org>, <http://www.genedb.org>). The table shows the number of hits, the systematic name, the annotated gene product, the predicted primary structure, annotated *Plasmodium* orthologues and a consecutive UAP (up-regulated in attenuated parasites) number. SP: signal peptide; exo: exonuclease domain; AAA: ATPase domain; TM: transmembrane domain; KRAB: krueppel associated box; FHA: forkhead-associated domain; RRM: RNA recognition motif; TFIIS_M: transcription factor S-II; COX: cytochrome oxidase.

More genes are specifically up-regulated in RAS. Amongst them the carbonic anhydrase UAP 12 (PB000654.03.0), the conserved protein UAP 14 (PB108189.00.0) probably involved in heat shock protein binding, the asparagin-rich antigen UAP 19 (PB402386.00.0), the osmophilic body protein UAP 20 (PB300550.00.0) probably involved in intracellular signalling and the cytochrome c oxidase UAP 21 (PY00149). Interestingly also the circumsporozoite protein (CSP) came up once during sequence analysis of transcripts up-regulated in RAS.

Other UAPs are found up-regulated in both attenuated parasite lines, RAS and GAP. Primarily the C2 domain-containing protein (UAP 1), which is the leading hit up-regulated in RAS. But also the small hypothetical proteins UAP 2, UAP 3, UAP 4 and UAP 7 are shared between RAS and GAP as well as the serine/threonine phosphatase UAP 6. Cellular functions during LS development of the different identified UAPs are so far unknown.

The distribution of the UAPs and the classification into functional groups are again illustrated in the circle diagram of figure 12. The classification of the identified gene sequences was supported by database annotations and predicted protein domains identified with the Simple Modular Architecture Research Tool (SMART) (smart.embl-heidelberg.de).

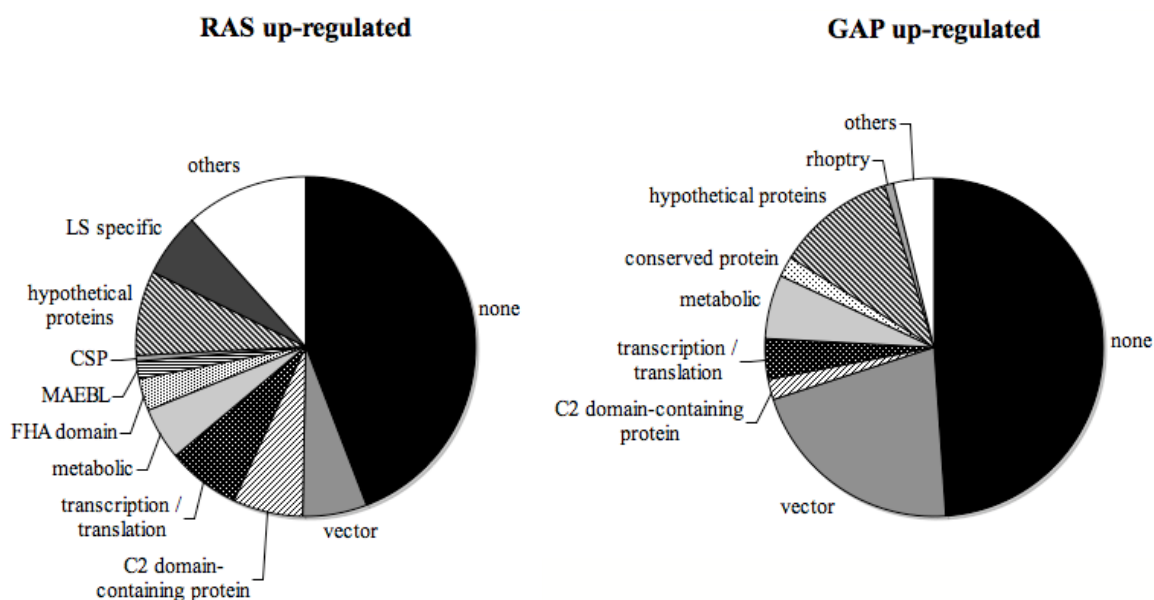


Figure 12. Genes differentially expressed in attenuated parasites in comparison to wild-type (WT) parasites during early liver-stage development (20h). The circle diagram shows the percentage of certain liver-stage transcripts identified in 200 analysed sequences of genetically-attenuated (GAP up-regulated) or radiation-attenuated (RAS up-regulated) parasites compared to WT sequences by suppression subtractive hybridisation (SSH). Sequence analysis was performed using the BLAST search on PlasmoDB and GeneDB homepages (<http://plasmodb.org>, <http://www.genedb.org>).

The BLAST search in the PlasmoDB and GeneDB databases (<http://plasmodb.org>, <http://www.genedb.org>) resulted in 49 % and 44 % of the searches, respectively, in no hits. These sequences were again entered in the NCBI database (<http://www.ncbi.nlm.nih.gov>) using the blastn algorithm to check for possible similarities to host-cell sequences, however no matching human sequences were found. More than 21 % and 6 % of the sequences, respectively, were identified as the pGEM-T Easy sequencing vector. Again it becomes apparent that a high percentage of transcription factors is up-regulated in attenuated parasites. In total it can also be seen that RAS express a much broader up-regulated repertoire if compared to GAP.

We also performed the reverse subtraction and thereby identified transcripts that are down-regulated in attenuated parasites in comparison to WT liver-stages. Results are shown in tables 4 and 5. Interestingly one gene up-regulated in RAS is down-regulated in GAP, namely the transcriptional repressor Not4hp (UAP 15). Other genes are specifically down-regulated in GAP, a tryptophan-rich antigen (PKH_120090) and several hypothetical proteins. The hypothetical proteins PY06363 and PY07366 as well as the reverse transcriptase PY07669 are assigned to one cluster according to the protein information on the GeneDB homepage.

pos	# hits	systematic name	product	primary structure	orthologs
1	11	PB402448.00.0	serine/threonine phosphatase	NA	-
2	5	PB401378.00.0	hypothetical protein	1 76 []	-
3	4	PY05684	transcriptional repressor Not4hp	1 [] TM domains [] 624	-
4	4	PB402624.00.0	hypothetical protein	1 67 [] SP	-
5	3	PKH_120090	tryptophan-rich antigen	1 [] 557 800 TryThrA_C	MAL13P1.269
6	3	PY06363	hypothetical protein	1 126 259 542 627 RVT_1 exo AAA	-
7	3	PY07366	hypothetical protein	1 109 392 452 477 exo AAA	-
8	3	PY07602	hypothetical protein	1 404	-
9	2	PY07668	endo/ exonuclease/ phosphatase family	1 15 246 Endo_exo_phos	-
10	2	PY07669	reverse transcriptase	1 227 484 RVT_1	-

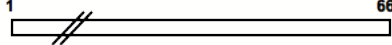
11	2	PB102146.00.0	conserved protein, unknown function		669	PY06038 PFE1095w
----	---	---------------	--	--	-----	---------------------

Table 4. Genes down-regulated in genetically-attenuated parasites (GAP) in comparison to wild-type (WT) parasites during early liver-stage development (20h). Listed are the 11 most abundant genes down-regulated in GAP liver-stages as identified by suppression subtractive hybridisation (SSH). More than 200 sequences were analysed using the BLAST search tool (blastn algorithm) from the PlasmoDB and GeneDB databases (<http://plasmodb.org>, <http://www.genedb.org>). The table shows the number of hits, the systematic name, the annotated gene product, the predicted primary structure and annotated *Plasmodium* orthologs. SP: signal peptide; exo: exonuclease domain; AAA: ATPase domain; TM: transmembrane domain; TryThra_C: Tryptophan-Threonine-rich plasmid antigen C terminal; RVT_1: reverse transcriptase.

Also the titin-L1-related fusion protein PY07613 down-regulated in RAS is part of this gene cluster. Furthermore we identified also in the down-regulated sequences genes that are shared between RAS and GAP. The reverse transcriptase PY07669 and PY07668 belonging to the endonuclease/exonuclease phosphatase family came up in both down-regulated populations.

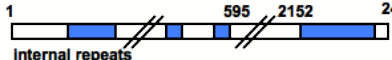
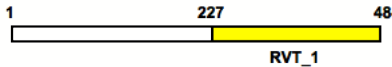
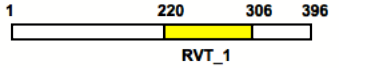
pos	# hits	systematic name	product	primary structure	orthologs	
1	7	PB300106.00.0	MAEBL		2476	PY01844 PFL0315c
2	5	PB402448.00.0	serine/threonine phosphatase	NA		-
3	3	PY07669	reverse transcriptase		484	-
4	2	PB401378.00.0	hypothetical protein		76	-
5	2	PB402624.00.0	hypothetical protein		67	-
6	2	PB001050.01.0	nucleolar preribosomal assembly protein		444	PY00572 PF08_0065
7	2	PY06985	endo/ exonuclease/ phosphatase family		277	-
8	2	PY07613	titin-L1 fusion protein-related		396	-
9	2	PY07668	endo/ exonuclease/ phosphatase family		246	-

Table 5. Genes down-regulated in radiation-attenuated sporozoites (RAS) in comparison to wild-type (WT) parasites during early liver-stage development (20h). Listed are the nine most abundant genes down-regulated in RAS liver-stages as identified by suppression subtractive hybridisation (SSH). More than 200 sequences were analysed using the BLAST search tool (blastn algorithm) from the PlasmoDB and GeneDB databases (<http://plasmodb.org>, <http://www.genedb.org>). The table shows the number of hits, the systematic name, the annotated gene product, the predicted primary structure and annotated *Plasmodium* orthologs. SP: signal peptide; CAF-1: chromosome assembly factor 1; RVT_1: reverse transcriptase.

Unfortunately we had to exclude some of the UAPs after analysis of the down-regulated genes as they came up in all subtracted populations, even in their own reverse subtraction. UAP 2, UAP 3 and UAP 6 can be considered as false positives and are therefore marked light grey in the above shown tables.

All mentioned annotations and sequence information are based on database searches from 2008 - 2010. Due to continuous updates regarding the *Plasmodium* genome sequencing not all identified sequences listed here are still available under the described annotations.

The up-regulation of the shared UAPs in GAP and RAS liver-stages was further validated and quantified by quantitative real-time PCR (qRT-PCR). As templates served *P. berghei* GAP, RAS and WT RNA isolated from liver-stages after 20 hours LS development and transcribed in cDNA. The used primer pairs were chosen according to the sequence fragments received after sequencing of the subtracted cDNA libraries resulting from the SSH screening. Figure 12 shows the copy numbers of mRNA of UAP 1, UAP 4 and UAP 7. The mRNA level for all investigated genes ranges from around 100 to 150 copies in WT LS, but is enhanced to a mean of 6032 and 7635 copies for UAP 1 in GAP and RAS LS, respectively. The number of mRNA copies for UAP 4 increased to a mean of 5223 and 6217 and for UAP 7 to a mean of 3994 and 4823 copies in GAP and RAS LS, respectively. The qRT-PCR results validate the results from the SSH screening.

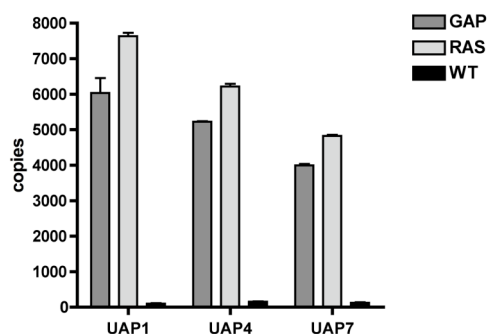


Figure 13. Quantitative real-time PCR of transcripts up-regulated in attenuated parasites (UAP). Quantitive real-time RT-PCR with total RNA isolated from 20 h *P. berghei* liver-stages from either wildtype (WT), radiation-attenuated (RAS) or genetically-attenuated (GAP) parasites as templates using gene-specific oligonucleotide primer pairs. Shown are the transcript levels of UAP 1, UAP 4 and UAP 7. Transcript quantity is represented as the number of copies (+/- SD) in comparison with an external standard curve produced with gene-specific plasmids.

In summary the SSH screening resulted in a set of specifically up-regulated transcripts in GAP and RAS liver-stage parasites if compared to WT liver-stages. These UAPs (up-regulated in attenuated parasites) display proteins mainly with unknown functions. Results could be validated by qRT-PCR. The antigenic capacity of the identified proteins will be determined.

3.2.2 The *Plasmodium* ferlin protein family

The *P. berghei* C2 domain-containing protein (C2CP) was identified as one of the most prominent transcripts up-regulated in attenuated parasites (UAP 1). C2 domains are generally involved in Ca^{2+} -sensing and -signalling and proteins containing C2 domains are described to mediate Ca^{2+} -dependent vesicular fusion events. The *C. elegans* and human ferlins are well characterised proteins with characteristic cytosolic C2 domains. Database searches for protein orthologues and paralogues revealed beside the *Pb* C2CP one annotated *Pb* ferlin (FER) and a ferlin-like protein (FLP). So far there is nothing known about the cellular role of Plasmodial C2 domain-containing proteins and ferlins. Although the previously mentioned screening should primarily serve new antigen identification, the ferlin protein family is also very interesting with respect to their cellular functions. A more precise look at the databases also revealed several ferlin proteins in other Apicomplexan parasites. The primary structures of these proteins are shown in figure 13. Shown are the *P. berghei* C2 domain-containing protein (PB402109.00.0) and the annotated *Pb* ferlin (PB000505.02.0) and *Pb* ferlin-like protein (PB101952.00.0) paralogues. In the *P. falciparum* genome there is also one ferlin (PF14_0530) and a ferlin-like protein (MAL8P1.134) annotated. The *Pb* and *Pf* FER share 63.7 % amino acid identity whereas the *Pb* and *Pf* FLP share even 71.5 % amino acid identity. Ferlin (TGVEG_073920) and FLP (TGVEG_093560) orthologues are also found in the Apicomplexan parasite *Toxoplasma gondii*. Except for the *Pb* C2CP, all other ferlin proteins contain at least five characteristic C2 domains. Moreover all ferlins and ferlin-like proteins carry transmembrane domains and a signal peptide is found for *Pb* C2CP.

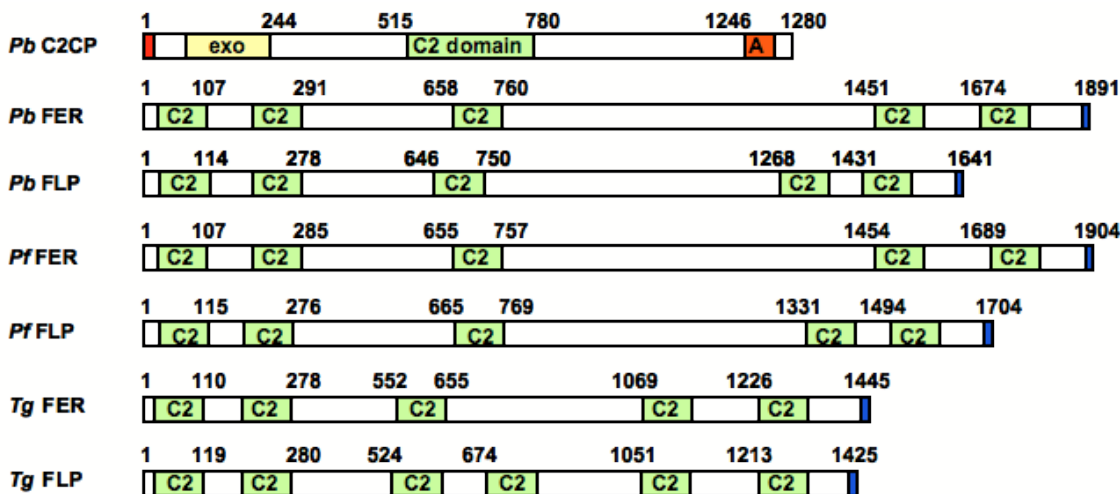


Figure 14. Primary structures of annotated Apicomplexan C2 domain-containing proteins (C2CP) and related ferlins. Shown are the *P. berghei* C2CP and related ferlin and FLP paralogues as well as the *P. falciparum* and *Toxoplasma gondii* orthologues. Characteristic C2 domains are involved in Ca^{2+} sensing and -signalling in other described ferlin proteins. Beside these domains SMART analysis (<http://smart.embl-heidelberg.de/>) revealed domains with predicted exonuclease (exo) and ATPase activity (A). Bold numbers represent amino acid positions. Signal peptides are shown in red, transmembrane domains are marked blue.

To get a first impression in when and where the *P. berghei* C2CP and ferlin are expressed during the parasite life cycle a reverse transcriptase PCR was performed on different stage-specific cDNAs.

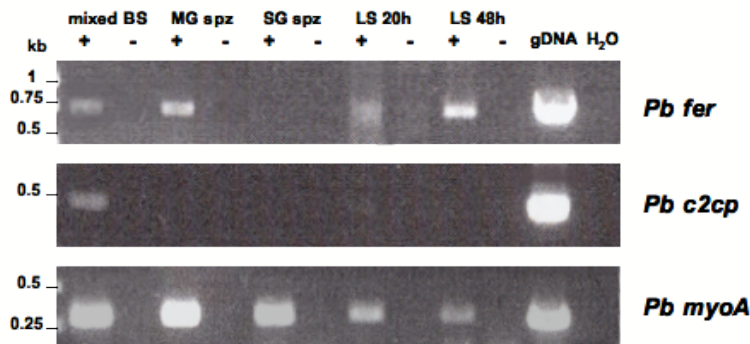


Figure 15. Reverse transcriptase PCR detects transcripts of *P. berghei* ferlin (*fer*) and C2 domain-containing protein (*c2cp*) in different parasite stages. As templates served stage-specific cDNAs synthesised from isolated *P. berghei* WT RNA from mixed blood-stages (mixed BS), midgut (MG spz) and salivary gland sporozoites (SG spz) and liver-stages after 20 hours (LS 20h) and 48 hours (LS 48h) *in vitro* development in human hepatoma cells. A standard PCR program was run with specific oligonucleotides for *Pb fer* and *Pb c2cp* fragments and *Pb myosin A* (*myoA*) as constitutively expressed control. DNA fragments were separated by agarose gel electrophoresis. +: cDNA samples prepared with reverse transcriptase; -: cDNA samples prepared without reverse transcriptase.

Transcripts of the *P. berghei* ferlin (*Pb fer*) could be amplified from cDNA of *P. berghei* WT mixed blood-stages, midgut sporozoites and late liver-stages (LS 48h). The *Pb fer* fragment amplified from early liver-stages (LS 20h) was very weak suggesting a rather low expression of *Pb fer* during this stage. The gene seems not to be expressed in salivary gland sporozoites as no fragment could be amplified from the respective cDNA preparation. The transcript of *P. berghei* C2CP (*Pb c2cp*) could only be detected in blood-stages. A hardly detectable DNA band was also found on the agarose gel when using *P. berghei* WT early liver-stage cDNA (LS 20h) as a template. The constitutively expressed *myosin A* could be amplified from the cDNA templates of all stages. This control showed the presence of cDNA in all preparations with reverse transcriptase (+) and no gDNA contaminations in the respective RNA preparations transcribed without reverse transcriptase (-).

3.2.3 *P. berghei* ferlins are essential during blood-stage development

In order to functionally characterise the *P. berghei* C2 domain-containing protein (C2CP) and the related ferlin (FER) a targeted gene depletion should be performed. Resulting depletion phenotypes could suggest potential functions of the protein. Targeted gene depletion in *Plasmodium* is conducted in blood-stage parasites. Therefore genes essential during blood-stage development cannot be targeted. A failing integration of the targeting construct, however, can also be due to poor accessibility of the genomic locus for homologous recombination. We therefore generated a knock-out construct and a complementation construct for *Pb fer* and *Pb c2cp*, that were transfected separately during the same experiment.

The different genetic strategies are shown in figure 15. For the knock-out targeting construct two fragments from the 5' and 3' untranslated regions (UTR) of the respective gene were amplified with specific oligonucleotides (for sequences see appendix 6.1). Expected fragments sizes were confirmed by agarose gel electrophoresis. The *Pb fer* fragments were 676 bp and 773 bp for the 5' and the 3' UTR fragment, respectively. The *Pb c2cp* fragments had a length of 678 bp and 612 bp, respectively. The two corresponding fragments were cloned into the targeting vector b3D (for vector map see appendix 6.2) as described, flanking the *TgDHFR/TS* selectable marker, resulting in the constructs pΔ*fer* and pΔ*c2cp*. For the control complementation constructs C-terminal fragments including the stop codon were amplified in two parts to insert a unique restriction site necessary for linearisation prior to transfection. The sizes of 952 bp and 744 bp for the *Pb fer* complementation and of 497 bp and 481 bp for the *Pb c2cp* complementation, respectively, were again confirmed by agarose gel electrophoresis. Cloning of two corresponding fragments one after another into the

clonign vector b3D+ (for vector map see appendix 6.2) resulted in the complementation constructs *pfer*CONT and *pc2cp*CONT.

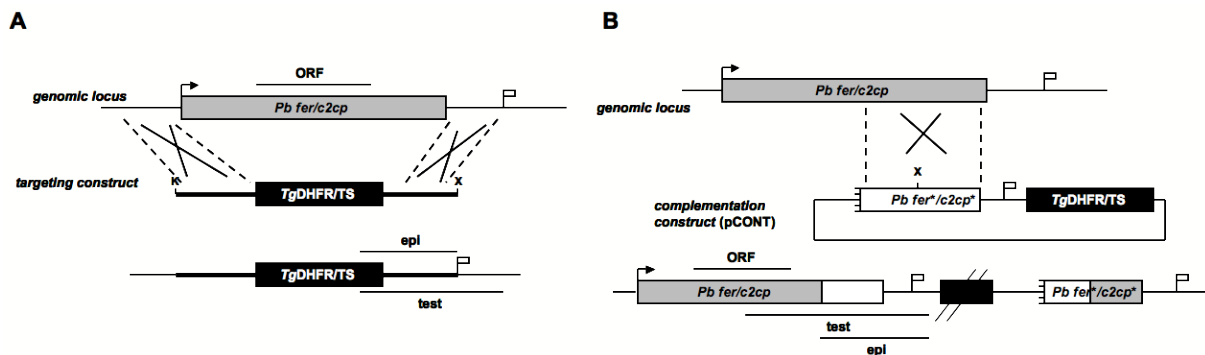


Figure 16. Knock-out (A) and complementation (B) strategy of the *P. berghei* ferlin (FER) and C2 domain-containing protein (C2CP). A. The replacement construct contains the 5' and 3' untranslated regions of the *P. berghei* *fer* or *c2cp* open reading frames flanking the *TgDHFR/TS* selectable marker. The wildtype (WT) genomic locus is targeted with the linearised *KpnI/XbaI* targeting vector. A double crossing-over event replaces the endogenous *fer* or *c2cp* ORF, respectively, by the selectable marker. B. The complementation control construct (pCONT) contains a N-terminal truncated version of the *P. berghei* *fer* or *c2cp* ORF (*fer**/*c2cp**) and the *TgDHFR/TS* selectable marker. A *XbaI*-linearised plasmid is targeting the *fer* or *c2cp* WT genomic locus, respectively, and inserts the selection marker and an additional truncated *fer** or *c2cp** copy.

The *P. berghei* ANKA GFPcon strain (Franke-Fayard et al. 2004) was transfected with the *KpnI/XbaI* digested *pΔfer* and *pΔc2cp* constructs, as well as with the *XbaI*-linearised constructs *pfer*CONT and *pc2cp*CONT according to the described AMAXA transfection protocol. Transfected merozoites were directly injected intravenously (*i.v.*) into NMRI mice. Parasitemia was checked by giemsa-stained blood smears on day 1 after transfection. Starting parasitemias were quite low with 0.1 % to 0.3 % for three independent experiments. From day 1 Pyrimethamine was provided with the drinking water to select for transfected parasites. On day 2 parasitemias decreased to undetectable levels in giemsa-stained blood smears. Under continuous drug selection resistant parasites first appeared from day 7 to 9 in the blood. Resistant parasites transfected with the knock-out constructs took on average 9 days for *pΔc2cp* and 8.5 days for *pΔfer* until detectable in thin blood smears. Parasites transfected with the complementation constructs, *pfer*CONT and *pc2cp*CONT, were slightly faster and respective mice got blood-stage positive on average 7.5 days after transfection. As soon as parasite levels in the blood increased to 0.5 % to 1 % mice were sacrificed. Infected blood was saved as cryo stock and isolated parasites were kept as parental populations for genomic DNA (gDNA). Around 50 to 100 µl infected blood was transferred intraperitonealy (*i.p.*) into naïve NMRI mice and parasitemia was monitored under drug selection. Upcoming parasites

were again collected from infected blood and kept as transfer population. Transfectants were checked by specific PCRs for integration of the targeting constructs (figure 17).

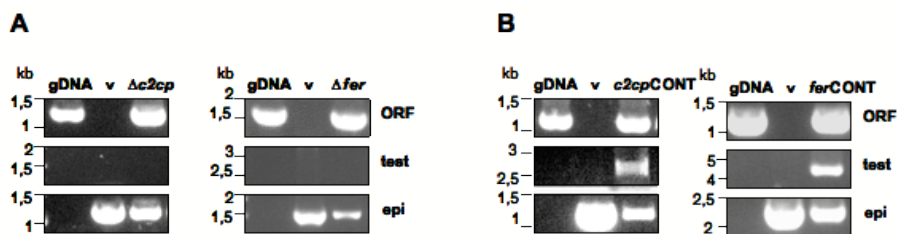


Figure 17. Genotyping PCR of *P. berghei* ferlin (*fer*) and C2 domain-containing protein (*c2cp*) knock-out (A) or complementation (B) transfectants. Standard PCRs were run with ORF, test and episomal (epi) specific oligonucleotide pairs (see figure 16). As templates served gDNA of the different transfer transfectants ($\Delta c2cp/\Delta fer/c2cpCONT/ferCONT$) and *P. berghei* wild-type gDNA (WT) or respective targeting constructs (v) as PCR controls. Specific DNA fragments were separated by agarose gel electrophoresis.

Specific oligonucleotide pairs ORF I and ORF II amplified different parts of the *Pb fer* or *Pb c2cp* open-reading frames. For the knock-out genotyping PCR (figure 16A) the DNA fragments amplified with ORF I oligonucleotides are expected to be 978 bp for *Pb c2cp* and 1696 bp for *Pb fer*. Respective bands could be seen on a agarose gel when using WT gDNA or $\Delta c2cp/\Delta fer$ gDNA as PCR templates. As expected there is no ORF I specific DNA fragment amplified when the targeting knock-out constructs were used as a template. The episomal specific oligonucleotide pairs epi I and epi II amplify vector specific fragments. Therefore epi I specific DNA bands, with the expected sizes of 1165 bp and 1326 bp for *Pb c2cp* and *Pb fer*, respectively, can be detected on a agarose gel when using respective targeting constructs, p $\Delta c2cp$ and p Δfer , as a template as well as the gDNA of resistant transfectants, $\Delta c2cp$ and Δfer , that carry the plasmids. Test oligonucleotide pairs test I and II prove integration of the targeting constructs into the parasite genome and can therefore only be amplified from gDNA of positive transfectants. The expected test I specific DNA fragments with sizes of 1301 bp and 1557 bp cannot be amplified from the transfectants gDNA indicating no integration of the targeting constructs, p $\Delta c2cp$ and p Δfer , and therefore no depletion of the respective genes, *Pb c2cp* and *Pb fer*. That looks different for the control complementation genotyping PCR. ORF II specific DNA fragments have a size of 978 bp or 1068 bp and can be visualised on a agarose gel when using WT gDNA or gDNA of the transfectants *c2cpCONT* and *ferCONT* as templates and not be amplified from the CONT complementation constructs. Epi II specific DNA bands can be detected on a agarose gel with a size of 1478 bp and 2196 bp, respectively, for transfectants' gDNA and vector control only.

The test II specific DNA fragments with sizes of 2879 bp for *c2cp*CONT and 4304 bp for *fer*CONT demonstrate a successful integration of the control complementation constructs, *pc2cp*CONT and *pfer*CONT. By that the accessibility of both genomic loci could be proven. Same genotyping results were achieved from three independent transfection experiments. In summary this experiment shows that the *Pb c2cp* and *Pb fer* genomic loci are accessible for homologous recombination, the genes, however, cannot be depleted by targeted gene disruption. From these results we conclude an essential role for *Pb C2CP* and *Pb FER* during blood-stage development.

3.2.4 Immunological characterisation of *P. berghei* C2 domain-containing protein (C2CP) reveals specific immune responses in immunised animals

The initial goal of this study was to identify new potential antigen candidates by comparative analysis of early GAP, RAS and WT liver-stage parasites. The attenuated parasite lines, GAP and RAS, arrest during liver-stage development, alert the immune system and by that confer to stage-specific protection. We hypothesised that due to this arrestment GAP and RAS liver-stages express a different, probably reduced set of transcripts in comparison to WT liver-stages. The expressed antigens, however, are sufficient for the induction of protection. This comparative analysis should therefore narrow down antigen candidates involved in pre-erythrocytic immunity.

The *P. berghei* C2 domain-containing protein (C2CP) was one of the most prominent up-regulated transcripts in attenuated parasites (UAP 1) if compared to WT. Its potential as antigen candidate became apparent as four predicted H-2^b-restricted CD8⁺ T-cell epitopes were detected with help of several prediction programs (table 6). Therefore we tested whether these *Pb* C2CP-derived peptides are specifically recognised in GAP and RAS immunised C57BL/6 mice.

The amino acid sequences of the predicted *Pb* C2CP CD8⁺ T cell epitopes, A9I, T9L, S8V and A8I are shown in table 6. In total two H-2^b-restricted nonamers and two octamers were predicted with help from the epitope prediction program SYFPEITHI (<http://www.syfpeithi.de>) and personal help from T-cell experts. The MHC-binding of T9L could later also be validated *in vitro* by a collaborating group in Copenhagen, Denmark (Harndahl et al. 2009).

The primary structure of *Pb* C2CP is shown as a horizontal bar from position 1 to 1280. It includes a signal peptide (SP) at the N-terminus, a C2 domain, and a C-terminal region ending in AAA. Four bold black bars indicate predicted CD8⁺ T-cell epitopes: A9I (positions 244-248), T9L (positions 417-425), S8V (positions 671-678), and A8I (positions 827-834). Below the bar, the sequence is divided into SP, exo, C2 domain, and AAA.

sequence	abbreviation	position	half-life [h]
AYIAPHTII	A9I	141-149	-
TIRSFYKRL	T9L	417-425	5.81
SPYLFNIV	S8V	671-678	-
AIYRFNAI	A8I	827-834	-

Table 6. Predicted CD8⁺ T-cell epitopes of the *P. berghei* C2 domain-containing protein (C2CP). Shown are the H-2^b-restricted CD8⁺ T-cell epitopes of *Pb* C2CP as predicted with help from the SYFPEITHI epitope prediction program (<http://www.syfpeithi.de>) and personal communication with T-cell experts. In the shown primary structure the bold black bars indicate the schematic localisation of the predicted T-cell epitopes. The amino acid sequences and positions of the epitopes are shown in the table. The binding affinity of T9L is determined as half-life of the MHC I-peptide complex as measured in an *in vitro* assay by collaborating partners in Copenhagen, Denmark and accounts for on average 5.81 h (mean of two independent measurements) (Harndahl et al. 2009).

Five independent immunisations with genetically-attenuated parasites (GAP; *uis3*(-)) and radiation-attenuated sporozoites (RAS) were performed according to the prime-two-boost protocol shown in figure 18. Injected sporozoites of these attenuated parasite lines invade hepatocytes and transform into liver-stages normally. But then parasites arrest during liver-stage development and do not proceed to blood-stage infection. These arresting parasites confer to stage-specific protection against subsequent WT sporozoite challenges. The attenuated parasite vaccination model is routinely used for experimental immunisations of rodents.

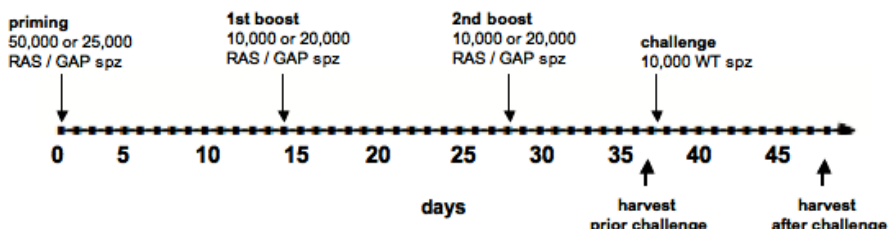


Figure 18. Schematic diagram of the prime-two-boost immunisation protocol. C57BL/6 mice were injected i.v. with *P. berghei* RAS or GAP on day 0. The first boost was typically administered 14 days later and the second boost 14 days thereafter. Booster doses were typically lower than the priming dose. 7 days after the final boost animals were either challenged with WT sporozoites (spz) or organs were dissected for immunological studies (harvest prior challenge). The challenged mice were sacrificed 7 days after the WT challenge (harvest after challenge).

Groups of five C57BL/6 mice were typically immunised in 14 days intervals according to the shown protocol (figure 18). Due to reasons of time the protocol was sometimes shorten. The first boost was then administered 7 days after the priming and the second boost 7 days thereafter. *P. berghei* GAP and WT sporozoites were isolated from mosquitoes' infected salivary glands on days 17 to 21 post infectious blood meal as described. WT sporozoites were γ -irradiated with a dose of 150 Gray resulting in RAS. The isolated sporozoite numbers per mosquito reached from 10,000 to 25,000 with a mean of 14,980 sporozoites per mosquito for GAP and 14,400 for WT. Either 7 days after the final boost or 7 days after a subsequent WT challenge, immunised mice were sacrificed and serum, livers and spleens were collected. All naïve challenge control mice developed blood-stage parasitemias of 0.3 % to 0.5 % when they were sacrificed on day 7 after the challenge, whereas all immunised mice remained blood-stage negative. Liver lymphocytes and splenocytes were isolated as described (2.12.2) and cultured over night in the presence of the *Pb* C2CP-derived peptides (2.12.4). Thereby lymphocytes from immunised mice specific to these peptides get restimulated, proliferate and produce cytokines.

The establishment of an effector memory T-cell response is important for vaccination and builds the basis for adaptive immune responses. We therefore had a look at the expression of specific surface marker of T-cells in the liver of GAP and RAS immunised animals.

The staining for surface activation marker of lymphocytes from GAP and RAS immunised mice showed a clearly enhanced effector memory T-cell population (T_{EM} ; $CD8^+CD44^{high}CD62L^{low}$) in comparison to naïve mice (figure 19). This indicates the establishment of a memory immune response during GAP immunisation which was hitherto unpublished. Mean percentages of T_{EM} -cells of 6.47 % in livers of naïve mice, increased significantly to 63.3 % in RAS immunised and to 47.3 % in GAP immunised animals ($p = 0.0003$ and $p = 0.024$; unpaired t test). In naïve WT challenged mice 18.8 % of the $CD8^+$ T-cells expressed the activation marker $CD44^{high}CD62L^{low}$, this did not differ significantly from naïve controls. Also the absolute cell numbers of T_{EM} -cells in the liver increased significantly after GAP and RAS immunisation. While a mean of 84,144 $CD8^+CD44^{high}CD62L^{low}$ cells could be counted in the liver of naïve mice, the number increased significantly to on average 1,889,755 T_{EM} -cells and 1,289,110 T_{EM} -cells in RAS and GAP immunised mice, respectively ($p = 0.0142$ and $p = 0.0089$; unpaired t test). In WT challenged mice the cell number also increased if compared to naïve mice, a mean of 405,262.5 T_{EM} -cells were detected in the liver. This increase, however, is not significant.

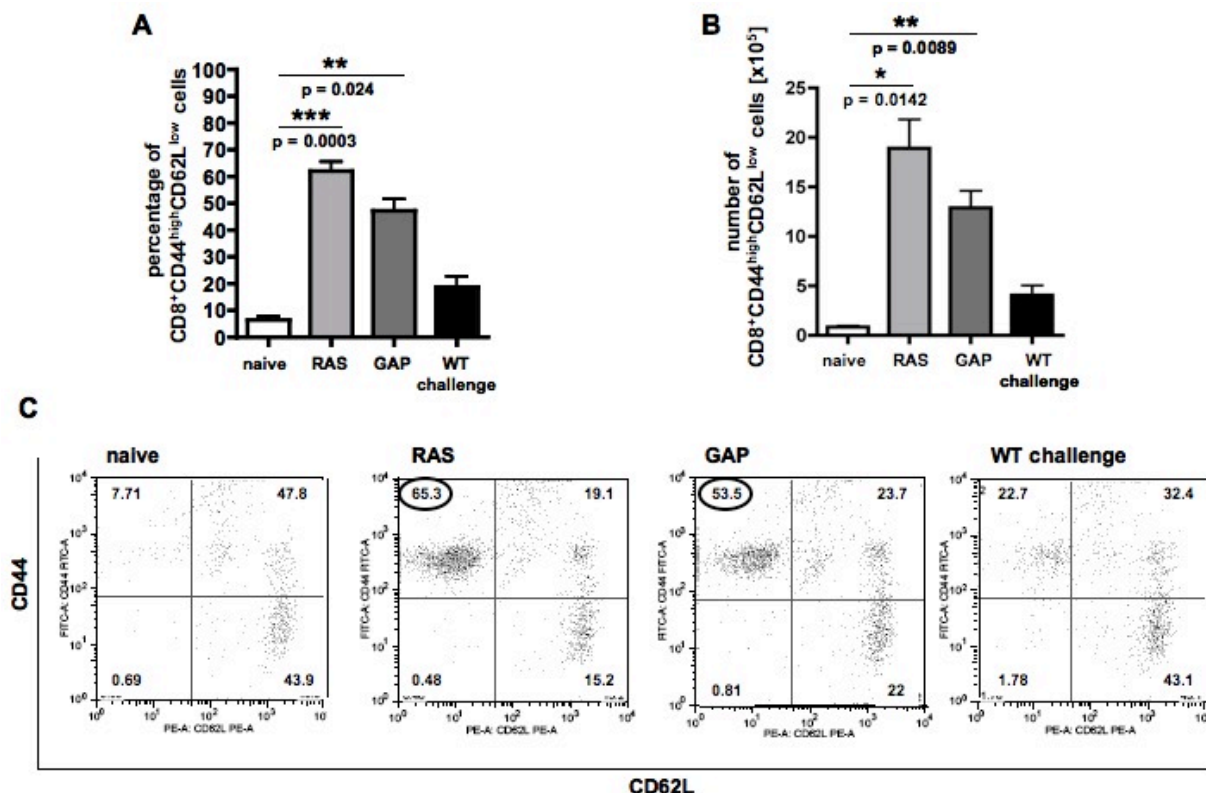


Figure 19. Effector memory T-cell population (CD8⁺CD44^{high}CD62L^{low}) in the liver increases after GAP and RAS immunisation. Liver lymphocytes of naïve, immunised and WT challenged animals were incubated over night with BMDCs and the *Pb* C2CP-specific peptide T9L. Surface staining was performed with anti CD8a-PacBlue conjugated antibody (1:100, BD biosciences), antiCD44-FITC (1:100, BD biosciences), anti CD62L-PE (1:200, BD biosciences) and anti CD25-Alexa647 (1:50, BD biosciences). Analysis of the stained cells was performed by flow cytometry using the FACSCanto system (BD biosciences). Resulting data were further analysed using the flowjo analysis software (<http://www.flowjo.com>). A. Mean percentages of CD8⁺CD44^{high}CD62L^{low} cells; B. Absolute cell numbers of CD8⁺CD44^{high}CD62L^{low} cells; C. Representative dot plots from single mice (n=5).

Subsequently an *in vivo* cytotoxicity assay should shed light on the capacity of GAP and RAS immunised animals to recognise and kill cells that carry *Pb* C2CP-derived peptides on their surface. Therefore a pool of either three (A9I, S8V and A8I) or all four predicted CD8⁺ T-cell epitope peptides A9I, T9L, S8V and A8I was loaded on CFSE-labelled splenocytes and injected *i.v.* into immunised mice together with a control cell population that carried no peptides and was labelled with a lower concentration of CFSE (2.12.3). Mice were sacrificed 18 hours later and liver lymphocytes and splenocytes were isolated as before. For the cytotoxicity assay some of these cells were directly tracked by flow cytometry where the CFSE-labelled cells can be seen in the FL1 channel of the BD FACSCalibur (excitation 488 nm, emission 517 nm). The percentage of specifically lysed cells was calculated with the following mathematical function:

$$\text{specific lysis } [\%] = 100 - \frac{\left(\text{ratio } \text{CFSE}^{\text{high}} / \text{CFSE}^{\text{low}} \text{ sample} \right)}{\left(\text{mean ratio } \text{CFSE}^{\text{high}} / \text{CFSE}^{\text{low}} \text{ naive controls} \right)} * 100$$

The percentages of specifically lysed cells in spleens and livers of RAS and GAP immunised mice 7 days after a subsequent WT challenge is shown in figures 20 and 21.

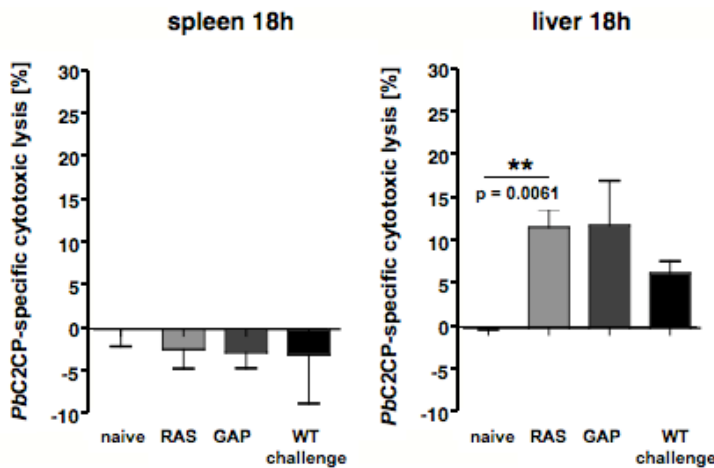


Figure 20. *In vivo* cytotoxicity assay shows lysis of target cells pulsed with the *Pb* C2CP-derived peptides A9I, S8V and A8I. Naïve splenocytes were loaded with *Pb* C2CP-derived peptides A9I, S8V and A8I and labelled with 2 µM CFSE (CFSE^{high}) (5-(and-6)-carboxyfluorescein diacetate, succinimidyl ester, Invitrogen). A control cell-population was labelled with 0.2 µM CFSE (CFSE^{low}). Cell-populations were mixed in equal numbers (1:1) resulting in final CFSE concentrations of 1 µM or 0.1 µM, respectively. 1 x 10⁷ cells of this mixed population were injected *i.v.* into tail veins of immunised or naïve control animals 18 hours prior to cell isolation. CFSE-labelled cells were tracked by flow cytometry in spleen and liver. The specific lysis was calculated as ratio of CFSE^{high} cells and CFSE^{low} cells and compared to the ratio detected in naïve animals. Shown are the mean percentages of lysed cells from groups of 3 - 5 mice.

There is no specific cytotoxic lysis detectable in the spleens of immunised and challenged animals when using a pool of the three *Pb* C2CP-derived peptides A9I, S8V, A8I. Specific lysis, however, could be observed in the liver. A significant increase from less than 0.0001 % in naïve animals to 11.6 % in RAS immunised animals could be observed. We could also detect an average of 11.8 % specific lysis in the livers of GAP immunised animals. Though this increase was not significant to naïve mice due to a very high standard deviation. The specific cytotoxic lysis in livers of WT challenged mice accounted for on average 6.3 %.

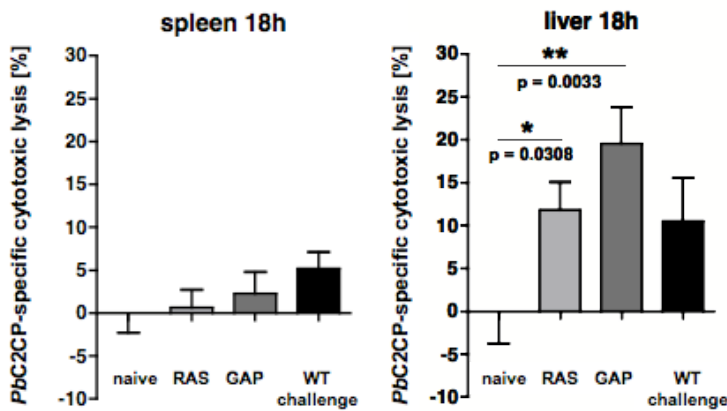


Figure 21. *In vivo* cytotoxicity assay shows lysis of target cells pulsed with a pool of all four *Pb* C2CP-derived peptides in immunised animals. Naïve splenocytes were loaded with a pool of all four *Pb* C2CP-derived peptides (A9I, T9L, S8V and A8I) and labelled with CFSE together with a control cell-population as described before. 1×10^7 cells were injected *i.v.* into tail veins of immunised or naïve control animals 18 hours prior to cell isolation. CFSE-labelled cells were tracked by flow cytometry in spleen and liver. The specific lysis was calculated as ratio of CFSE^{high} cells and CFSE^{low} cells and compared to the ratio detected in naïve animals. Shown are the mean percentages of lysed cells in three independent experiments, each with 3 - 5 mice per group.

When adding the peptide T9L to the pool there was also no specific cytotoxic lysis detected in the spleen of immunised animals. In the livers of RAS and GAP immunised mice, however, 11.8 % and 19.6 % *Pb* C2CP-specific cells, respectively, get lysed. This is significantly more than in naïve control animals where on average less than 0.001 % of the fluorescently labelled *Pb* C2CP-specific cells get lysed. In WT challenged mice also 10.5 % of the *Pb* C2CP-specific are killed. These mice had seen *P. berghei* WT liver-stages before but in contrast to immunised mice had developed a blood-stage infection. These results demonstrate that *Pb* C2CP-specific cells get indeed recognised and killed in immunised or exposed animals. Immune responses directed against the *Pb* C2CP-derived peptides could be detected.

To decipher *Pb* C2CP-specific immune responses in RAS and GAP immunised animals in more detail, the single *Pb* C2CP-derived peptides A9I, S8V, A8I T9L were used for restimulation in the following experiments. Below mice were not challenged with WT sporozoites after GAP and RAS immunisation.

The ELISpot (Enzyme-linked immunosorbent spot) is an extremely sensitive assay that allows the detection of cytokines on single cell level. We therefore applied this method to measure low IFN- γ responses in the livers and spleens of RAS and GAP immunised mice that could not be detected by FACS (data not shown). Purified liver lymphocytes or total

splenocytes from immunised mice were restimulated over night with the *Pb* C2CP-derived peptides A9I, S8V, A8I and T9L as described before. Prior to the transfer of restimulated cells to IFN- γ coated MultiScreen filter plates, culture medium was exchanged by fresh medium to dilute secreted IFN- γ in the culture supernatant and reduce background. After 24 hours incubation of the stimulated cells on filter plates spots were detected by a secondary biotinylated anti IFN- γ antibody. Every spot that developed on the membrane represented a single reactive cell. Spots were counted under a dissection microscope. Controls for the stimulated cells from immunised animals were cells incubated without stimulus and cells isolated from naïve animals. A positive control, naïve lymphocytes activated with an anti-CD3 antibody, was run along to prove that the assay is working.

In two independent immunisation experiments we restimulated with the three single *Pb* C2CP-derived peptides A9I, S8V and A8I. The measured IFN- γ responses in spleens and livers are shown in figure 22.

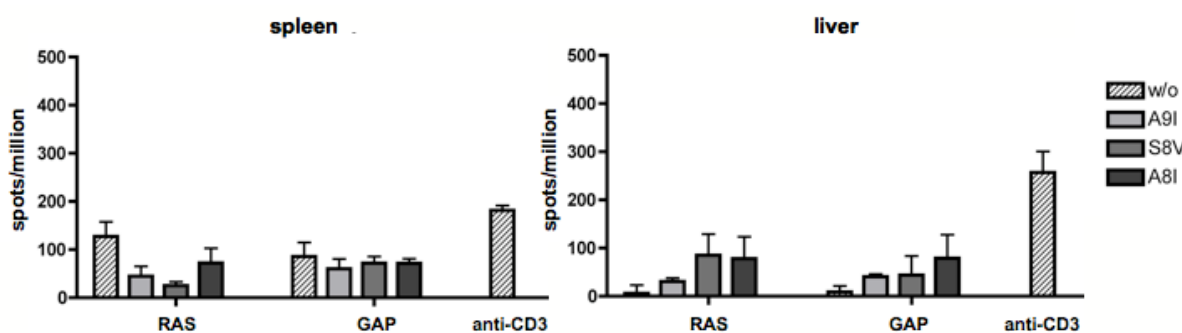


Figure 22. Interferon- γ (IFN- γ) responses of effector T-cells measured by cytokine-based ELISpot after restimulation with the *Pb* C2CP-derived peptides A9I, S8V, A8I. Cultured lymphocytes from immunised animals were restimulated over night with 1 μ M of the *Pb* C2CP-derived peptides A9I, S8V, A8I or incubated without stimulus (w/o). Cells were subsequently transferred to MultiScreen filter plates coated with 5 μ g/ml IFN- γ antibody. The IFN- γ response is shown as counted spots per million cultivated cells. Counts of naïve control animals were subtracted. Shown are the means of counted triplets from two independent experiments ($n = 5$).

The detected IFN- γ responses were low in spleens of immunised animals reaching from 25 to 125 reactive cells per million cultivated splenocytes. We measured no differences in the IFN- γ production of restimulated cells if compared to non-stimulated controls in the spleen. In the liver of immunised animals the IFN- γ responses are also unexpectedly low. This was due to extremely high responses in naïve animals that were subtracted. The data analysis revealed no

enhanced IFN- γ responses in livers of immunised animals after restimulation with the *Pb* C2CP-derived peptides A9I, S8V and A8I.

In two more independent immunisation experiments we used the single *Pb* C2CP-derived peptide T9L for specific restimulation of splenocytes and liver lymphocytes after RAS and GAP immunisation. The respective results are shown in figure 23.

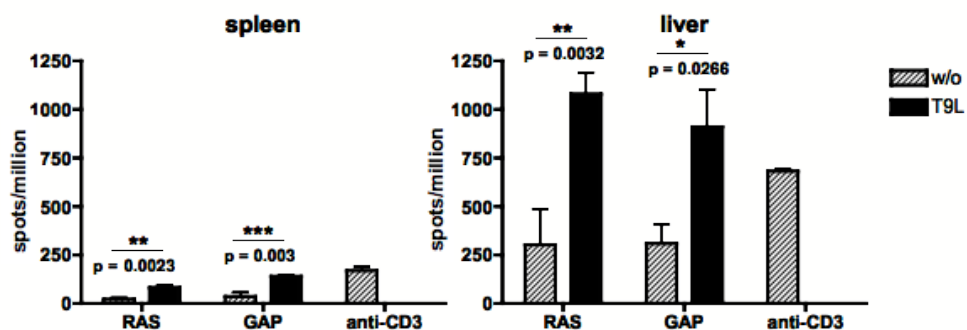


Figure 23. Cytokine-based ELISpot measures Interferon- γ (IFN- γ) responses of effector T-cells from RAS and GAP immunised mice. Cultured lymphocytes from immunised animals were restimulated over night with 1 μ M of the *Pb* C2CP-derived peptide T9L or incubated without stimulus (w/o). Cells were subsequently transferred to MultiScreen filter plates coated with 5 μ g/ml IFN- γ antibody. The detected IFN- γ response is shown as counted spots per million cultivated cells. Counts of naïve control animals were subtracted. Shown are the means of counted triplets from two independent experiments ($n = 5$).

The IFN- γ responses of restimulated splenocytes after GAP and RAS immunisation were also low (figure 21). The anti-CD3 positive control, however, showed similar responses compared to the T9L stimulated cells, with a mean of 168 spots per million total splenocytes. This indicates a low number of IFN- γ producing cells in the spleen. Though the IFN- γ response increased significantly in spleens of RAS and GAP immunised C57BL/6 mice when restimulated with the *Pb* C2CP-derived peptide T9L ($p = 0.0023$ and $p = 0.003$; unpaired t test). The IFN- γ responses of purified liver lymphocytes were in total higher than those of the splenocytes suggesting more activated T-cells in the liver were the parasite infection occurs. When specifically restimulating liver lymphocytes from GAP-immunised animals with *Pb* C2CP-derived peptide T9L the responses of 911 reactive cells, from RAS-immunised animals even 1078 responding lymphocytes per million cells were detected. As control, unspecific stimulation of naïve cells with anti-CD3 antibody resulted in on average 681 reactive cells per one million liver lymphocytes. The detected IFN- γ responses after restimulation with T9L were significantly enhanced in RAS and GAP immunised animals (p

= 0.0032 and p = 0.0266; unpaired t test). These results shown, that T-cells from GAP and RAS immunised C57BL/6 mice can indeed be specifically restimulated with at least one *Pb* C2CP-derived peptide.

3.2.5 First immunisation studies with *P. berghei* C2CP-derived peptide T9L

Cells carrying *P. berghei* C2CP-derived peptides were recognised and attacked by the immune system in GAP and RAS immunised mice and the peptide T9L was able to specifically restimulate T-cells. Therefore immunisation studies with this peptide should be performed in C57BL/6 mice in order to have a first impression in the protective potential of this single peptide. For immunisations with peptides a suitable adjuvant system is very important. Here we used the TargoSphere® delivery system from Rodos Bio Target GmbH (RBT; <http://www.biotargeting.eu>). These nanocarrier target professional antigen-presenting cells (APCs) via their C-type lectin receptors (CLRs) on the surface and enter the cells' endolysosomal system. The content of the nanocarrier by that gain access to the intracellular antigen presentation pathways. The *Pb* C2CP-derived peptide T9L was packed by the company into nanocarrier then called RBT06.01 TS. The packing efficiency was 10 % resulting in a Targosphere solution with a final peptide concentration of 21.277 µg/ml. As control served nanocarrier packed with a FITC:Dextran mixture (FITC:Dextran TS). The final FITC:Dextran concentration in the Targosphere solution was 172.8 µg/ml.

Groups of C57BL/6 mice (n = 3) were immunised with 5 µg or 1 µg peptide or FITC:Dextran, respectively. Per mouse aliquots of 47 µl or 235 µl RBT06.01 TS or 5.8 µl or 29 µl FITC:Dextran TS were prepared. In order to inject same volumes the FITC:Dextran TS solution was filled up to 47 µl or 235 µl, respectively, with PBS. The solutions were administered subcutaneously into a skin fold at the back. Immunisation was performed according to the shorten prime-two-boost protocol described earlier (3.2.4; figure 17). That means injections were made every 7 days. Seven days after the final boost immunised mice were exposed to the bites of 5 infected mosquitoes each. As challenge control three naïve mice were also exposed. Subsequent dissection of the mosquitoes revealed a rather low infectivity with only around 8,000 salivary gland sporozoites per mosquito. Parasitemia was followed by daily giemsa-stained blood smears from day 3 post challenge.

vaccine	dose	challenge	pre-patency
RBT06.01 TS	1 µg	5 infected mosquitoes	4.3 days (3 / 3)
RBT06.01 TS	5 µg	5 infected mosquitoes	6.3 days (3 / 3)
FITC:Dextran	1 µg	5 infected mosquitoes	5 days (3 / 3)
FITC:Dextran	5 µg	5 infected mosquitoes	5 days (3 / 3)
no		5 infected mosquitoes	5 days (3 / 3)

Table 7. Pre-patency of mice immunised with nanocarrier RBT06.01 TS packed with *P. berghei* C2CP-derived peptide T9L. The peptide T9L was packed into specialised nanocarrier (TargoSpheres®) by the Rodos Bio Target GmbH. Different doses of RBT06.01 TS or control nanocarrier packed with FITC:Dextran were administered subcutaneously into C57BL/6 mice thrice in a 7 days interval. Seven days after the last boost mice were exposed to bites of infected mosquitoes. All mice developed blood-stage parasitemia as observed by daily giemsa-stained blood smears from day 3 post challenge. The pre-patency was determined as time until the first appearance of a single parasites in the peripheral blood.

The *P. berghei* NK65 CS-GFP strain was used for sporozoite challenge (Natarajan et al. 2001). This strain expresses the cytoplasmic green fluorescent protein (GFP) under the control of the stage-specific circumsporozoite protein (CSP) promotor. Sporozoites of this strain therefore fluoresce bright green. This again allows the pre-selection of infected mosquitoes under a fluorescent stereo-microscope. All challenged mice developed a blood-stage parasitemia between day 4 and day 7 post infection. The non-immunised mice developed a detectable blood-stage parasitemia by day 5. This is rather late as parasites are expected to come up on day 3 to 4 in naïve animals after sporozoite challenge. Interestingly a slight delay in pre-patency was observed in animals immunised with 5 µg RBT06.01 TS in comparison to FITC:Dextran immunised controls. The time until the first parasites could be detected in giemsa-stained blood smears extended on average from 5 to 6.3 days post wild-type sporozoite challenge.

Eight days post challenge animals were sacrificed, lymphocytes were isolated from livers spleens and lymph nodes and cells were prepared for cytokine ELISpot as described earlier (2.12.2 / 2.12.4 / 2.12.6). As a control organs from naïve C57BL/6 mice were treated equally. Cells from the groups were pooled and restimulated with T9L or cultured without stimulus over night prior to transfer on the MultiScreen filter plates. IFN-γ production was measured as a read-out for activated T-cells.

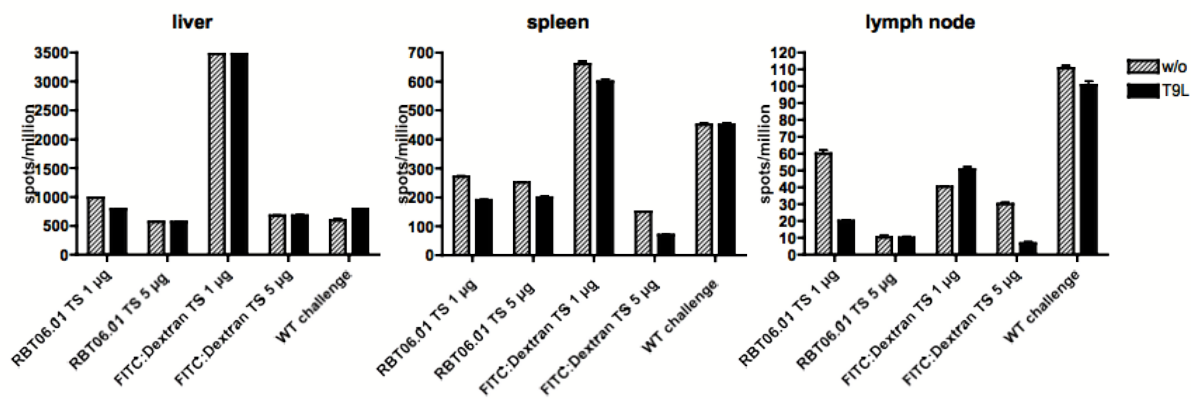


Figure 24. Cytokine-based ELISpot to measure Interferon- γ (IFN- γ) responses of activated T-cells from RBT06.01 TS immunised mice. Pools of cultured lymphocytes from immunised animals were restimulated over night with 1 μ M of the *Pb* C2CP-derived peptide T9L or incubated without stimulus (w/o). Cells were subsequently transferred to MultiScreen filter plates coated with 5 μ g/ml IFN- γ antibody. The detected IFN- γ response is shown as counted spots per million cultivated cells. Counts of naïve control animals were subtracted. Shown are the means of counted triplets from groups of three mice.

Measured T-cell responses varied quite strong between the different organs as seen on the scale of the y axis. In total the IFN- γ responses were the highest in the liver and only little responding cells were detected in the lymph nodes. The group treated with 1 μ g FITC:Dextran Targospheres shows exceptional high responses if compared to the other groups. This however was not due to a single outlier.

In summary we detected no enhanced IFN- γ responses after specific restimulation of effector T-cells in mice immunised with the *P. berghei* C2CP-derived peptide T9L packed in specialised nanocarrier (RBT06.01). This suggests that either this system is not suitable for immunisation with single peptides or the single peptide alone has not enough potential in stimulating protective immune responses.

3.2.6 Recombinant expression of *P. berghei* C2 domain-containing protein (C2CP)

For recombinant over-expression in *E. coli* the *P. berghei* C2CP was divided in three parts. This should simplify expression and improve solubility of the otherwise very large protein. The division of the protein was done on the one hand with respect to hydrophobic regions as determined by the ProtScale analysis tool on the ExPASy Proteomics Server (<http://www.expasy.ch/tools/protscale.html>) using the Kyte & Doolittle scale. Numbers > 0 display hydrophilic regions, whereas number < 0 display hydrophobic regions. Thus the *Pb* C2CP parts I - III (table 8) were defined at the end of hydrophilic protein regions expecting a better solubility of the expressed protein parts. On the other hand the protein was also divided

with respect to the guanine/cytosine (GC) content of the DNA sequence coding for *Pb* C2CP. This was important to consider in order to design suitable oligonucleotides for cloning of the expression constructs. The positions of the different chosen protein parts are shown in table 8.

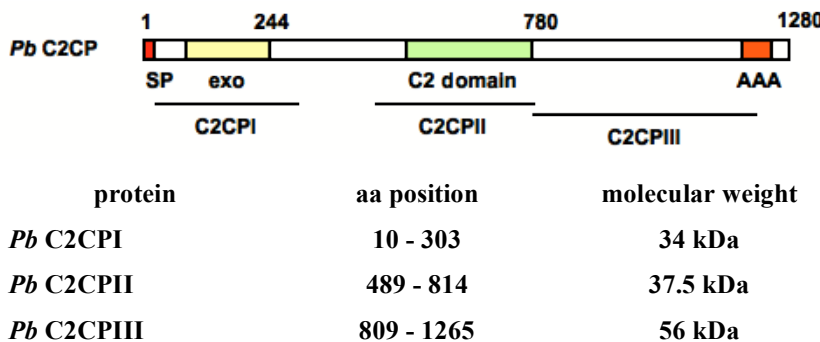


Table 8. Division of the *P. berghei* C2 domain-containing protein (C2CP) for recombinant expression. The 1280 amino acid protein *Pb* C2CP was sub-divided into the three parts C2CPI, C2CPII and C2CPIII for easier expression. The rough position is indicated by the black bars in the primary structure. Detailed amino acid (aa) positions and calculated molecular weights are listed in the table. The molecular weight was calculated with help of the ProtParam tool on the ExPASy Proteomics Server (<http://www.expasy.ch/tools/protparam.html>).

The sequences coding for *Pb* C2CPI - III were cloned into the expression vector pET15b (Novagen). This results in the expression of fusion proteins with a N-terminal 6 x Histidin-tag (C2CPI-III-His). The DNA sequences coding for C2CPI, C2CPII and C2CPIII with a size of 882 bp, 978 bp and 1371 bp, respectively, were cloned using the restriction endonuclease recognition sites *Nde*I and *Xho*I. Cloning was successful for all three constructs (vector maps attached under 6.2), however, expression was only performed for C2CPI-His.

For recombinant over-expression codon optimised *E. coli* BL21 competent cells (BL21-CodonPlus (DE3)-RIPL, Stratagene) were transformed with the pETc2cpI construct. Expression was performed in 25 ml LB-medium with ampicillin (100 µg/ml). The culture starting with an OD₆₀₀ of 0.1 - 0.2 was cultivated shaking at 37 °C until an OD₆₀₀ of 0.5 was reached. Expression was induced by the addition of 1 mM IPTG to the culture and good expression was achieved after 4 hours at 37 °C, 250 rpm, as tested by applying samples on a SDS-PAGE after different time points. To test the solubility of the expressed C2CPI-His bacteria cells were lysed by sonication. For this the cell pellet was resuspended in a lysis buffer containing 0.05 % Tween 20 and lysozyme (1 mg/ml). The lysozyme was allowed to crack the bacterial cell wall for 30 minutes on ice, a subsequent sonication for 2 x 30 seconds should completely lyse the cells. After centrifugation soluble protein was in the supernatant,

whereas insoluble protein expressed as inclusion bodies or potentially bound to membranes would be in the pellet together with the cell debris.

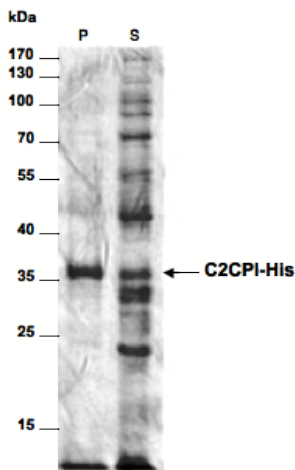


Figure 25. Recombinant overexpression of the *P. berghei* C2CPI-His fusion protein in *E. coli* BL21. The Coomassie stained SDS gel shows insoluble pellet (P) fraction alongside with the soluble supernatant (S) fraction. Expression was performed in codon optimised *E. coli* BL21 (Stratagene) at 37 °C, 250 rpm. 4 hours after induction with 1 mM IPTG cells were centrifuged and sonicated in lysis buffer. Supernatant and pellet in 8 M urea were mixed 1 : 1 with 2 x SDS loading dye and heated for 5 minutes at 95 °C prior to loading on the gel. As protein standard served the PageRuler™ Prestained Protein Ladder (Fermentas).

As seen in figure 25 only around half of the expressed C2CPI-His with a calculated molecular weight of 34 kDa was found in the supernatant. Efforts to increase the amount of soluble protein unfortunately failed. Neither induction with lower IPTG concentrations (0.1 mM, 0.25 mM or 0.5 mM) nor expression at lower temperatures (room temperature or 16 °C) improved the solubility. Even when scaling-up the culture volume to 100 ml in order to obtain more protein the solubility was impaired. Therefore the expression was finally performed in 4 flasks with 25 ml culture each as described initially. Supernatants were combined and C2CPI-His was purified by nickel ion affinity chromatography. For an optimal binding of the His-tagged fusion protein on the HIS-Select® Nickel Affinity Gel (Sigma) lysis of the cells was performed in a sodium phosphate buffer with a pH of 8.0.

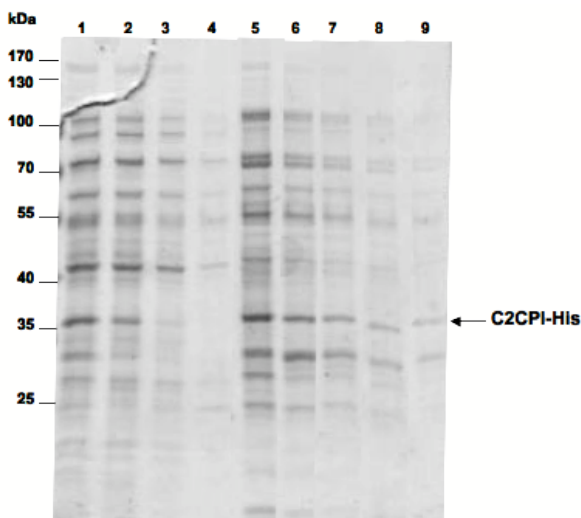


Figure 26. Purification of the C2CPI-His fusion protein by nickel ion affinity chromatography. The Coomassie stained SDS gel shows the single fractions collected during column purification of the C2CPI-His fusion protein using the HIS-Select® Nickel Affinity Gel (Sigma). 1. cell lysate prior to purification; 2. flow-through; 3./4. washing steps; 5. - 9. elution. The samples were mixed with 2 x SDS loading dye and heated for 5 minutes at 95 °C prior to loading on the gel. As protein standard served the PageRuler™ Prestained Protein Ladder (Fermentas).

All fractions collected during column purification were applied to a SDS gel shown in figure 26. The fusion protein did not bind properly on the column matrix. Therefore C2CPI-His could partly be detected in the flow-through and the two following washing steps. The His-tagged fusion protein, however, could be concentrated by elution with 250 mM imidazol in 5 fractions with 1 ml each. Fractions 1 to 4 were combined and dialysed against PBS to remove the imidazol.

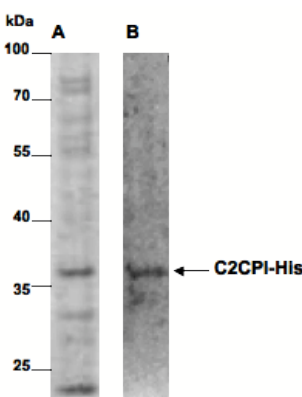


Figure 27. Coomassie stained SDS gel (A) and Western Blot (B) of purified C2CPI-His after dialysis against PBS. Pb C2CPI-His was purified by nickel ion affinity chromatograph and subsequently dialysed against PBS to remove the imidazol from the elution buffer. The sample was mixed with 2 x SDS loading dye and heated for 5 minutes at 95 °C prior to loading on the gel. As protein standard served the PageRuler™ Prestained Protein Ladder (Fermentas).

The purified C2CPI-His sample was not absolutely clean. Therefore the purification should be optimised by the addition of low concentrations of imidazol to the equilibration and washing buffer. Imidazol concentrations between 2 and 6 mM resulted in no improved purification and showed similar protein patterns on a SDS-PAGE in the purified protein samples. An imidazol concentration of 10 mM however was too high as the C2CPI-His protein did not bind on the column at all and the complete protein was found in the flow-through. Finally no cleanly purified protein sample could be obtained with the used protocols. Different expression conditions or buffers have to be tested in order to improve solubility and purity of the protein sample.

4. Discussion

Even more than 60 years after its discovery the malaria liver-stage still remains the most elusive stage of the *Plasmodium* life cycle (Shortt and Garnham 1948). Though this clinically silent stage provides an ideal target for causal-prophylactic drugs and vaccination as it is the only stage that can be completely eliminated by sterilising protective immunity. Administration of radiation-attenuated sporozoites (RAS) remains still the "gold standard" in vaccination against malaria (Nussenzweig et al. 1967). Recently, a new generation of attenuated parasites have been generated by depletion of a single liver-stage essential gene, the genetically-attenuated parasites (GAP) (Mueller et al. 2005a). Like RAS, GAP arrest during liver-stage development and by that confer stage-specific sterile protection against subsequent WT sporozoite challenges. Thereby these live-attenuated parasites provide us with an ideal tool to study protective pre-erythrocytic immune responses in the mammalian host.

To date only little is known about GAP-mediated immunity. Studies in knock-out mice revealed that CD8⁺ T-cells are the major players in conferring this protection (Mueller et al. 2007). In order to study the underlying mechanisms, however, and to specifically enhance effector T-cell numbers *in vitro* we need immunogenic antigens recognised in GAP-immunised mice for specific restimulation of T-cells *ex vivo*. Unfortunately, no defined and presented antigen epitope so far exist in the here used GAP experimental vaccine model. In Balb/c inbred mice around 90 % protection can be achieved with a single dose of RAS, this is associated with a strong immune response against the main surface protein of the sporozoites, the circumsporozoite protein (CSP). The presentation of a single protective H-2K^d-restricted CD8⁺ T-cell epitope of CSP, SYIPSAEKI for *P. berghei* and SYVPSAEQI for *P. yoelii*, could be shown (Rodrigues M. M. et al. 1991). For the GAP vaccination model in this study, however, the rodent strain *Plasmodium berghei* was used, whose most susceptible host for liver-stage development is the inbred mouse strain C57BL/6 (Scheller et al. 1994). In the C57BL/6 genetic mouse background there is no CSP epitope defined as these mice express the MHC haplotype H-2^b. Protective immunity, however, can be achieved when using a prime-two-boost immunisation protocol (Mueller et al. 2005a). We therefore believe that other pre-erythrocytic antigens must mediate this immunity that are so far not identified. The goal of this study was to perform a detailed analysis and dissect protective immune responses induced by GAP. In particular we firstly wanted to validate that GAP-mediated immunity is independent of immune responses specific to CSP and secondly we searched for new antigen candidates involved in GAP-mediated immunity, whose identified epitopes might then be

used for a specific and in-depth immunological study by e.g. restimulation of antigen-specific T-cells.

***P. yoelii* CSP CD8⁺ T-cell epitope mutants - different strategies and unexpected outcomes**

CSP has historically been considered the major antigen involved in pre-erythrocytic immunity. Strong immune responses against defined epitopes were characterised extensively (Nardin and Nussenzweig 1993). Recently, several studies showed immune responses independent of CSP (Gruner et al. 2007) (Kumar et al. 2006) and also in the GAP model used in here protection is achieved despite the absence of CSP-specific immune responses (Mueller et al. 2007). As CSP is essential for sporozoite development (Menard et al. 1997), CSP disruption by targeted gene depletion results in no infectious sporozoites and consequently no CSP knock-out liver-stages are available. Therefore it is difficult to study pre-erythrocytic immune responses independent of CSP. We designed an experimental tool by mutating the *P. yoelii* CD8⁺ T-cell epitope so that the epitope will no longer be recognised by the host's immune system without affecting CSP functionality within the parasite. As we were not fully aware of which amino acids might be essential for proper folding and therefore protein function, we inserted different mutations into the sequence coding for the CD8⁺ T-cell epitope inside the *Py csp* gene. Mutation of the DNA sequence was successful for basically two different approaches leading to alanisation of either the two amino acids that are important for anchoring the *P. yoelii* CSP CD8⁺ T-cell epitope onto MHC class I complex (V₂₈₂ and Q₂₈₇; mutant me01) or the alanisation of the amino acids whose residues are potentially not important for folding and functionality (S₂₈₀, V₂₈₂, S₂₈₄ and I₂₈₈; mutant me03) as predicted by a protein expert colleague (see table 1). When inserting these mutated sequences into the parasite's genome via homologous recombination, however, we had to face several problems. The initial complementation targeting construct pcspΔepi me01 successfully integrated into the genomic locus after *P. yoelii* transfection (see figures 5 and 6). After parasite cloning by limited dilution, however, the mutated sequence coding for the CSP CD8⁺ T-cell epitope reverted to the wild-type epitope sequence by DNA repair mechanisms. This was detected after subsequent sequence analysis of the resulting clones. The analysed sequences still showed integration of the targeting construct as both the selectable marker and the inserted restriction sites could be confirmed within the analysed DNA sequence (figure 38). Indeed, there are several DNA repair mechanisms reported in *Plasmodium*. It was shown that a cell-free lysate of asexual *P. falciparum* blood-stage parasites repaired DNA lesions by the long-patch base excision repair (BER) pathway. This pathway fills apurinic/apyrimidinic sites (AP

sites) with several nucleotides, whereas in other organisms like yeast, *E. coli* and also humans AP sites are predominantly repaired by the replacement of single nucleotides (short-patch BER pathway) (Haltiwanger et al. 2000). Further studies demonstrated, that bulky DNA lesions induced by ultraviolet (UV) light could also be repaired by a *P. falciparum* lysate (Trotta et al. 2004). This indicates the presence of the nucleotide excision repair (NER) pathway, that is involved in the repair of larger DNA lesions than the BER pathway. Interestingly, this repair mechanisms is impaired in the highly drug-resistant human *P. falciparum* W2 isolate and therefore defects in DNA repair may be one mechanism of the rapid development of drug resistance in *Plasmodium* (Trotta et al. 2004). This was recently supported by another study, where a third DNA repair mechanism in *P. falciparum*, the mismatch repair (MMR), was also linked to the development of resistance (Castellini et al. 2011). This MMR pathway generally corrects mismatch DNA during replication. Disruption of the MMR gene MSH2-2 in *P. berghei* indeed led to an increased number of DNA polymorphisms in comparison to a control parasite after less than 40 life cycles (Bethke et al. 2007). The most supposable DNA repair mechanism that reverted the *P. yoelii* CSP CD8⁺ T-cell epitope in this study may be the BER pathway, because we modified at most two or three consecutive nucleotides in the respective DNA sequence.

Subsequently we wanted to transmit the mutated parental population *Py* CSP me01 to mosquitoes, but we observed an unexpected exflagellation defect prior to transmission. As this exflagellation defect could not be explained with the described CSP function we had a closer look at the *P. yoelii* *csp* genomic locus and its surrounding genetic environment. And indeed, in the PlasmoDB database we found an extremely closely located gene upstream of the *P. yoelii* *csp* annotated as a hypothetical protein, for now, called *csprae* (PY07369) (see figure 7). The flanking regions of the two genes, probably involved in regulation of gene expression, overlap because of this extremely close proximity meaning that *csprae* most likely is located within the *csp* 5' UTR and *csp* is found within the *csprae* 3' UTR. For that it would be difficult to target *csp* by insertion of a large complementation construct without affecting the 3' regulatory region of the neighbouring gene. The integration of the whole targeting construct into the *csp* genomic locus disrupts the natural genomic sequence and thereby potentially interrupts the 3' UTR of the upstream located gene (see figure 5). That 3' regulatory regions are highly important for expression in *Plasmodium* was described before. The 3' UTR of group A *var* genes, that code for *PfEMP1* proteins, for example regulates the expression of these genes (Muhle et al. 2009). It was demonstrated that the DownsA 3' UTR of this *var* genes can regulate gene expression by the suppression of the UpsA promotor. For

the *P. falciparum* pfs25 protein, a surface protein important for parasite development inside the mosquito, it was shown that several elements in the 3' gene-flanking region are necessary for expression (Oguariri et al. 2006). This study revealed the required role of an AT-rich region 137-231 nucleotides (nt) from the stop codon for gene expression, as well as the presence of a specific nonamer sequence 360 nt from the stop codon, that enhanced expression by more than 50 %. With our genetic strategy we indeed targeted the genomic sequence 140 nt from the stop codon of *csprae* by insertion of the complete targeting construct, even though the first additional nucleotides were inserted about 880 nt from the stop codon, namely the *XbaI* recognition site (see figure 5).

Therefore it should be proven whether this exflagellation phenotype was indeed a consequence of affecting *P. yoelii* *csprae* gene expression. The targeting construct *pΔcsprae* was generated to functionally degrade *csprae* by deletion of the sequence coding for the first 9 amino acids (see figure 8). With this strategy the promotor region of the *csp* gene should be untouched as the deletion would be inserted around 1 kb upstream of the *csp* start codon. Despite the close proximity of *Py csp* and the small hypothetical protein *Py csprae*, this was possible because of two large introns in the *csprae* coding sequence. The *csprae* endogenous locus could not be genetically depleted in at least two independent transfection experiments. Unfortunately it could not be solved whether the transfactions failed because *csprae* is essential during blood-stage development or because of technical issues. Maybe the damage of the *csprae* 3' regulatory region by insertion of the knock-in construct *pcspΔepi* only reduced the *csprae* expression to a lower extent leading to an exflagellation defect, similar to the above described region downstream of the *pfs25* gene, that regulates expression intensity (Oguariri et al. 2006). Whereas depletion of parts of the gene coding sequence by integration of the *pΔcsprae* targeting construct resulted in a complete loss-of-function and therefore in non-viable parasites. Similar annotations of this closely located gene upstream of *csp* were not found for the *P. berghei* or *P. falciparum* genome in the PlasmoDB database. The neighbouring annotated genes localise 1.5 kb and 1.4 kb upstream of the *Pb* and the *Pf csp* coding sequence, respectively (from stop codon neighbouring gene to start codon *csp*).

In order to circumvent the initially observed repair mechanisms we subsequently focussed on another genetic strategy to insert the mutations into the *P. yoelii* genome (figure 9). The initial complementation strategy left the sequence coding for the WT CD8⁺ T-cell epitope in a truncated *csp* gene, that is not expressed as a functional protein. As this WT epitope sequence might have been served as a template for the observed repair mechanisms we then inserted the mutated sequences by a double cross-over event. Another advantage of this so-called

replacement strategy is the more stable integration of the targeting construct into the parasite genome in comparison to the initial complementation strategy. After parasite transfection with the targeting constructs *pcsp**replΔepi* me01 and me03 genotyping PCRs showed successful integration of the constructs (figure 11). However cloning never succeeded for unknown reasons. Unfortunately, both parental mutant lines me01 and me03 generated by integration of the replacement construct *pcsp**replΔepi* did not complete the parasite life cycle within the mosquito. Maybe the functionality of CSP was yet affected due to the inserted point mutations in the epitope sequence. Recently, the protein structure of recombinant *P. falciparum* CSP was analysed showing the folding of the C-terminal located thrombospondin-like type I repeat (TSR) domain and therein the localisation of disulfid bonds important for stabilisation of the protein (Plassmeyer et al. 2009). If not protein folding maybe also function of the TSR domain (amino acids 297-345 for *P. yoelii* CSP) might be impaired by the mutation of closely located amino acid residues inside the *Py* CSP CD8⁺ T-cell epitope (amino acids 280-288).

What exactly caused the observed phenotypes is not known. In order to overcome all these challenges probably more mutations and maybe even other genetic strategies have to be considered. Like for the *csp* knock-out generated by Menard *et al.* where an additional 1.4 kb fragment upstream of the *csp* gene was included into the targeting vector (Menard et al. 1997). This at least would prevent double-strand breaks in the endogenous *csp* promotor and ensure normal expression of the gene. In the long run we aimed at generating *P. yoelii* CSP CD8⁺ T-cell epitope mutants in the GAP (*uis3(-)*) background. Immunisation studies with such mutant GAPs would finally aid dissecting the role of CSP in GAP-mediated immunity. These GAP CSP-mutants, that do not induce CSP-specific CD8⁺ T-cells clones, would provide a tool to study induced protective immune responses independent of CSP. If animals immunised with the CSP-mutant GAPs were still protected, this would further validate that GAP-induced protection is independent to immune responses specific to CSP.

RAS liver-stages express a broader up-regulated transcript repertoire in comparison to GAP

Within this part of my thesis we aimed at identifying possible novel antigen candidates involved in GAP-mediated immunity, that may potentially act as vaccine targets, when comparing the transcriptional repertoire expressed by RAS, GAP and WT liver-stages by suppression subtractive hybridisation (SSH). This approach differs fundamentally from recent studies, that also aimed at the identification of potential target antigens. For example another comparative transcriptional analysis identified differentially expressed transcripts in *P. yoelii* WT and RAS sporozoites as well as in early (24 h) and late (48 h) WT and RAS LS in comparison to mixed blood-stages (Williams and Azad 2010). This analysis, however, does not comprise potential multi-stage antigen candidates as transcripts that are expressed in pre-erythrocytic as well as in blood-stages are excluded with this method. In the here presented study we compared the transcript repertoire expressed in attenuated parasites to that expressed in WT parasites during early liver-stage development. We believe that in the protection-inducing attenuated parasites antigens may accumulate, due to developmental arrest, that are important for protection. The time point of 20 hours liver-stage development was chosen as the *uis3(-)* GAPs arrest at mid liver-stage development (24 hours) and therefore antigens expressed at this early time point must be sufficient to induce the GAP-mediated protective immunity. The SSH screening identified a set of specifically up-regulated transcripts in attenuated parasites (UAPs) in comparison to WT liver-stages. The reverse subtractions also revealed several transcripts that are down-regulated in attenuated parasites if compared to WT. Unfortunately we had to exclude the three UAPs 2, 3 and 6 after analysis of the down-regulated transcripts as they were detected in all subtracted populations tested. The down-regulated transcripts were not investigated in detail as they can be considered as not important for protective immunity induced by RAS or GAP, respectively. In the here performed SSH screening transcripts are enriched that are more abundant in one cDNA population if compared to another. Therefore down-regulation in attenuated parasites concurrently means that these transcripts are up-regulated in WT liver-stages. As WT LS *per se* do not confer sterile protection, this suggests that transcripts that are more abundant in WT in comparison to attenuated LS do not code for antigens involved in protective immune responses.

Although some of the identified UAPs are shared between RAS and GAP liver-stages there are also differences in the up-regulated transcript repertoire of the two attenuated parasite lines (tables 2 and 3; figure 12). RAS liver-stages expressed a more diverse up-regulated transcript repertoire whereas we identified less differentially expressed transcripts in GAP

liver-stages. This is conceivable if considering that irradiation of sporozoites results in multiple random point mutations, while GAPs are generated by specific gene depletion of a single liver-stage essential gene, in this study *uis3*. Therefore GAP liver-stages differ from WT only by one single gene, whereas RAS comprise a heterogenous parasite population with an undefined genetic background. This is why RAS liver-stages arrest at different time points and thereby different developmental stages resulting in the expression of a more heterogeneous set of transcripts. Whereas transcript expression by GAP is similar to this of WT liver-stages. The most striking difference between the up-regulated transcript repertoire of RAS and GAP liver-stages is the circumsporozoite protein (CSP). In RAS liver-stages CSP appeared as up-regulated transcript in comparison to WT liver-stages. In contrast there was no CSP transcript up-regulated in GAP liver-stages. This might serve as a proof-of-concept for the here performed screening. While CSP plays a dominant role as protective antigen in RAS-mediated immunity [reviewed in (Nardin and Nussenzweig 1993)], no CSP-specific immune responses were detected for the here used GAP vaccination model (Mueller et al. 2007). This demonstrates that the here performed screening indeed enriched transcripts that code for antigens involved in RAS and GAP mediated immunity, respectively.

UAPs - up-regulated in attenuated parasites

In total 21 UAPs were identified, of which some are specific for RAS or GAP, respectively, but interestingly also several UAPs are shared between both attenuated parasite lines. The most prominent transcript identified as up-regulated in RAS and GAP, UAP 1, coded for a putative C2 domain-containing protein (C2CP; plasmoDB annotation PB402109.00.0). Such C2 domains are found in several proteins and are characteristic for the ferlin protein family (see below). Beside one C2 domain the *P. berghei* C2CP had a predicted exonuclease domain and a predicted triple A domain (AT_nPases Asociated with diverse cellular Activities; AAA+ ATPase). Although these AAA+ ATPases are known to mediate diverse cellular processes, like proteolysis, membrane fusion, microtubule serving or biogenesis of endosomes. A common underlying mechanism of all described functions of AAA+ proteins is the energy-dependent unfolding of proteins (Lupas and Martin 2002). Such a AAA+ ATPase was recently described as energy source of the *P. falciparum* protein export machine PTEX transporting proteins beyond the PVM (de Koning-Ward et al. 2009).

Furthermore the small hypothetical proteins UAP 4 and UAP 7 are up-regulated in both attenuated parasite lines if compared to WT liver-stages. UAP 4 holds a predicted Krueppel-associated box (KRAB domain) and may therefore mediate transcriptional repression (see below). The hypothetical protein UAP 7 has a pexel export signal and a transmembrane (TM)

domain. This export signal was shown to be important for the transport of proteins through the parasitophorous vacuole membrane (PVM) (Marti et al. 2004). UAP 7 may therefore either be located within the PVM, because of its TM domain, or its final destination may be the cytoplasm of the host hepatocyte. There *Plasmodium* proteins can facilitate liver-stage development e.g. by adapting the host's gene expression like it is described for CSP (Singh A. P. et al. 2007).

Interestingly several predicted domains characteristic for eukaryotic transcription factors or domains involved in post-transcriptional regulation were identified for UAP 4, UAP 8, UAP 11, UAP 13, UAP 15 and UAP 16. In *Plasmodium* transcriptional regulation is only poorly understood. A genome-wide database search for transcription factors in *P. falciparum* revealed that most detected transcription factors were CCCH-type zinc finger proteins (Coulson et al. 2004). This type of zinc finger is described to bind to mRNA indicating rather post-transcriptional control in *Plasmodium* (Lai et al. 2000). The Krueppel-associated box (KRAB domain) as predicted for UAP 4 is present in the largest family of zinc finger transcription factors where the N-terminally located KRAB domain acts as a transcriptional repressor by binding to corepressor proteins whereas the zinc finger motif binds to DNA. By that these KRAB domain containing zinc finger repressor proteins function as transcriptional repressors [reviewed in (Urrutia 2003)]. Whether this type of transcriptional repression is also present in *Plasmodium* is not described so far. The translation elongation factor UAP 8 belongs to the EF-1 alpha (EF-Tu) type, which binds GTP and an aminoacyl-tRNA and delivers the latter to the A site of ribosomes. Another predicted domain potentially involved in transcriptional regulation is the forkhead-associated domain (FHA domain) of UAP 11. This FHA domain was initially/historically called like that because it have been found in a small subset of forkhead-type transcription factors (Hofmann and Bucher 1995). Meanwhile the FHA domain could be associated with proteins involved in numerous processes including intracellular signal transduction, transcription, protein transport, DNA repair and protein degradation by recognising phosphothreonine epitopes on proteins [reviewed in (Durocher and Jackson 2002)]. The function of FHA domains in *Plasmodium* is unknown. In at least two genome-wide database searches no forkhead transcription factors were described in *Plasmodium* (Templeton et al. 2004) (Coulson et al. 2004). A second predicted protein domain of UAP 11 is the RNA-recognition motifs (RRM). This domain typically binds to mRNA and is involved in post-transcriptional regulation. Recently, also protein-protein interactions were described for RRM domains [reviewed in (Clery et al. 2008)]. The WW domain of UAP 13 is described for the human phosphorylated CTD interacting factor 1

(PCIF1), which interacts with the phosphorylated C-terminal domain of the RNA polymerase II (Fan et al. 2003). Further characterisation of PCIF1 suggests a role in negative regulation of gene expression (Hirose et al. 2008). Furthermore UAP 15 is annotated as potential transcriptional repressor Not4hp and the TFSII_M domain of UAP 16 is characteristic for the transcription factor S-II. This transcription factor binds to RNA polymerase II and by that induces mRNA cleavage (Kettenberger et al. 2003). In total it is not as surprising that transcriptional regulation is extremely important during early liver-stage development. During the complex reorganisation of the extracellular sporozoite to the intracellular liver-stage and the fast growth of the parasite the regulation of gene expression have to built the basis for the morphological changes. How this critical developmental step is accomplished remains elusive and is under extensive investigations (Prudencio et al. 2006). However, recently, two protein families were described that may be involved in gene regulation in *Plasmodium*. The AP2 (Apetala2)-integrase DNA binding domains were discovered in different apicomplexan parasites and especially expression was shown in *Plasmodium* blood-stages (Balaji et al. 2005). Furthermore the sporozoite and liver-stages asparagine-rich protein SLARP/SAP1 was described as transcriptional regulator during liver-stage development (Silvie et al. 2008) (Aly et al. 2011). The large *P. falciparum* genome with more than 5000 genes (Gardner et al. 2002), that are differentially expressed during the various stages of the complex life cycle, is one of the impediments in malaria vaccine development and hinders the selection of highly immunogenic and potentially protective antigen candidates. Therefore the detailed understanding of gene regulation in *Plasmodium* may also help to identify potential antigen candidates and be important for the development of an effective malaria vaccine.

Predicted export signals like signal peptides or PEXEL motifs as well as transmembrane domains make some of the UAPs even more interesting with respect to their antigenic function. At first glance it seems to be important that potential antigens have to be exported or at least protrude into the host-cell cytoplasm in order to gain access to the host's immune system. Such intracellular antigens inside the host-cell are typically coupled to MHC class I molecules and transported to the host's cell surface. Recently, it was described that processing and presentation of sporozoite antigen is dependent on TAP-mediated transport of MHC class I epitopes to the endoplasmic reticulum (Cockburn et al. 2011). MHC class I presented antigens can then be recognised by CD8⁺ cytotoxic T-cells and target cells are subsequently killed. But there are also modes of action how intracellular antigens inside the parasite can get access to recognition by CD8⁺ T-cells. One way may be the cross-presentation of extracellular antigens released after apoptosis of host-cells by dendritic cells (DCs). Indeed cross-

presentation of sporozoite antigens by DCs to CD8⁺ T-cells was described in the skin-draining lymph nodes after bite immunisation (Chakravarty et al. 2007). While WT liver-stages prevent infected hepatocytes to undergo apoptosis (van de Sand et al. 2005) (Leiriao et al. 2005b) it is reported that apoptosis is increased in RAS infected hepatocytes (Leiriao et al. 2005a). Moreover it was demonstrated that GAP infected hepatocytes undergo apoptosis even more frequently than WT or RAS infected ones (van Dijk et al. 2005). Thereby the chance increases that antigens of attenuated parasites are indeed released into the extracellular matrix of the liver. Interestingly cross-presentation was also reported for intracellular antigens from live HIV-infected cells (Maranon et al. 2004). The active uptake of intracellular antigens from live cells by DCs is contact-dependent but the mechanism behind this transfer is unknown. Importantly this cross-presentation is more effective in activating CD8⁺ T-cells than antigen presentation by infected cells. Additionally a recent study indicated that antigen presentation of CSP to CD8⁺ T cells may not depend on the presence of the PEXEL signal, that is required for the export of *Plasmodium* proteins into the erythrocyte cytosol (Cockburn et al. 2011) (Marti et al. 2004). This suggests that parasite proteins do not necessarily have to hold export signals in order to reach the host-cell cytoplasm. In summary this shows that all identified parasite proteins may act as potential antigens independent of their localisation in the parasite or the host-cell or the existence of at first glance important domains or characteristics.

The ferlin protein family

Beside the potential antigenic function of the identified UAPs the *P. berghei* C2CP (UAP 1) also have awakened our interest with respect to its cellbiological function in the *Plasmodium* parasite. The function of C2 domains in general and C2 domain-containing proteins, like the identified UAP 1 or other Plasmodial ferlins, in particular are not described so far. In other organisms, however, C2 domains are attributed conserved functions in Ca²⁺-dependent membrane fusion events [reviewed in (Lek et al. 2012)]. As *Plasmodium* has a complex life cycle with different invasive and intracellular stages, where membrane fusion might play an important role, Plasmodial ferlins may take over several conceivable functions (see below). We therefore believe that Plasmodial ferlins may also be involved in vesicular trafficking and membrane fusion e.g. during host-cell invasion, establishment of the parasitophorous vacuole or parasite release from hepatocytes. The comprehensive understanding of the complex cellular processes that lead to successful parasite invasion and establishment of an infection are also important for the selection of new potential antigen targets and the development of an effective malaria vaccine.

Searching the PlasmoDB and GeneDB databases (www.plasmodb.org and www.genedb.org) for orthologues and paralogues in other apicomplexan parasites revealed an annotated putative *P. berghei* ferlin (PB000505.02.0), a *P. berghei* ferlin-like protein (PB101952.00.0) and a the *P. falciparum* orthologues PF14_0530 (FER) and MAL8P1.134 (FLP), two putative *P. yoelii* ferlins (PY05745 and PY04695) and annotated genes for a *Toxoplasma gondii* ferlin (TGVEG_073920) and a *Tg* FLP (TGVEG_093560) parologue. Although ferlins are ubiquitous proteins well characterised in *Caenorhabditis elegans* and humans, there is nothing known about their function in apicomplexan parasites. Recently, the *Pf* ferlin was evolutionary classified as ferlin-like gene with at least five C2 domains and a C2-FerI-C2 motif (Lek et al. 2010). The ferlin protein family is generally characterised by multiple tandem C2 domains and a C-terminal transmembrane domain (Bansal and Campbell 2004). Such tandem C2 domains are also present in other proteins and have been well characterised in synaptotagmin [reviewed in (Bai and Chapman 2004)]. The C2 domains of synaptotagmin bind Ca²⁺ and by that mediate protein-protein interactions between the SNAREs (soluble N-ethyl-maleimide-sensitive fusion protein (NSF) attachment protein receptor), synaptobrevin and syntaxin. This triggers the fast exocytotic membrane fusion and thereby the release of neurotransmitter at the synaptic cleft (Chapman 2002). The first described ferlin, the *C. elegans* FER-1, is required for Ca²⁺-mediated membrane fusion during spermatogenesis (Washington and Ward 2006). Mutations in *fer-1* thus led to a fertilisation defect, an effect that was eponymous for the ferlin protein family (Achanzar and Ward 1997). Furthermore the human dysferlin is important for Ca²⁺-dependent resealing of the sarcolemma in muscle fibres (Bansal and Campbell 2004). And additionally, the human otoferlin serves as a calcium sensor that regulates SNARE-mediated membrane fusion in cochlear hair cells (Johnson and Chapman 2010). Mutations in both human ferlins, dysferlin as well as otoferlin, are associated with inherited diseases like muscular dystrophy and deafness, respectively. All this suggests the common function of Ca²⁺-sensing and Ca²⁺-dependent membrane fusion for C2 domains in general and ferlin proteins in particular. The cellular function and subcellular localisation of ferlins and ferlin-like proteins in Apicomplexan parasites, however, is so far not defined and was focus of this work.

The *P. berghei* C2 domain-containing protein and related ferlin perform vital functions in blood-stages

Targeted gene disruption is a commonly used method to study potential protein functions in *Plasmodium*. The resulting phenotypes of knock-out parasites subsequently allow conclusions of the protein function. The fact that *Plasmodium* is haploid almost throughout its entire life

cycle facilitates this purpose and leads to distinct phenotypes in most cases. As targeted gene disruptions are typically performed in *Plasmodium* blood-stages the depletion of genes essential for blood-stage development lead to non-viable parasites. This was the case for the *P. berghei* *fer* and *c2cp*. We were not able to specifically deplete the one or the other gene in three independent transfection experiments and at the same time a control complementation constructs proved that the genomic locus is generally accessible and hence not resistant to gene-targeting. Therefore we conclude a vital function of *P. berghei* ferlin and C2 domain-containing protein during blood-stage development.

The expression profile of *Pb fer* and *c2cp* supports their essential role in blood-stages as transcripts of both genes were found in *P. berghei* blood-stage parasites. This probably also explains why no Plasmodial ferlin was detected in RAS liver-stages during a previous screen, where the transcriptional profile of RAS and WT sporozoites as well as liver-stages was compared to mixed blood-stages (Williams and Azad 2010). Proteins that are expressed during liver-stage as well as blood-stage development were not detect by this experimental set-up. Furthermore transcripts of *Pb c2cp* were found in early WT liver-stages (20 h). A respective band is only very slightly shown in figure 15. This suggests an extremely weak expression of *Pb c2cp* in early liver-stages. This is in agreement with the quantitative real-time PCR data (figure 13) where the *Pb c2cp* is also only expressed very weak in WT liver-stages after 20 hours development (100 copies in qRT-PCR). In contrast transcripts of *Pb fer* were detected in WT midgut sporozoites and late liver-stages (48 h). Whereas the expression was only very weak in early liver-stages (20 h) and no transcripts could be detected in salivary gland sporozoites. This indicated a *Pb fer* expression in intracellular stages (blood-stages, midgut sporozoites and liver-stages) rather than extracellular stages (salivary gland sporozoites). In order to prove this hypothesis other extracellular parasite stages like purified merozoites or ookinetes have to be tested. Typically intracellular *Plasmodium* blood and liver-stages build a surrounding parasitophorous vacuole (PV) immediately after invasion of the respective host-cell. This involves a rapid assembly of the PV membrane (PVM) around the intracellular parasite. Other described ferlins play important roles in different membrane fusion events. For example the above described human ferlins, dysferlin and otoferlin. Additionally the *C. elegans* FER-1, that mediates the fusion of specialized membranous organelles during spermatogenesis (Washington and Ward 2006) or the ferlin of the sea urchin, that regulates ATP release from vesicles after membrane wounding (Covian-Nares et al. 2010). Thus a potential role of the Plasmodial ferlins in establishment of the PVM is more than conceivable. This hypothesis is supported by described interaction partners of Plasmodial

ferlins. In a yeast two-hybrid (Y2H) screening the *P. berghei* C2CP was identified as an interaction partner of the N-terminal portion of UIS4, a small protein that protrude into the PV of intrahepatic liver-stages (Sabine Fraschka, unpublished) (Mueller et al. 2005b). We hypothesize that this interaction may serve as a trigger for e.g. membrane fusion of vesicles containing UIS4 with the PVM and furthermore across the PVM to other compartments of the infected cell e.g. the host's sorting compartment. Additionally a high-throughput yeast two-hybrid assay revealed the interaction of a putative *P. falciparum* ferlin-like protein (FLP, MAL8P1.134) with the parasitophorous vacuole resident protein exported protein 2 (EXP-2, PF14_0678) (LaCount et al. 2005). EXP-2 is associated with the PVM potentially via an N-terminal amphipathic helix and directed into the vacuolar space, the cellular function of the protein, however, are not described so far (Fischer et al. 1998). Recently, EXP-2 was also associated with the PTEX export machinery that exports parasite proteins into the cytosol of infected erythrocytes. In the PTEX protein complex EXP-2 is suggested to form the pore because of its strong membrane association (de Koning-Ward et al. 2009). This interaction further supports the hypothesis that Plasmodial ferlins may transport vesicles to and maybe beyond the PVM. Interestingly, these two interactions of *Pb* C2CP and *Pf* FLP with the two stage-specific PVM resident proteins UIS4 and EXP-2 suggest a role of ferlin proteins during liver-stage as well as blood-stage development in *Plasmodium*.

As a protein family of 18 SNAREs is described for *P. falciparum* (Ayong et al. 2007) it may also be reasonable that C2 domains of Plasmodial ferlins are involved in SNARE-mediated membrane fusion events. SNARE molecules typically mediate the fusion of synaptic vesicles with the pre-synaptic plasma membrane, resulting in the release of neurotransmitter. Thereby SNAREs are involved in all stages of the fusion process, from bringing the two opposing membranes into close proximity up to the expansion of the fusion pore (Risselada and Grubmuller 2012). Nevertheless it is debated whether SNAREs are indeed essential for membrane merger or whether they just establish membrane attachment by formation of a *trans*-SNARE complex between complementary SNAREs in the two membranes, while fusion itself is then executed by other proteins. Evidence therefore provide several studies on the fusion of yeast vacuoles (Wickner and Haas 2000). For example it was shown that protein phospholipase 1 and calmodulin are involved in the final bilayer mixing step of membrane fusion (Peters et al. 1999) (Peters and Mayer 1998). Thus, also ferlin proteins may contribute to the fusion process initiated by SNAREs in *Plasmodium*.

In summary the RT-PCR data support the results from the screening and the functional analysis. The low expression of *Pb c2cp* (UAP 1) in early WT LS is in good agreement with

the SSH screening. An up-regulation of *Pb c2cp* in attenuated parasites means low abundance in WT LS, because we always compared to WT as a reference and this was also shown by qRT-PCR. Additionally the expression of *Pb c2cp* and *Pb fer* in blood-stage parasites supports a functional role of these proteins during the erythrocytic phase. Finally both, the expression of *Pb C2CP* in attenuated liver-stages as shown by the SSH screening and the here demonstrated expression and essential role also in blood-stages, makes the *Pb C2CP* and interesting candidate for incorporation into a multi-stage malaria vaccine.

GAP immunisation establishes a memory T-cell response

Immunisation with genetically-attenuated parasites (GAP) leads to sterile protection in C57BL/6 mice. This protection can be achieved by injection of *uis3(-)* sporozoites according to a three dose immunisation protocol (figure 18). Two booster dose are required to establish full protection in this vaccination model as no immunodominant CD8⁺ T-cell epitope is available in C57BL/6 mice expressing the H-2^b MHC I haplotype. A similar observation has been described for experimental RAS immunisation in a transgenic mouse model that is tolerant to the immunodominant CSP (Kumar et al. 2006). Suggesting that other probably less immunodominant antigens, hitherto unidentified, can also induce protection and may also be involved in GAP-mediated immunity.

In this study we showed that GAP immunisation induces effector T-cells and establishes a memory T-cell response. FACS analysis revealed an enhanced CD8⁺CD44^{high}CD62L^{low} effector memory T-cell population in the liver after immunisation if compared to non-immunised controls (figure 19). The induction of effector cells and the development of memory-recall responses following a pathogen infection are hallmarks of adaptive immunity and the basis of vaccination. In order to study underlying mechanisms like the induced effector cytokines produced by this T-cell subset, however, T-cell numbers have to be enhanced *ex vivo* as low responses of a small number of specific effector T-cells can hardly be detected in whole organs e.g. in the liver. One approach in our lab is the generation of stage-specific ovalbumin (OVA)-expressing model parasites. The strong immunogenic and easy to track OVA is used in many models as both a general and strong T-cell activator [reviewed in (Plebanski et al. 2010)]. Though the here presented study aimed at another more specific approach. Antigen-specific T-cell clones are activated during immunisation and migrate to the liver, where they direct their cytotoxic activity against infected hepatocytes. These T-cell clones are difficult to track, as specific T-cell numbers are low compared to the number of liver infiltrating cells. Especially in the GAP vaccination model no presented antigen is described making it impossible to study specific T-cell responses. Therefore the aim of this

study was the identification and characterisation of new potential antigens involved in GAP-mediated immunity, essentially to specifically restimulate T-cells from immunised animals *in vitro*. The *P. berghei* C2 domain-containing protein (C2CP) was considered a promising candidate. This candidate antigen was identified by comparative analysis of early *Plasmodium* liver-stages as one of the most abundant transcript up-regulated in attenuated parasites (UAP 1). We believe that one characteristic of potential antigens involved in GAP-induced protection may be the high expression of the respective protein during early liver-stage development. Additionally we found several predicted C2CP-specific strong binding MHC class I epitopes, that are H-2^b-restricted and may therefore be presented in the here used C57BL/6 mouse background. Hence we investigated this antigen candidate with respect to its potential in elicit specific immune responses after GAP and RAS immunisation.

***Plasmodium berghei* C2CP-specific cells are recognised and killed in GAP and RAS immunised animals**

The *P. berghei* C2CP (UAP 1) contains the four predicted H-2^b-restricted CD8⁺ T-cell epitopes A9I, T9L, S8V and A8I. The MHC class I binding of the peptide T9L, that showed the highest binding affinity to H-2^b MHC molecules also by prediction, was further validated and *in vitro* binding affinity was determined by colleagues from Copenhagen with an adapted LOCI assay (luminescent oxygen channelling immunoassay) (Harndahl et al. 2009).

Naïve splenocytes were pulsed with a pool of either three (A9I, S8V and A8I) or all four peptides and injected into RAS and GAP immunised mice. After 18 hours we had a look if these cells became specifically lysed in spleens and livers. Although there was no specific lysis of *Pb* C2CP-specific cells shown in spleens of immunised animals, these cells were recognised and lysed in livers of immunised and WT infected C57BL/6 mice. When using the three *Pb* C2CP-derived peptides A9I, S8V and A8I this cytotoxic lysis increased significantly in the livers of RAS immunised mice when compared to naïve animals. In order to achieve a significant higher cytotoxic lysis after RAS and GAP immunisation, however, we had to add the fourth *Pb* C2CP-derived peptide T9L. Interestingly, activated cytotoxic CD8⁺ T-cells are primarily located in the liver after GAP or RAS immunisation. Indeed it has been demonstrated that CSP-specific effector CD8⁺ T-cells have to home to the liver in order to induce protective immunity in the RAS model while effector T-cells located in lymphoid organs were not sufficient for protection (Morrot et al. 2005). Cytotoxic CD8⁺ T-cells accomplish their anti-parasitic activity via recognition of MHC class I-presented epitopes by infected hepatocytes (White et al. 1996). By that infected hepatocytes get specifically lysed by so far not fully understood effector mechanisms. The injected peptide-pulsed splenocytes

probably became recognised and killed by similar effector mechanisms by the antigen specific cytotoxic T-lymphocytes that were activated during immunisation. The observation that *Pb* C2CP-specific cells were also lysed in WT infected animals is not really surprising as WT sporozoites also induce immune responses under natural malaria transmission. Repeated exposure to WT sporozoites leads to a degree of protection in endemic areas. This naturally acquired immunity protects against severe symptoms rather than infection (Artavanis-Tsakonas et al. 2003) and primarily depends on antibodies, but T-cells seem to be important to develop and maintain immunity (Langhorne et al. 2008). Immune responses induced by WT sporozoites, however, can even be protective if blood-stage infection is prohibited (Belnoue et al. 2004) and therefore may potentially be similar to the protective immune responses induced by GAP and RAS.

That activated effector T-cells indeed home to the liver where infection occurs and antigen is presented was further supported by a cytokine-based ELISpot analysis.

***P. berghei* C2CP-derived peptides are able to specifically restimulate T-cells from GAP and RAS immunised animals**

For a long time it is known that CD8⁺ T-cells perform an important role in protective immunity after immunisation with RAS (Schofield et al. 1987b) (Weiss et al. 1988). Later it was shown that transferred CD8⁺ T-cell clones against the immunodominant CD8⁺ T-cell epitope of CSP confer this protection and are capable of killing malaria liver stages (Rodrigues M. M. et al. 1991). For GAP-mediated immunity it could also be demonstrated that CD8⁺ T-cells are the key players in mediating protective immunity (Mueller et al. 2007). The role of IFN- γ as the effector cytokine in RAS mediated immunity was demonstrated in several studies (Ferreira et al. 1986) (Schofield et al. 1987b) (Tsuji et al. 1995). Recently, however, the contribution of IFN- γ in liver-stage immunology was questioned as protective immune responses induced by recombinant viral vaccines expressing CSP were independent of IFN- γ (Rodrigues E. G. et al. 2000) (Chakravarty et al. 2008). Though in GAP-mediated immunity IFN- γ plays an important role as protection was abrogated in IFN- γ (-/-) mice (Mueller et al. 2007).

In this study we therefore measured IFN- γ responses as a read-out for effector T-cell function after RAS and GAP immunisation in a cytokine-based ELISpot. Effector T-cells from immunised animals were specifically restimulated *in vitro* for 24 hours with *P. berghei* C2CP-derived peptides. In two independent experiments the *Pb* C2CP-derived peptides A9I, S8V and A8I were not able to restimulate T-cells in the spleen or the liver of immunised animals.

Though the predicted H-2^b-restricted CD8⁺ T-cell epitope T9L was highly immunogenic and hence potent to specifically enhance IFN- γ responses after restimulation *in vitro* in RAS and GAP immunised C57BL/6 mice in comparison to naïve controls. Ultimately, in very good agreement with the previous described cytotoxicity assay this suggests the peptide T9L derived from *Plasmodium* C2CP displays high immunogenicity in GAP-vaccinated animals. This is the very first immunogenic peptide specified in the herein described *P. berghei* GAP model and the first specific restimulation of T-cells in this vaccination model.

The basis of this study will now facilitate to examine underlying effector mechanisms of protective immune responses induced by GAP. Hence, an extensive FACS analysis could help to decipher antigen-specific T-cell populations and respective phenotypes involved in GAP-mediated immunity. For this T-cell numbers may probably be increased by prolonged antigen exposure e.g. by administration of additional booster dose or decrease of the periods between the single boosts. It then would be interesting to also study the contribution of CD4⁺ T-cells and innate immune responses in GAP mediated pre-erythrocytic immunity.

Immunisation study with *Pb* C2CP-derived peptides and recombinant overexpression of *P. berghei* C2CP - first results

Apparently the question emerges, if the *Pb*C2CP-derived peptide T9L is highly immunogenic, is it also protective? Indeed it could be shown, that mice immunised with the protective CD8⁺ T-cell epitope SYVPSAEQI of *P. yoelii* CSP alone, developed a strongly proliferating CD8⁺ T-cell response, indicating that the peptide itself is strongly immunogenic. This T-cell population, however, failed to acquire effector functions, when administrating the peptide in PBS (Overstreet et al. 2010). Hence we carried out a first immunisation trial using the peptide T9L delivered in specialised nanocarrier, called TargoSpheres, from the Rodos BioTarget GmbH (RBT; www.biotargeting.eu). These Targospheres directly target antigen-presenting cells (APCs) and release their content into the APCs. Thereby the peptide should gain access to the professional antigen-presentation pathway via MHC molecules. Of course we had to test both the administered dose and the administration route. The decision was made to inject two different dose into the skin of mice. The skin is also the entry port of Plasmodial antigens during natural transmission and distinct subsets of skin-resident migratory DCs have been characterised, Langerhans cells, dermal DCs and, recently, langerin⁺CD103⁺ dermal DCs (Eidsmo et al. 2009). As some sporozoites stay in the skin for more than one hour after an infectious bite (Yamauchi et al. 2007) skin-resident DCs may play an important role, as they may acquire sporozoite antigen directly in the skin before they migrate to the draining lymph-nodes to prime CD8⁺ T-cells (Chakravarty et al. 2007).

Firstly we examined the pre-patency of immunised animals. All immunised as well as control animals developed a blood-stage parasitemia after WT sporozoite challenge. Though a slight delay in pre-patency could be observed in the group of mice immunised with the higher peptide dose (5 µg). The delay of on average 1.3 days if compared to FITC:Dextran injected controls could be interesting with respect to disease outcome. Early studies showed that the *P. berghei* ANKA clone present mature liver schizonts as early as 43 hours after inoculation of infectious sporozoites, whereas the less virulent *P. berghei* NK65 clone showed first mature schizonts not before 51 hours after infection in the liver (Bafort et al. 1968). This extended liver phase might be coupled with a milder disease outcome as the latter does not cause cerebral symptoms. A vaccine that will prevent malaria symptoms and saves patients from death rather than inhibiting an infection completely would probably also be useful for endemic areas. Such a vaccine virtual mimics naturally acquired immunity that is dependent on repeated exposure and develops only slowly in the course of time. One high risk group, however, suffering from severe malaria and associated deaths are children under the age of five. A vaccine that would overcome the exposure-dependence of naturally acquired immunity and rapidly elicit protection against severe malaria would therefore especially help to reduce mortality in children.

Secondly, an immunological examination of the immunised animals was performed 8 days after sporozoite challenge. Lymphnode dissection was included in this analysis as we immunised subcutaneously into the skin of the animals. In by bite immunisations, where sporozoites passage the skin, the draining lymph nodes are ascribed an important role in CD8⁺ T-cell priming (Chakravarty et al. 2007). Not all sporozoites injected into the skin enter blood vessels to reach the liver, in fact some sporozoites are drained with the lymphatic system to regional lymph nodes (Amino et al. 2006). There sporozoites get internalised by resident dendritic cells and antigens are cross-presented to naïve CD8⁺ T-cells. T-cell priming in the lymph nodes is followed by dissemination of effector T-cells into different organs including spleen and liver (Chakravarty et al. 2007). In these organs specifically activated T-cells were analysed by IFN-γ ELISpot. High immune responses could be detected in the liver. We counted between 500 and 1000 IFN-γ producing T-cells per million liver lymphocytes in all immunised and control groups (see figure 24). An exception was the control group injected with 1 µg FITC:Dextran, that showed up to 3480 responding cells per one million liver lymphocytes. This result was not caused by a single outlier, but high IFN-γ responses were rather consistent throughout the whole group. Interestingly the high responses of the 1 µg FITC:Dextran group proceed also in the spleen. These responses might possibly have been

due to a contamination in the respective vial. The same FITC:Dextran and PBS solutions, however, from the same vials were used for injection of the group treated with 5 µg FITC:Dextran that did not show this high responses. In the spleen IFN- γ responses were lower than in the liver reaching from 200 to 300 responding cells per million splenocytes in the immunised groups. This is consistent with the previous ELISpot, where most of the IFN- γ producing effector T-cells were localised to the liver rather than the spleen (see figure 23) and published results, where effector T-cells had to localise to the liver in order to induce protection in RAS immunised animals (Morrot et al. 2005). The IFN- γ responses were the lowest in the draining lymph nodes, only 10 to 60 responding cells were measured per one million lymphocytes in all immunised groups. Interestingly, the not immunised challenged group showed more than 100 IFN- γ producing cells per million lymphocytes in the lymph nodes. This skin-draining lymph nodes are the priming site for IFN- γ producing effector CD8 $^{+}$ T-cell that subsequently migrate to the liver in order to kill infected hepatocytes (Chakravarty et al. 2007). Another explanation might be that sporozoites inoculated into the skin, in this experiment by bite of infected mosquitoes, are partly drained with the lymphatics to the proximal lymph nodes, where they can even start to differentiate into exo-erythrocytic stages (Amino et al. 2006). These parasite stages probably may also be attacked by IFN- γ producing effector T-cells, like it was shown for exo-erythrocytic forms in the liver (Schofield et al. 1987a). This may explain the presence of IFN- γ producing cells in the lymph node of naïve challenged mice. Maybe the lower IFN- γ responses in lymph nodes of immunised animals could be due to induced immune responses in the skin that potentially capture sporozoites already at the entry. In total, however, for all measured IFN- γ responses after immunisation with these nanocarrier we did not observe any specificity after restimulation with the peptide T9L. In future studies other adjuvant systems should be tested with the *Pb* C2CP-derived peptide T9L and also in combination with other antigens identified in the here presented screen. Maybe also coupling of the peptide to a highly immunogenic carrier should be tested like e.g. the tetanus toxoid, that was coupled to CSP-derived peptides, inducing high antibody titres and protection against malaria infection (Zavala et al. 1987) (Etlinger et al. 1988). A more promising approach, however, would probably be the delivery of the recombinant C2CP protein in its native form and formulated with the right adjuvant. That a strong and suitable adjuvant system is very important shows the development of the RTS,S vaccine. Only the formulation with the novel clinically approved AS adjuvant system lead to strong humoral and cell-mediated responses in rhesus monkeys and partial protection in human volunteers [reviewed in (Cohen et al. 2010)].

We also aimed at the recombinant expression of the *P. berghei* C2CP. Therefore we used the codon-optimised *E. coli* BL21-CodonPlus (DE3)-RIPL strain provided as transformation competent cells from Stratagene. Recombinant expression of *Pb* C2CP protein parts fused to a 6x-histidin-tag was performed according to standard *E. coli* expression protocols (see 3.2.6). The expressed fusion protein C2CPI-his was only partly expressed as soluble protein and solubility was not improved by different strategies like reduction of expression temperature or induction of protein expression with a low concentration of IPTG. Also the purification via column chromatography succeeded only partially and could not be improved by using different imidazol concentrations. The AT-rich *Plasmodium* genome may hamper the high-level expression in *E. coli*. Therefore the use of codon-optimised protein-constructs was described for other *Plasmodium* proteins e.g. the *Pf* falcipain-2 in order to achieve good expression results in *E. coli* (Salas Sarduy et al. 2012). The usage of codon-optimised synthetic genes specifically generated for the respective organism, that is used for recombinant expression, was also described for *Pf* CSP in *E. coli* and also in *Pichia pastoris* yeast cells (Plassmeyer et al. 2009). Probably the endogenous gene sequence we used for the generation of the expression-constructs was not suitable for high-level expression in *E. coli*. But also the use of different host organisms for recombinant expression of *Plasmodium* protein is demonstrated reaching from bacterial and viral cells to eukaryotic yeast cells, but also the use of more unusual hosts is described e.g. the slime mold *Dictyostelium discoideum* (van Bemmelen et al. 2000) (Birkholtz et al. 2008). Therefore the expression of the *Pb* C2CP could probably be optimised to a valuable amount when testing different other expression systems. Also new technologies including new promotor systems, like the Gateway System using the tightly manageable *araBAD* promoter, were successfully applied for high-throughput cloning and expression of functional proteins in *P. falciparum* (Aguiar et al. 2004). There is a multitude of distinct heterologous expression systems used for the recombinant expression of Plasmodial proteins, although the here used pET/BL21 combination seems to be the most popular one, the suitable system has to be found for each protein [reviewed in (Birkholtz et al. 2008)].

The recombinant *P. berghei* C2CP then enables e.g. the production of antibodies by immunisation of animals with the protein. On the one hand we could show the intracellular localisation of C2CP in fixed and immunofluorescently labelled preparations with specific antibodies. This would further uncover potential cellular functions of the protein. Secondly Western blot analysis of stage-specific parasite lysates would eventually demonstrate expression on protein level rather than transcripts. Finally recombinant *Pb* C2CP could be

formulated and tested as subunit vaccine candidate. The most advanced recombinant protein subunit vaccines is RTS,S based on the recombinant *P. falciparum* circumsporozoite protein (CSP). Only a long lasting journey, however, led to the today's vaccine currently tested in a clinical phase III trial (Leach et al. 2011) (Casares et al. 2010). The expression in *Saccharomyces cerevisiae* in combination with the hepatitis B virus surface antigen as a matrix carrier and the assembly of the fusion protein in virus-like particles was important for proper delivery of the CSP antigen (Cohen et al. 2010). Additionally the formulation with a strong and appropriate adjuvant system was necessary in order to reach sufficient immunogenicity of the antigen. This development of a safe, immunogenic and partly protective vaccine lasts already more than 25 years, but also started with the expression of a recombinant protein (Ballou 2009).

Concluding remarks

The here presented study describes the identification and characterisation of the first specific antigen *Pb* C2CP and its immunogenic CD8⁺ T-cell epitope T9L involved in GAP-mediated immunity. It shows the first antigen-specific immune response of C57BL/6 mice immunised with GAP. This now enables the investigation of GAP-induced effector mechanisms in more detail. Hence T-cells from GAP-immunised animals can be specifically restimulated and thereby T-cell numbers can be enhanced *in vitro*. This facilitates the analysis of the whole cascade of downstream effector mechanisms following immunisation. Therefore this work is of fundamental importance to understanding the mechanisms of pre-erythrocytic immunity to malaria. In the long run this work may further pave the way for the composition of an anti-infective multi-component subunit malarial vaccine in combination with antigens derived from the herein described differential profiling and known malarial pre-erythrocytic vaccine candidates such as CSP. This finally would emulate the attenuated parasite in a safe and effective malaria vaccine.

5. References

- Achanzar WE, Ward S. 1997.** A nematode gene required for sperm vesicle fusion. *J Cell Sci* 110 (Pt 9): 1073-1081.
- Agnandji ST, et al. 2011.** First results of phase 3 trial of RTS,S/AS01 malaria vaccine in African children. *N Engl J Med* 365: 1863-1875.
- Aguiar JC, et al. 2004.** High-throughput generation of *P. falciparum* functional molecules by recombinational cloning. *Genome Res* 14: 2076-2082.
- Alonso PL, et al. 2004.** Efficacy of the RTS,S/AS02A vaccine against *Plasmodium falciparum* infection and disease in young African children: randomised controlled trial. *Lancet* 364: 1411-1420.
- Aly AS, Lindner SE, MacKellar DC, Peng X, Kappe SH. 2011.** SAP1 is a critical post-transcriptional regulator of infectivity in malaria parasite sporozoite stages. *Mol Microbiol* 79: 929-939.
- Amino R, Thibierge S, Martin B, Celli S, Shorte S, Frischknecht F, Menard R. 2006.** Quantitative imaging of *Plasmodium* transmission from mosquito to mammal. *Nat Med* 12: 220-224.
- Ancsin JB, Kisilevsky R. 2004.** A binding site for highly sulfated heparan sulfate is identified in the N terminus of the circumsporozoite protein: significance for malarial sporozoite attachment to hepatocytes. *J Biol Chem* 279: 21824-21832.
- Anderson RJ, Hannan CM, Gilbert SC, Laidlaw SM, Sheu EG, Korten S, Sinden R, Butcher GA, Skinner MA, Hill AV. 2004.** Enhanced CD8+ T cell immune responses and protection elicited against *Plasmodium berghei* malaria by prime boost immunization regimens using a novel attenuated fowlpox virus. *J Immunol* 172: 3094-3100.
- Artavanis-Tsakonas K, Tongren JE, Riley EM. 2003.** The war between the malaria parasite and the immune system: immunity, immunoregulation and immunopathology. *Clin Exp Immunol* 133: 145-152.
- Avril M, et al. 2010.** Immunization with VAR2CSA-DBL5 recombinant protein elicits broadly cross-reactive antibodies to placental *Plasmodium falciparum*-infected erythrocytes. *Infect Immun* 78: 2248-2256.
- Ayong L, Pagnotti G, Tobon AB, Chakrabarti D. 2007.** Identification of *Plasmodium falciparum* family of SNAREs. *Mol Biochem Parasitol* 152: 113-122.
- Baer K, Klotz C, Kappe SH, Schnieder T, Frevert U. 2007.** Release of hepatic *Plasmodium yoelii* merozoites into the pulmonary microvasculature. *PLoS Pathog* 3: e171.
- Bafort J, Timperman G, Delbar T. 1968.** Observations on tissue schizogony and sporogony of rodent malaria. *Ann Soc Belges Med Trop Parasitol Mycol* 48: 535-540.
- Bai J, Chapman ER. 2004.** The C2 domains of synaptotagmin--partners in exocytosis. *Trends Biochem Sci* 29: 143-151.
- Balaji S, Babu MM, Iyer LM, Aravind L. 2005.** Discovery of the principal specific transcription factors of Apicomplexa and their implication for the evolution of the AP2-integrase DNA binding domains. *Nucleic Acids Res* 33: 3994-4006.
- Ballou WR. 2009.** The development of the RTS,S malaria vaccine candidate: challenges and lessons. *Parasite Immunol* 31: 492-500.
- Bansal D, Campbell KP. 2004.** Dysferlin and the plasma membrane repair in muscular dystrophy. *Trends Cell Biol* 14: 206-213.
- Barbosa A, et al. 2009.** Plasmodium falciparum-specific cellular immune responses after immunization with the RTS,S/AS02D candidate malaria vaccine in infants living in an area of high endemicity in Mozambique. *Infect Immun* 77: 4502-4509.

- Barnes KI, Watkins WM, White NJ. 2008.** Antimalarial dosing regimens and drug resistance. *Trends Parasitol* 24: 127-134.
- Beaudoin RL, Strome CP, Mitchell F, Tuberger TA. 1977.** Plasmodium berghei: immunization of mice against the ANKA strain using the unaltered sporozoite as an antigen. *Exp Parasitol* 42: 1-5.
- Beckers CJ, Dubremetz JF, Mercereau-Puijalon O, Joiner KA. 1994.** The *Toxoplasma gondii* rhoptry protein ROP 2 is inserted into the parasitophorous vacuole membrane, surrounding the intracellular parasite, and is exposed to the host cell cytoplasm. *J Cell Biol* 127: 947-961.
- Bejon P, et al. 2008.** Efficacy of RTS,S/AS01E vaccine against malaria in children 5 to 17 months of age. *N Engl J Med* 359: 2521-2532.
- Belnoue E, Costa FT, Frankenberg T, Vigario AM, Voza T, Leroy N, Rodrigues MM, Landau I, Snounou G, Renia L. 2004.** Protective T cell immunity against malaria liver stage after vaccination with live sporozoites under chloroquine treatment. *J Immunol* 172: 2487-2495.
- Bethke L, Thomas S, Walker K, Lakhia R, Rangarajan R, Wirth D. 2007.** The role of DNA mismatch repair in generating genetic diversity and drug resistance in malaria parasites. *Mol Biochem Parasitol* 155: 18-25.
- Birkholtz LM, et al. 2008.** Heterologous expression of plasmodial proteins for structural studies and functional annotation. *Malar J* 7: 197.
- Bojang KA, et al. 2001.** Efficacy of RTS,S/AS02 malaria vaccine against *Plasmodium falciparum* infection in semi-immune adult men in The Gambia: a randomised trial. *Lancet* 358: 1927-1934.
- Cardoso FC, Roddick JS, Groves P, Doolan DL. 2011.** Evaluation of approaches to identify the targets of cellular immunity on a proteome-wide scale. *PLoS One* 6: e27666.
- Carvalho LH, Sano G, Hafalla JC, Morrot A, Curotto de Lafaille MA, Zavala F. 2002.** IL-4-secreting CD4+ T cells are crucial to the development of CD8+ T-cell responses against malaria liver stages. *Nat Med* 8: 166-170.
- Casares S, Richie TL. 2009.** Immune evasion by malaria parasites: a challenge for vaccine development. *Curr Opin Immunol* 21: 321-330.
- Casares S, Brumeau TD, Richie TL. 2010.** The RTS,S malaria vaccine. *Vaccine* 28: 4880-4894.
- Castellini MA, Buguliskis JS, Casta LJ, Butz CE, Clark AB, Kunkel TA, Taraschi TF. 2011.** Malaria drug resistance is associated with defective DNA mismatch repair. *Mol Biochem Parasitol* 177: 143-147.
- Cerami C, Frevert U, Sinnis P, Takacs B, Clavijo P, Santos MJ, Nussenzweig V. 1992.** The basolateral domain of the hepatocyte plasma membrane bears receptors for the circumsporozoite protein of *Plasmodium falciparum* sporozoites. *Cell* 70: 1021-1033.
- Chakravarty S, Baldeviano GC, Overstreet MG, Zavala F. 2008.** Effector CD8+ T lymphocytes against liver stages of *Plasmodium yoelii* do not require gamma interferon for antiparasite activity. *Infect Immun* 76: 3628-3631.
- Chakravarty S, Cockburn IA, Kuk S, Overstreet MG, Sacci JB, Zavala F. 2007.** CD8+ T lymphocytes protective against malaria liver stages are primed in skin-draining lymph nodes. *Nat Med* 13: 1035-1041.
- Chapman ER. 2002.** Synaptotagmin: a Ca(2+) sensor that triggers exocytosis? *Nat Rev Mol Cell Biol* 3: 498-508.
- Chen DH, Tigelaar RE, Weinbaum FI. 1977.** Immunity to sporozoite-induced malaria infection in mice. I. The effect of immunization of T and B cell-deficient mice. *J Immunol* 118: 1322-1327.
- Clery A, Blatter M, Allain FH. 2008.** RNA recognition motifs: boring? Not quite. *Curr Opin Struct Biol* 18: 290-298.

- Cockburn IA, Chen YC, Overstreet MG, Lees JR, van Rooijen N, Farber DL, Zavala F. 2010.** Prolonged antigen presentation is required for optimal CD8+ T cell responses against malaria liver stage parasites. *PLoS Pathog* 6: e1000877.
- Cockburn IA, Tse SW, Radtke AJ, Srinivasan P, Chen YC, Sinnis P, Zavala F. 2011.** Dendritic cells and hepatocytes use distinct pathways to process protective antigen from plasmodium in vivo. *PLoS Pathog* 7: e1001318.
- Cohen J, Nussenzweig V, Nussenzweig R, Vekemans J, Leach A. 2010.** From the circumsporozoite protein to the RTS, S/AS candidate vaccine. *Hum Vaccin* 6: 90-96.
- Coppi A, Tewari R, Bishop JR, Bennett BL, Lawrence R, Esko JD, Billker O, Sinnis P. 2007.** Heparan sulfate proteoglycans provide a signal to Plasmodium sporozoites to stop migrating and productively invade host cells. *Cell Host Microbe* 2: 316-327.
- Coppi A, Natarajan R, Pradel G, Bennett BL, James ER, Roggero MA, Corradin G, Persson C, Tewari R, Sinnis P. 2011.** The malaria circumsporozoite protein has two functional domains, each with distinct roles as sporozoites journey from mosquito to mammalian host. *J Exp Med* 208: 341-356.
- Coulson RM, Hall N, Ouzounis CA. 2004.** Comparative genomics of transcriptional control in the human malaria parasite Plasmodium falciparum. *Genome Res* 14: 1548-1554.
- Covian-Nares JF, Koushik SV, Puhl HL, 3rd, Vogel SS. 2010.** Membrane wounding triggers ATP release and dysferlin-mediated intercellular calcium signaling. *J Cell Sci* 123: 1884-1893.
- Cummings JF, et al. 2010.** Recombinant Liver Stage Antigen-1 (LSA-1) formulated with AS01 or AS02 is safe, elicits high titer antibody and induces IFN-gamma/IL-2 CD4+ T cells but does not protect against experimental Plasmodium falciparum infection. *Vaccine* 28: 5135-5144.
- de Koning-Ward TF, et al. 2009.** A newly discovered protein export machine in malaria parasites. *Nature* 459: 945-949.
- Diatchenko L, et al. 1996.** Suppression subtractive hybridization: a method for generating differentially regulated or tissue-specific cDNA probes and libraries. *Proc Natl Acad Sci U S A* 93: 6025-6030.
- Doolan DL, Hoffman SL. 1999.** IL-12 and NK cells are required for antigen-specific adaptive immunity against malaria initiated by CD8+ T cells in the Plasmodium yoelii model. *J Immunol* 163: 884-892.
- Doolan DL, Hoffman SL. 2000.** The complexity of protective immunity against liver-stage malaria. *J Immunol* 165: 1453-1462.
- Doolan DL, Khamboonruang C, Beck HP, Houghten RA, Good MF. 1993.** Cytotoxic T lymphocyte (CTL) low-responsiveness to the Plasmodium falciparum circumsporozoite protein in naturally-exposed endemic populations: analysis of human CTL response to most known variants. *Int Immunol* 5: 37-46.
- Doolan DL, Hedstrom RC, Rogers WO, Charoenvit Y, Rogers M, de la Vega P, Hoffman SL. 1996.** Identification and characterization of the protective hepatocyte erythrocyte protein 17 kDa gene of Plasmodium yoelii, homolog of Plasmodium falciparum exported protein 1. *J Biol Chem* 271: 17861-17868.
- Draper SJ, Goodman AL, Biswas S, Forbes EK, Moore AC, Gilbert SC, Hill AV. 2009.** Recombinant viral vaccines expressing merozoite surface protein-1 induce antibody- and T cell-mediated multistage protection against malaria. *Cell Host Microbe* 5: 95-105.
- Draper SJ, Moore AC, Goodman AL, Long CA, Holder AA, Gilbert SC, Hill F, Hill AV. 2008.** Effective induction of high-titer antibodies by viral vector vaccines. *Nat Med* 14: 819-821.
- Dunachie SJ, et al. 2006.** A DNA prime-modified vaccinia virus ankara boost vaccine encoding thrombospondin-related adhesion protein but not circumsporozoite protein partially protects healthy malaria-naïve adults against Plasmodium falciparum sporozoite challenge. *Infect Immun* 74: 5933-5942.
- Durocher D, Jackson SP. 2002.** The FHA domain. *FEBS Lett* 513: 58-66.

- Eichinger DJ, Arnot DE, Tam JP, Nussenzweig V, Enea V. 1986.** Circumsporozoite protein of Plasmodium berghei: gene cloning and identification of the immunodominant epitopes. *Mol Cell Biol* 6: 3965-3972.
- Eidsmo L, Allan R, Caminschi I, van Rooijen N, Heath WR, Carbone FR. 2009.** Differential migration of epidermal and dermal dendritic cells during skin infection. *J Immunol* 182: 3165-3172.
- Enayati A, Hemingway J. 2010.** Malaria management: past, present, and future. *Annu Rev Entomol* 55: 569-591.
- Etlinger HM, et al. 1988.** Assessment in humans of a synthetic peptide-based vaccine against the sporozoite stage of the human malaria parasite, Plasmodium falciparum. *J Immunol* 140: 626-633.
- Fan H, Sakuraba K, Komuro A, Kato S, Harada F, Hirose Y. 2003.** PCIF1, a novel human WW domain-containing protein, interacts with the phosphorylated RNA polymerase II. *Biochem Biophys Res Commun* 301: 378-385.
- Ferreira A, Schofield L, Enea V, Schellekens H, van der Meide P, Collins WE, Nussenzweig RS, Nussenzweig V. 1986.** Inhibition of development of exoerythrocytic forms of malaria parasites by gamma-interferon. *Science* 232: 881-884.
- Fischer K, Marti T, Rick B, Johnson D, Benting J, Baumeister S, Helmbrecht C, Lanzer M, Lingelbach K. 1998.** Characterization and cloning of the gene encoding the vacuolar membrane protein EXP-2 from Plasmodium falciparum. *Mol Biochem Parasitol* 92: 47-57.
- Florens L, et al. 2002.** A proteomic view of the Plasmodium falciparum life cycle. *Nature* 419: 520-526.
- Franke-Fayard B, Trueman H, Ramesar J, Mendoza J, van der Keur M, van der Linden R, Sinden RE, Waters AP, Janse CJ. 2004.** A Plasmodium berghei reference line that constitutively expresses GFP at a high level throughout the complete life cycle. *Mol Biochem Parasitol* 137: 23-33.
- Frevert U. 2004.** Sneaking in through the back entrance: the biology of malaria liver stages. *Trends Parasitol* 20: 417-424.
- Friesen J, Silvie O, Putrianti ED, Hafalla JC, Matuschewski K, Borrman S. 2010.** Natural immunization against malaria: causal prophylaxis with antibiotics. *Sci Transl Med* 2: 40ra49.
- Gardner MJ, et al. 2002.** Genome sequence of the human malaria parasite Plasmodium falciparum. *Nature* 419: 498-511.
- Gonzalez-Aseguinolaza G, et al. 2000.** alpha-galactosylceramide-activated Valpha 14 natural killer T cells mediate protection against murine malaria. *Proc Natl Acad Sci U S A* 97: 8461-8466.
- Gruner AC, Snounou G, Brahimi K, Letourneur F, Renia L, Druilhe P. 2003.** Pre-erythrocytic antigens of Plasmodium falciparum: from rags to riches? *Trends Parasitol* 19: 74-78.
- Gruner AC, et al. 2007.** Sterile protection against malaria is independent of immune responses to the circumsporozoite protein. *PLoS One* 2: e1371.
- Guinovart C, et al. 2009.** Insights into long-lasting protection induced by RTS,S/AS02A malaria vaccine: further results from a phase IIb trial in Mozambican children. *PLoS One* 4: e5165.
- Hall N, et al. 2005.** A comprehensive survey of the Plasmodium life cycle by genomic, transcriptomic, and proteomic analyses. *Science* 307: 82-86.
- Haltiwanger BM, Matsumoto Y, Nicolas E, Dianov GL, Bohr VA, Taraschi TF. 2000.** DNA base excision repair in human malaria parasites is predominantly by a long-patch pathway. *Biochemistry* 39: 763-772.
- Harndahl M, Justesen S, Lamberth K, Roder G, Nielsen M, Buus S. 2009.** Peptide binding to HLA class I molecules: homogenous, high-throughput screening, and affinity assays. *J Biomol Screen* 14: 173-180.
- Heppner DG, Jr., et al. 2005.** Towards an RTS,S-based, multi-stage, multi-antigen vaccine against falciparum malaria: progress at the Walter Reed Army Institute of Research. *Vaccine* 23: 2243-2250.

- Hill AV, et al. 1992.** Molecular analysis of the association of HLA-B53 and resistance to severe malaria. *Nature* 360: 434-439.
- Hirose Y, Iwamoto Y, Sakuraba K, Yunokuchi I, Harada F, Ohkuma Y. 2008.** Human phosphorylated CTD-interacting protein, PCIF1, negatively modulates gene expression by RNA polymerase II. *Biochem Biophys Res Commun* 369: 449-455.
- Hodder AN, Crewther PE, Anders RF. 2001.** Specificity of the protective antibody response to apical membrane antigen 1. *Infect Immun* 69: 3286-3294.
- Hoffman SL, Franke ED. 1994.** Inducing protective immune responses against the sporozoite and liver stages of Plasmodium. *Immunol Lett* 41: 89-94.
- Hoffman SL, Oster CN, Plowe CV, Woollett GR, Beier JC, Chulay JD, Wirtz RA, Hollingdale MR, Mugambi M. 1987.** Naturally acquired antibodies to sporozoites do not prevent malaria: vaccine development implications. *Science* 237: 639-642.
- Hoffman SL, et al. 2002.** Protection of humans against malaria by immunization with radiation-attenuated Plasmodium falciparum sporozoites. *J Infect Dis* 185: 1155-1164.
- Hoffman SL, et al. 2010.** Development of a metabolically active, non-replicating sporozoite vaccine to prevent Plasmodium falciparum malaria. *Hum Vaccin* 6: 97-106.
- Hofmann K, Bucher P. 1995.** The FHA domain: a putative nuclear signalling domain found in protein kinases and transcription factors. *Trends Biochem Sci* 20: 347-349.
- Hollingdale MR, Zavala F, Nussenzweig RS, Nussenzweig V. 1982.** Antibodies to the protective antigen of Plasmodium berghei sporozoites prevent entry into cultured cells. *J Immunol* 128: 1929-1930.
- Hollingdale MR, Leland P, Leef JL, Schwartz AL. 1983.** Entry of Plasmodium berghei sporozoites into cultured cells, and their transformation into trophozoites. *Am J Trop Med Hyg* 32: 685-690.
- Hutchings CL, Birkett AJ, Moore AC, Hill AV. 2007.** Combination of protein and viral vaccines induces potent cellular and humoral immune responses and enhanced protection from murine malaria challenge. *Infect Immun* 75: 5819-5826.
- Ishino T, Chinzei Y, Yuda M. 2005.** A Plasmodium sporozoite protein with a membrane attack complex domain is required for breaching the liver sinusoidal cell layer prior to hepatocyte infection. *Cell Microbiol* 7: 199-208.
- Jin Y, Kebaier C, Vanderberg J. 2007.** Direct microscopic quantification of dynamics of Plasmodium berghei sporozoite transmission from mosquitoes to mice. *Infect Immun* 75: 5532-5539.
- Johnson CP, Chapman ER. 2010.** Otoferlin is a calcium sensor that directly regulates SNARE-mediated membrane fusion. *J Cell Biol* 191: 187-197.
- Jung S, et al. 2002.** In vivo depletion of CD11c+ dendritic cells abrogates priming of CD8+ T cells by exogenous cell-associated antigens. *Immunity* 17: 211-220.
- Kaba SA, Brando C, Guo Q, Mittelholzer C, Raman S, Tropel D, Aebi U, Burkhard P, Lanar DE. 2009.** A nonadjuvanted polypeptide nanoparticle vaccine confers long-lasting protection against rodent malaria. *J Immunol* 183: 7268-7277.
- Kariu T, Ishino T, Yano K, Chinzei Y, Yuda M. 2006.** CelTOS, a novel malarial protein that mediates transmission to mosquito and vertebrate hosts. *Mol Microbiol* 59: 1369-1379.
- Kester KE, et al. 2009.** Randomized, double-blind, phase 2a trial of falciparum malaria vaccines RTS,S/AS01B and RTS,S/AS02A in malaria-naive adults: safety, efficacy, and immunologic associates of protection. *J Infect Dis* 200: 337-346.
- Kettenberger H, Armache KJ, Cramer P. 2003.** Architecture of the RNA polymerase II-TFIIS complex and implications for mRNA cleavage. *Cell* 114: 347-357.

- Khusmith S, Sedegah M, Hoffman SL. 1994.** Complete protection against Plasmodium yoelii by adoptive transfer of a CD8+ cytotoxic T-cell clone recognizing sporozoite surface protein 2. *Infect Immun* 62: 2979-2983.
- Kumar KA, Sano G, Boscardin S, Nussenzweig RS, Nussenzweig MC, Zavala F, Nussenzweig V. 2006.** The circumsporozoite protein is an immunodominant protective antigen in irradiated sporozoites. *Nature* 444: 937-940.
- Kyes S, Horrocks P, Newbold C. 2001.** Antigenic variation at the infected red cell surface in malaria. *Annu Rev Microbiol* 55: 673-707.
- LaCount DJ, et al. 2005.** A protein interaction network of the malaria parasite Plasmodium falciparum. *Nature* 438: 103-107.
- Lai WS, Carballo E, Thorn JM, Kennington EA, Blackshear PJ. 2000.** Interactions of CCCH zinc finger proteins with mRNA. Binding of tristetraprolin-related zinc finger proteins to AU-rich elements and destabilization of mRNA. *J Biol Chem* 275: 17827-17837.
- Langhorne J, Ndungu FM, Sponaas AM, Marsh K. 2008.** Immunity to malaria: more questions than answers. *Nat Immunol* 9: 725-732.
- Leach A, et al. 2011.** Design of a phase III multicenter trial to evaluate the efficacy of the RTS,S/AS01 malaria vaccine in children across diverse transmission settings in Africa. *Malar J* 10: 224.
- Leiriao P, Mota MM, Rodriguez A. 2005a.** Apoptotic Plasmodium-infected hepatocytes provide antigens to liver dendritic cells. *J Infect Dis* 191: 1576-1581.
- Leiriao P, Albuquerque SS, Corso S, van Gemert GJ, Sauerwein RW, Rodriguez A, Giordano S, Mota MM. 2005b.** HGF/MET signalling protects Plasmodium-infected host cells from apoptosis. *Cell Microbiol* 7: 603-609.
- Lek A, Lek M, North KN, Cooper ST. 2010.** Phylogenetic analysis of ferlin genes reveals ancient eukaryotic origins. *BMC Evol Biol* 10: 231.
- Lek A, Evesson FJ, Sutton RB, North KN, Cooper ST. 2012.** Ferlins: regulators of vesicle fusion for auditory neurotransmission, receptor trafficking and membrane repair. *Traffic* 13: 185-194.
- Lupas AN, Martin J. 2002.** AAA proteins. *Curr Opin Struct Biol* 12: 746-753.
- Maranon C, Desoutter JF, Hoeffel G, Cohen W, Hanau D, Hosmalin A. 2004.** Dendritic cells cross-present HIV antigens from live as well as apoptotic infected CD4+ T lymphocytes. *Proc Natl Acad Sci U S A* 101: 6092-6097.
- Marti M, Good RT, Rug M, Knuepfer E, Cowman AF. 2004.** Targeting malaria virulence and remodeling proteins to the host erythrocyte. *Science* 306: 1930-1933.
- Mathias DK, et al. 2012.** Expression, immunogenicity, histopathology, and potency of a mosquito-based malaria transmission-blocking recombinant vaccine. *Infect Immun* 80: 1606-1614.
- Matuschewski K, Nunes AC, Nussenzweig V, Menard R. 2002.** Plasmodium sporozoite invasion into insect and mammalian cells is directed by the same dual binding system. *EMBO J* 21: 1597-1606.
- Mauduit M, Tewari R, Depinay N, Kayibanda M, Lallemand E, Chavatte JM, Snounou G, Renia L, Gruner AC. 2010.** Minimal role for the circumsporozoite protein in the induction of sterile immunity by vaccination with live rodent malaria sporozoites. *Infect Immun* 78: 2182-2188.
- McKenna KC, Tsuji M, Sarzotti M, Sacci JB, Jr., Witney AA, Azad AF. 2000.** gammadelta T cells are a component of early immunity against preerythrocytic malaria parasites. *Infect Immun* 68: 2224-2230.
- Menard R, Sultan AA, Cortes C, Altszuler R, van Dijk MR, Janse CJ, Waters AP, Nussenzweig RS, Nussenzweig V. 1997.** Circumsporozoite protein is required for development of malaria sporozoites in mosquitoes. *Nature* 385: 336-340.

- Mitchell GH, Thomas AW, Margos G, Dluzewski AR, Bannister LH. 2004.** Apical membrane antigen 1, a major malaria vaccine candidate, mediates the close attachment of invasive merozoites to host red blood cells. *Infect Immun* 72: 154-158.
- Molano A, Park SH, Chiu YH, Nosseir S, Bendelac A, Tsuji M. 2000.** Cutting edge: the IgG response to the circumsporozoite protein is MHC class II-dependent and CD1d-independent: exploring the role of GPIs in NK T cell activation and antimalarial responses. *J Immunol* 164: 5005-5009.
- Morrot A, Hafalla JC, Cockburn IA, Carvalho LH, Zavala F. 2005.** IL-4 receptor expression on CD8+ T cells is required for the development of protective memory responses against liver stages of malaria parasites. *J Exp Med* 202: 551-560.
- Mota MM, Rodriguez A. 2001.** Migration through host cells by apicomplexan parasites. *Microbes Infect* 3: 1123-1128.
- Mueller AK, Labaied M, Kappe SH, Matuschewski K. 2005a.** Genetically modified Plasmodium parasites as a protective experimental malaria vaccine. *Nature* 433: 164-167.
- Mueller AK, Kohlhepp F, Hammerschmidt C, Michel K. 2010.** Invasion of mosquito salivary glands by malaria parasites: prerequisites and defense strategies. *Int J Parasitol* 40: 1229-1235.
- Mueller AK, Deckert M, Heiss K, Goetz K, Matuschewski K, Schluter D. 2007.** Genetically attenuated Plasmodium berghei liver stages persist and elicit sterile protection primarily via CD8 T cells. *Am J Pathol* 171: 107-115.
- Mueller AK, Camargo N, Kaiser K, Andorfer C, Frevert U, Matuschewski K, Kappe SH. 2005b.** Plasmodium liver stage developmental arrest by depletion of a protein at the parasite-host interface. *Proc Natl Acad Sci U S A* 102: 3022-3027.
- Muhle RA, Adjalley S, Falkard B, Nkrumah LJ, Muhle ME, Fidock DA. 2009.** A var gene promoter implicated in severe malaria nucleates silencing and is regulated by 3' untranslated region and intronic cis-elements. *Int J Parasitol* 39: 1425-1439.
- Murray CJ, Rosenfeld LC, Lim SS, Andrews KG, Foreman KJ, Haring D, Fullman N, Naghavi M, Lozano R, Lopez AD. 2012.** Global malaria mortality between 1980 and 2010: a systematic analysis. *Lancet* 379: 413-431.
- Nardin EH, Nussenzweig RS. 1993.** T cell responses to pre-erythrocytic stages of malaria: role in protection and vaccine development against pre-erythrocytic stages. *Annu Rev Immunol* 11: 687-727.
- Natarajan R, Thathy V, Mota MM, Hafalla JC, Menard R, Vernick KD. 2001.** Fluorescent Plasmodium berghei sporozoites and pre-erythrocytic stages: a new tool to study mosquito and mammalian host interactions with malaria parasites. *Cell Microbiol* 3: 371-379.
- Nussenzweig RS, Vanderberg J, Most H, Orton C. 1967.** Protective immunity produced by the injection of x-irradiated sporozoites of plasmodium berghei. *Nature* 216: 160-162.
- Nussler AK, Renia L, Pasquetto V, Miltgen F, Matile H, Mazier D. 1993.** In vivo induction of the nitric oxide pathway in hepatocytes after injection with irradiated malaria sporozoites, malaria blood parasites or adjuvants. *Eur J Immunol* 23: 882-887.
- O'Donnell RA, de Koning-Ward TF, Burt RA, Bockarie M, Reeder JC, Cowman AF, Crabb BS. 2001.** Antibodies against merozoite surface protein (MSP)-1(19) are a major component of the invasion-inhibitory response in individuals immune to malaria. *J Exp Med* 193: 1403-1412.
- Offeddu V, Thathy V, Marsh K, Matuschewski K. 2012.** Naturally acquired immune responses against Plasmodium falciparum sporozoites and liver infection. *Int J Parasitol* 42: 535-548.
- Ogulari RM, Dunn JM, Golightly LM. 2006.** 3' gene regulatory elements required for expression of the Plasmodiumfalciparum developmental protein, Pfs25. *Mol Biochem Parasitol* 146: 163-172.

- Ogutu BR, et al. 2009.** Blood stage malaria vaccine eliciting high antigen-specific antibody concentrations confers no protection to young children in Western Kenya. PLoS One 4: e4708.
- Olotu A, et al. 2011.** Circumsporozoite-specific T cell responses in children vaccinated with RTS,S/AS01E and protection against *P falciparum* clinical malaria. PLoS One 6: e25786.
- Ouattara A, et al. 2010.** Lack of allele-specific efficacy of a bivalent AMA1 malaria vaccine. Malar J 9: 175.
- Overstreet MG, Freyberger H, Cockburn IA, Chen YC, Tse SW, Zavala F. 2010.** CpG-enhanced CD8+ T-cell responses to peptide immunization are severely inhibited by B cells. Eur J Immunol 40: 124-133.
- Peters C, Mayer A. 1998.** Ca²⁺/calmodulin signals the completion of docking and triggers a late step of vacuole fusion. Nature 396: 575-580.
- Peters C, Andrews PD, Stark MJ, Cesaro-Tadic S, Glatz A, Podtelejnikov A, Mann M, Mayer A. 1999.** Control of the terminal step of intracellular membrane fusion by protein phosphatase 1. Science 285: 1084-1087.
- Pied S, Roland J, Louise A, Voegtle D, Soulard V, Mazier D, Cazenave PA. 2000.** Liver CD4-CD8- NK1.1+ TCR alpha beta intermediate cells increase during experimental malaria infection and are able to exhibit inhibitory activity against the parasite liver stage in vitro. J Immunol 164: 1463-1469.
- Pinder M, et al. 2004.** Cellular immunity induced by the recombinant *Plasmodium falciparum* malaria vaccine, RTS,S/AS02, in semi-immune adults in The Gambia. Clin Exp Immunol 135: 286-293.
- Plassmeyer ML, et al. 2009.** Structure of the *Plasmodium falciparum* circumsporozoite protein, a leading malaria vaccine candidate. J Biol Chem 284: 26951-26963.
- Plebanski M, Hill AV. 2000.** The immunology of malaria infection. Curr Opin Immunol 12: 437-441.
- Plebanski M, Aidoo M, Whittle HC, Hill AV. 1997.** Precursor frequency analysis of cytotoxic T lymphocytes to pre-erythrocytic antigens of *Plasmodium falciparum* in West Africa. J Immunol 158: 2849-2855.
- Plebanski M, Katsara M, Sheng KC, Xiang SD, Apostolopoulos V. 2010.** Methods to measure T-cell responses. Expert Rev Vaccines 9: 595-600.
- Polley SD, et al. 2004.** Human antibodies to recombinant protein constructs of *Plasmodium falciparum* Apical Membrane Antigen 1 (AMA1) and their associations with protection from malaria. Vaccine 23: 718-728.
- Potocnjak P, Yoshida N, Nussenzweig RS, Nussenzweig V. 1980.** Monovalent fragments (Fab) of monoclonal antibodies to a sporozoite surface antigen (Pb44) protect mice against malarial infection. J Exp Med 151: 1504-1513.
- Prudencio M, Rodriguez A, Mota MM. 2006.** The silent path to thousands of merozoites: the *Plasmodium* liver stage. Nat Rev Microbiol 4: 849-856.
- Putrianti ED, Silvie O, Kordes M, Borrmann S, Matuschewski K. 2009.** Vaccine-like immunity against malaria by repeated causal-prophylactic treatment of liver-stage *Plasmodium* parasites. J Infect Dis 199: 899-903.
- Ramirez JL, Garver LS, Dimopoulos G. 2009.** Challenges and approaches for mosquito targeted malaria control. Curr Mol Med 9: 116-130.
- Renggli J, Hahne M, Matile H, Betschart B, Tschopp J, Corradin G. 1997.** Elimination of *P. berghei* liver stages is independent of Fas (CD95/Apo-I) or perforin-mediated cytotoxicity. Parasite Immunol 19: 145-148.
- Renia L, Rodrigues MM, Nussenzweig V. 1994.** Intrasplenic immunization with infected hepatocytes: a mouse model for studying protective immunity against malaria pre-erythrocytic stage. Immunology 82: 164-168.
- Riley EM, Allen SJ, Bennett S, Thomas PJ, O'Donnell A, Lindsay SW, Good MF, Greenwood BM. 1990.** Recognition of dominant T cell-stimulating epitopes from the circumsporozoite protein of *Plasmodium falciparum* and relationship to malaria morbidity in Gambian children. Trans R Soc Trop Med Hyg 84: 648-657.

- Riley EM, Allen SJ, Wheeler JG, Blackman MJ, Bennett S, Takacs B, Schonfeld HJ, Holder AA, Greenwood BM. 1992.** Naturally acquired cellular and humoral immune responses to the major merozoite surface antigen (PfMSP1) of Plasmodium falciparum are associated with reduced malaria morbidity. *Parasite Immunol* 14: 321-337.
- Risselada HJ, Grubmuller H. 2012.** How SNARE molecules mediate membrane fusion: recent insights from molecular simulations. *Curr Opin Struct Biol* 22: 187-196.
- Rodrigues EG, Claassen J, Lee S, Wilson JM, Nussenzweig RS, Tsuji M. 2000.** Interferon-gamma-independent CD8+ T cell-mediated protective anti-malaria immunity elicited by recombinant adenovirus. *Parasite Immunol* 22: 157-160.
- Rodrigues M, Nussenzweig RS, Zavala F. 1993.** The relative contribution of antibodies, CD4+ and CD8+ T cells to sporozoite-induced protection against malaria. *Immunology* 80: 1-5.
- Rodrigues MM, Cordey AS, Arreaza G, Corradin G, Romero P, Maryanski JL, Nussenzweig RS, Zavala F. 1991.** CD8+ cytolytic T cell clones derived against the Plasmodium yoelii circumsporozoite protein protect against malaria. *Int Immunol* 3: 579-585.
- Roestenberg M, et al. 2009.** Protection against a malaria challenge by sporozoite inoculation. *N Engl J Med* 361: 468-477.
- Romero P, Maryanski JL, Corradin G, Nussenzweig RS, Nussenzweig V, Zavala F. 1989.** Cloned cytotoxic T cells recognize an epitope in the circumsporozoite protein and protect against malaria. *Nature* 341: 323-326.
- Romero PJ, Tam JP, Schlesinger D, Clavijo P, Gibson H, Barr PJ, Nussenzweig RS, Nussenzweig V, Zavala F. 1988.** Multiple T helper cell epitopes of the circumsporozoite protein of Plasmodium berghei. *Eur J Immunol* 18: 1951-1957.
- Sagara I, et al. 2009.** A randomized controlled phase 2 trial of the blood stage AMA1-C1/Alhydrogel malaria vaccine in children in Mali. *Vaccine* 27: 3090-3098.
- Saiki RK, Scharf S, Faloona F, Mullis KB, Horn GT, Erlich HA, Arnheim N. 1985.** Enzymatic amplification of beta-globin genomic sequences and restriction site analysis for diagnosis of sickle cell anemia. *Science* 230: 1350-1354.
- Salas Sarduy E, Cabrera Munoz A, Trejo SA, Chavez Planes Mde L. 2012.** High-level expression of Falcipain-2 in Escherichia coli by codon optimization and auto-induction. *Protein Expr Purif* 83: 59-69.
- Scheller LF, Azad AF. 1995.** Maintenance of protective immunity against malaria by persistent hepatic parasites derived from irradiated sporozoites. *Proc Natl Acad Sci U S A* 92: 4066-4068.
- Scheller LF, Wirtz RA, Azad AF. 1994.** Susceptibility of different strains of mice to hepatic infection with Plasmodium berghei. *Infect Immun* 62: 4844-4847.
- Schofield L, Ferreira A, Altszuler R, Nussenzweig V, Nussenzweig RS. 1987a.** Interferon-gamma inhibits the intrahepatocytic development of malaria parasites in vitro. *J Immunol* 139: 2020-2025.
- Schofield L, Villaquiran J, Ferreira A, Schellekens H, Nussenzweig R, Nussenzweig V. 1987b.** Gamma interferon, CD8+ T cells and antibodies required for immunity to malaria sporozoites. *Nature* 330: 664-666.
- Schofield L, McConville MJ, Hansen D, Campbell AS, Fraser-Reid B, Grusby MJ, Tachado SD. 1999.** CD1d-restricted immunoglobulin G formation to GPI-anchored antigens mediated by NKT cells. *Science* 283: 225-229.
- Shimizu S, Osada Y, Kanazawa T, Tanaka Y, Arai M. 2010.** Suppressive effect of azithromycin on Plasmodium berghei mosquito stage development and apicoplast replication. *Malar J* 9: 73.
- Shortt HE, Garnham PC. 1948.** Pre-erythrocytic stage in mammalian malaria parasites. *Nature* 161: 126.

- Siddiqui WA, Tam LQ, Kramer KJ, Hui GS, Case SE, Yamaga KM, Chang SP, Chan EB, Kan SC. 1987.** Merozoite surface coat precursor protein completely protects Aotus monkeys against Plasmodium falciparum malaria. Proc Natl Acad Sci U S A 84: 3014-3018.
- Silvie O, Goetz K, Matuschewski K. 2008.** A sporozoite asparagine-rich protein controls initiation of Plasmodium liver stage development. PLoS Pathog 4: e1000086.
- Silvie O, Semblat JP, Franetich JF, Hannoun L, Eling W, Mazier D. 2002.** Effects of irradiation on Plasmodium falciparum sporozoite hepatic development: implications for the design of pre-erythrocytic malaria vaccines. Parasite Immunol 24: 221-223.
- Singh AP, Buscaglia CA, Wang Q, Levay A, Nussenzweig DR, Walker JR, Winzeler EA, Fujii H, Fontoura BM, Nussenzweig V. 2007.** Plasmodium circumsporozoite protein promotes the development of the liver stages of the parasite. Cell 131: 492-504.
- Singh B, Kim Sung L, Matusop A, Radhakrishnan A, Shamsul SS, Cox-Singh J, Thomas A, Conway DJ. 2004.** A large focus of naturally acquired Plasmodium knowlesi infections in human beings. Lancet 363: 1017-1024.
- Sirima SB, Cousens S, Druilhe P. 2011.** Protection against malaria by MSP3 candidate vaccine. N Engl J Med 365: 1062-1064.
- Slifka MK, Pagarigan RR, Whitton JL. 2000.** NK markers are expressed on a high percentage of virus-specific CD8+ and CD4+ T cells. J Immunol 164: 2009-2015.
- Smith JD, Chitnis CE, Craig AG, Roberts DJ, Hudson-Taylor DE, Peterson DS, Pinches R, Newbold CI, Miller LH. 1995.** Switches in expression of Plasmodium falciparum var genes correlate with changes in antigenic and cytoadherent phenotypes of infected erythrocytes. Cell 82: 101-110.
- Spring MD, et al. 2009.** Phase 1/2a study of the malaria vaccine candidate apical membrane antigen-1 (AMA-1) administered in adjuvant system AS01B or AS02A. PLoS One 4: e5254.
- Stewart VA, et al. 2007.** Priming with an adenovirus 35-circumsporozoite protein (CS) vaccine followed by RTS,S/AS01B boosting significantly improves immunogenicity to Plasmodium falciparum CS compared to that with either malaria vaccine alone. Infect Immun 75: 2283-2290.
- Sturm A, Amino R, van de Sand C, Regen T, Retzlaff S, Rennenberg A, Krueger A, Pollok JM, Menard R, Heussler VT. 2006.** Manipulation of host hepatocytes by the malaria parasite for delivery into liver sinusoids. Science 313: 1287-1290.
- Sultan AA, Thathy V, Frevert U, Robson KJ, Crisanti A, Nussenzweig V, Nussenzweig RS, Menard R. 1997.** TRAP is necessary for gliding motility and infectivity of plasmodium sporozoites. Cell 90: 511-522.
- Tarun AS, Dumpit RF, Camargo N, Labaied M, Liu P, Takagi A, Wang R, Kappe SH. 2007.** Protracted sterile protection with Plasmodium yoelii pre-erythrocytic genetically attenuated parasite malaria vaccines is independent of significant liver-stage persistence and is mediated by CD8+ T cells. J Infect Dis 196: 608-616.
- Tarun AS, Peng X, Dumpit RF, Ogata Y, Silva-Rivera H, Camargo N, Daly TM, Bergman LW, Kappe SH. 2008.** A combined transcriptome and proteome survey of malaria parasite liver stages. Proc Natl Acad Sci U S A 105: 305-310.
- Templeton TJ, Iyer LM, Anantharaman V, Enomoto S, Abrahante JE, Subramanian GM, Hoffman SL, Abrahamsen MS, Aravind L. 2004.** Comparative analysis of apicomplexa and genomic diversity in eukaryotes. Genome Res 14: 1686-1695.
- Tewari R, Spaccapelo R, Bistoni F, Holder AA, Crisanti A. 2002.** Function of region I and II adhesive motifs of Plasmodium falciparum circumsporozoite protein in sporozoite motility and infectivity. J Biol Chem 277: 47613-47618.
- Thera MA, et al. 2006.** Safety and allele-specific immunogenicity of a malaria vaccine in Malian adults: results of a phase I randomized trial. PLoS Clin Trials 1: e34.

- Thera MA, et al. 2010.** Safety and immunogenicity of an AMA1 malaria vaccine in Malian children: results of a phase 1 randomized controlled trial. PLoS One 5: e9041.
- Thera MA, et al. 2011.** A field trial to assess a blood-stage malaria vaccine. N Engl J Med 365: 1004-1013.
- Todryk SM, Bejon P, Mwangi T, Plebanski M, Urban B, Marsh K, Hill AV, Flanagan KL. 2008.** Correlation of memory T cell responses against TRAP with protection from clinical malaria, and CD4 CD25 high T cells with susceptibility in Kenyans. PLoS One 3: e2027.
- Tomas AM, et al. 2001.** P25 and P28 proteins of the malaria oocinete surface have multiple and partially redundant functions. EMBO J 20: 3975-3983.
- Topley E, Bruce-Chwatt LJ, Dorrell J. 1970.** Haematological study of a rodent malaria model. J Trop Med Hyg 73: 1-8.
- Trotta RF, Brown ML, Terrell JC, Geyer JA. 2004.** Defective DNA repair as a potential mechanism for the rapid development of drug resistance in Plasmodium falciparum. Biochemistry 43: 4885-4891.
- Tsuji M, Corradin G, Zavala F. 1992.** Monoclonal antibodies recognize a processing dependent epitope present in the mature CS protein of various plasmodial species. Parasite Immunol 14: 457-469.
- Tsuji M, Romero P, Nussenzweig RS, Zavala F. 1990.** CD4+ cytolytic T cell clone confers protection against murine malaria. J Exp Med 172: 1353-1357.
- Tsuji M, Mombaerts P, Lefrancois L, Nussenzweig RS, Zavala F, Tonegawa S. 1994.** Gamma delta T cells contribute to immunity against the liver stages of malaria in alpha beta T-cell-deficient mice. Proc Natl Acad Sci U S A 91: 345-349.
- Tsuji M, Miyahira Y, Nussenzweig RS, Aguet M, Reichel M, Zavala F. 1995.** Development of antimalaria immunity in mice lacking IFN-gamma receptor. J Immunol 154: 5338-5344.
- Urrutia R. 2003.** KRAB-containing zinc-finger repressor proteins. Genome Biol 4: 231.
- van Bemmelen MX, Beghdadi-Rais C, Desponds C, Vargas E, Herrera S, Reymond CD, Fasel N. 2000.** Expression and one-step purification of Plasmodium proteins in dictyostelium. Mol Biochem Parasitol 111: 377-390.
- van de Sand C, Horstmann S, Schmidt A, Sturm A, Bolte S, Krueger A, Lutgehetmann M, Pollok JM, Libert C, Heussler VT. 2005.** The liver stage of Plasmodium berghei inhibits host cell apoptosis. Mol Microbiol 58: 731-742.
- van den Berg H. 2009.** Global status of DDT and its alternatives for use in vector control to prevent disease. Environ Health Perspect 117: 1656-1663.
- van Dijk MR, et al. 2005.** Genetically attenuated, P36p-deficient malarial sporozoites induce protective immunity and apoptosis of infected liver cells. Proc Natl Acad Sci U S A 102: 12194-12199.
- van Schaijk BC, et al. 2008.** Gene disruption of Plasmodium falciparum p52 results in attenuation of malaria liver stage development in cultured primary human hepatocytes. PLoS One 3: e3549.
- VanBuskirk KM, et al. 2009.** Preerythrocytic, live-attenuated Plasmodium falciparum vaccine candidates by design. Proc Natl Acad Sci U S A 106: 13004-13009.
- Vanderberg JP. 1977.** Plasmodium berghei: quantitation of sporozoites injected by mosquitoes feeding on a rodent host. Exp Parasitol 42: 169-181.
- Vissing H, Meyer WK, Aagaard L, Tommerup N, Thiesen HJ. 1995.** Repression of transcriptional activity by heterologous KRAB domains present in zinc finger proteins. FEBS Lett 369: 153-157.
- Washington NL, Ward S. 2006.** FER-1 regulates Ca²⁺ -mediated membrane fusion during *C. elegans* spermatogenesis. J Cell Sci 119: 2552-2562.

- Weiss WR, Sedegah M, Beaudoin RL, Miller LH, Good MF. 1988.** CD8+ T cells (cytotoxic/suppressors) are required for protection in mice immunized with malaria sporozoites. *Proc Natl Acad Sci U S A* 85: 573-576.
- White KL, Snyder HL, Krzych U. 1996.** MHC class I-dependent presentation of exoerythrocytic antigens to CD8+ T lymphocytes is required for protective immunity against Plasmodium berghei. *J Immunol* 156: 3374-3381.
- Wickner W, Haas A. 2000.** Yeast homotypic vacuole fusion: a window on organelle trafficking mechanisms. *Annu Rev Biochem* 69: 247-275.
- Williams CT, Azad AF. 2010.** Transcriptional analysis of the pre-erythrocytic stages of the rodent malaria parasite, Plasmodium yoelii. *PLoS One* 5: e10267.
- Woehlbier U, Epp C, Hackett F, Blackman MJ, Bujard H. 2010.** Antibodies against multiple merozoite surface antigens of the human malaria parasite Plasmodium falciparum inhibit parasite maturation and red blood cell invasion. *Malar J* 9: 77.
- Wu Y, et al. 2008.** Phase 1 trial of malaria transmission blocking vaccine candidates Pfs25 and Pvs25 formulated with montanide ISA 51. *PLoS One* 3: e2636.
- Yamauchi LM, Coppi A, Snounou G, Sinnis P. 2007.** Plasmodium sporozoites trickle out of the injection site. *Cell Microbiol* 9: 1215-1222.
- Yoeli M, Most H. 1965.** Studies on sporozoite-induced infections of rodent malaria. I. The pre-erythrocytic tissue stage of Plasmodium berghei. *Am J Trop Med Hyg* 14: 700-714.
- Yoshida N, Potocnjak P, Nussenzweig V, Nussenzweig RS. 1981.** Biosynthesis of Pb44, the protective antigen of sporozoites of Plasmodium berghei. *J Exp Med* 154: 1225-1236.
- Zavala F, Tam JP, Barr PJ, Romero PJ, Ley V, Nussenzweig RS, Nussenzweig V. 1987.** Synthetic peptide vaccine confers protection against murine malaria. *J Exp Med* 166: 1591-1596.

6. Appendix

6.1 Oligonucleotide sequences

6.1.1 PyCSP complementation

<i>PyCSP_complI_EcoRI_for</i>	5'-CGGAATTCATGAAGAAGTGTACC-3'
<i>PyCSP_complII_XbaI_rev</i>	5'-GCTCTAGACTTTAACAAATTC-3'
<i>PyCSP_complIII_XbaI_for</i>	5'-GCTCTAGAATAAGTAGTCAACTC-3'
<i>PyCSP_complIII_NotI_rev</i>	5'-ATTTCGGCCGCTGGTTGCTTGTAC-3'
<i>PyCSP_int_test_for</i>	5'-CCCGCACGGACGAATCCAGATGG-3'
<i>PyCSP_int_test_rev</i>	5'-GTTTCGATATCGTCATAACAAG-3'
<i>PyCSP_int_epi_for</i>	5'-CCCGCACGGACGAATCCAGATGG-3'
<i>PyCSP_int_epi_rev</i>	5'-ATTTCGGCCGCTGGTTGCTTGTAC-3'

6.1.2 PyCSP epitope mutagenesis

<i>PyCSP_me01_for</i>	5'-GAAGATTCTTATGCCCAAGCGCGAACGAAACTAGAATTG-3'
<i>PyCSP_me01_rev</i>	5'-CAAATTCTAGTATTGCTTCCCGCTGGGCATAAGAACATCTTC-3'
<i>PyCSP_me02_for</i>	5'-GAAGATGCTTATGCCCAAGCCCGGCACAGCAACTAGAATTG-3'
<i>PyCSP_me02_rev</i>	5'-CAAATTCTAGTGCTTGCCCGGGCTGGGCATAAGCATCTTC-3'
<i>PyCSP_me03_for</i>	5'-GAAGATGCTTATGCCCAAGCCCGGGAACAGCAACTAGAATTG-3'
<i>PyCSP_me03_rev</i>	5'-CAAATTCTAGTGCTTCCCGGGCTGGGCATAAGCATCTTC-3'
<i>PyCSP_me04_for</i>	5'-GAAGATTCTGCTGCGAACAGCGGGAGCAAACTAGAATTG-3'
<i>PyCSP_me04_rev</i>	5'-CAAATTCTAGTATTGCTGCCCGCTGCGACAGCAGAACATCTTC-3'

6.1.3 PyCSprae knock-out

<i>PyCSprae_5'UTR_XbaI_for</i>	5'-GCTCTAGACCGTTGGTACAAATCTGCAAGCTTG-3'
<i>PyCSprae_5'UTR_BamHI_rev</i>	5'-CGGGATCCGCATATTGTTACGTAGGGAAATAC-3'
<i>PyCSprae_Nterm_HindIII_for</i>	5'-CCCAAGCTGGGGCTATTGTACATAAAAGTTGTTTC-3'
<i>PyCSprae_Nterm_KpnI_rev</i>	5'-GGGGTACCGCATAACACATTACCAACAAATTATGC-3'
<i>PyCSprae_5' test_for</i>	5'-CTCTCTCTTCTCGCTCTCTCTC-3'
<i>PyCSprae_test_rev</i>	5'-CCCGCACGGACGAATCCAGATGG-3'

6.1.4 PyCSP replacement

<i>PyCSP_ORF_XbaI_for</i>	5'-GCTCTAGAATGAAGAAGTGTACCATTTAG-3'
<i>PyCSP_ORF_BamHI_rev</i>	5'-CGGGATCCTTAATTAAAGAACATCAATAC-3'

<i>PyCSP_3'UTR_HindIII_for</i>	5'-CCCAAGCTTGTATGACGATATCGAAC-3'
<i>PyCSP_3'UTR_KpnI_rev</i>	5'-GGGGTACCGCTAGTTGGAATTATTTAC-3'
<i>PyCSP_repl_test_for</i>	5'-CGCATTATATGAGTTCATTTACACAATCC-3'
<i>PyCSP_repl_test_rev</i>	5'-CCTTCTTGTTGTATTAACCTG-3'
<i>PyCSP_repl_epi_for</i>	5'-CCCGCACGGACGAATCCAGATGG-3'
<i>PyCSP_repl_epi_rev</i>	5'-GCTCTAGAATGAAGAAGTGTACCATTAG-3'

6.1.5 *PbFER* knock-out and complementation

<i>PbFER_5'UTR_KpnI_for</i>	5'-GGGGTACCGCGTGTATGCTCCAATAAAATAC-3'
<i>PbFER_5'UTR_HindIII_rev</i>	5'-CCCAAGCTCCAAGATTGAGATCTGCCTCAATGTAAG-3'
<i>PbFER_3'UTR_BamHI_for</i>	5'-CGGGATCCGACGCTGGACTATGGGACCTATGG-3'
<i>PbFER_3'UTR_XbaI_rev</i>	5'-GCTCTAGAGCAGCTCGTCAACGAATTGTTACCC-3'
<i>PbFER_ORFI_for</i>	5'-TCCCCGCGGCCATCGAGTTCGGTCATGGAATATTGG-3'
<i>PbFER_ORFI_rev</i>	5'-GGACTAGTTATAGCAACATGGCGGGATAAATAAAGG-3'
<i>PbFER_testI_for</i>	5'-CCCGCACGGACGAATCCAGATGG-3'
<i>PbFER_testI_rev</i>	5'-CAATCCGATACTCACATATCTTCC-3'
<i>PbFER_epil_for</i>	5'-CCCGCACGGACGAATCCAGATGG-3'
<i>PbFER_epil_rev</i>	5'-GCTCTAGAGCAGCTCGTCAACGAATTGTTACCC-3'
<i>PbFER_complII_SacII_for</i>	5'-TCCCCGCGGCCATCGAGTTCGGTCATGGAATATTGG-3'
<i>PbFER_complII_XbaI_rev</i>	5'-GCTCTAGAGACCCACATTCAAGCAACCC-3'
<i>PbFER_complIII_XbaI_for</i>	5'-GCTCTAGAGAAATTATGGCTATGAAGAGGCAGC-3'
<i>PbFER_complIII_BamHI_rev</i>	5'-CGGGATCCTTATAGCAACATGGCGGGATAAATAAAGG-3'
<i>PbFER_ORFII_for</i>	5'-CCGCTCGAGATGGGTTCTATACTTGTAAATTAG-3'
<i>PbFER_ORFII_rev</i>	5'-CGGGATCCAATGGCACATCAAATCAAAATTTC-3'
<i>PbFER_testII_for</i>	5'-CCGCTCGAGATGGGTTCTATACTTGTAAATTAG-3'
<i>PbFER_testII_rev</i>	5'-CCTTGCTCATTACCTGCTAATACGATTGC-3'
<i>PbFER_epilII_for</i>	5'-TCCCCGCGGCCATCGAGTTCGGTCATGGAATATTGG-3'
<i>PbFER_epilII_rev</i>	5'-CCTTGCTCATTACCTGCTAATACGATTGC-3'

6.1.6 *PbC2CP* knock-out and complementation

<i>PbC2CP_5'UTR_KpnI_for</i>	5'-GGGGTACCGCAGTAAGGGAGAAAGGTC-3'
<i>PbC2CP_5'UTR_HindIII_rev</i>	5'-CCCAAGCTCCTTGATGAGTATGAAGTG-3'
<i>PbC2CP_3'UTR_BamHI_for</i>	5'-CGGGATCCGAAAACACATGAAACTCAAG-3'
<i>PbC2CP_3'UTR_XbaI_rev</i>	5'-GCTCTAGAGCTCATTACATTCCAATGC-3'
<i>PbC2CP_ORFI_for</i>	5'-GGAATTCCATATGCAGACCTCAAAGAAGATC-3'

<i>PbC2CP_ORFI_rev</i>	5'-CCGCTCGAGGCCAATCCATGAGCATGGGAG-3'
<i>PbC2CP_testI_for</i>	5'-CCCGCACGGACGAATCCAGATGG-3'
<i>PbC2CP_testI_rev</i>	5'-GTGAACAGCTACACTTCAGCCTCCCTATC-3'
<i>PbC2CP_epI_for</i>	5'-CCCGCACGGACGAATCCAGATGG-3'
<i>PbC2CP_epI_rev</i>	5'-GCTCTAGAGCTCATTACATTCCAATGC-3'
<i>PbC2CP_complII_SacII_for</i>	5'-TCCCCGCGGGATCCATTCTATCTCCTTGAC-3'
<i>PbC2CP_complII_XbaI_rev</i>	5'-GCTCTAGAGTGAGGTGGAATCTCAGGGTTG-3'
<i>PbC2CP_complIII_XbaI_for</i>	5'-GCTCTAGAACCAAGTCAGAATGGCTAAGATC-3'
<i>PbC2CP_complIII_SpeI_rev</i>	5'-GGACTAGTCTAATATCCACTTATCAGTGAGTAC-3'
<i>PbC2CP_ORFII_for</i>	5'-GGAATTCCATATGCAGACCTCAAAGAACATC-3'
<i>PbC2CP_ORFII_rev</i>	5'-CCGCTCGAGGCCAATCCATGAGCATGGGAG-3'
<i>PbC2CP_testII_for</i>	5'-GGAATTCCATATGCAGACCTCAAAGAACATC-3'
<i>PbC2CP_testII_rev</i>	5'-CCTTGCTCATTACCTGCTAATACGATTGC-3'
<i>PbC2CP_epII_for</i>	5'-TCCCCGCGGGATCCATTCTATCTCCTTGAC-3'
<i>PbC2CP_epII_rev</i>	5'-CCTTGCTCATTACCTGCTAATACGATTGC-3'

6.1.7 Reverse transcriptase PCR

Cloning oligonucleotides for the *pferCONT* and *pc2cpCONT* constructs were also used for reverse transcriptase PCR (RT PCR).

<i>PbFER_complIII_XbaI_for</i>	5'-GCTCTAGAGAAATTATGGGCTATGAAGAGGCAGC-3'
<i>PbFER_complII_BamHI_rev</i>	5'-CGGGATCCTTATAGCAACATGGCGGGATAAATAAAGG-3'
<i>PbC2CP_complII_XbaI_for</i>	5'-GCTCTAGAACCAAGTCAGAATGGCTAAGATC-3'
<i>PbC2CP_complIII_SpeI_rev</i>	5'-GGACTAGTCTAATATCCACTTATCAGTGAGTAC-3'

6.1.8 Quantitative RT PCR

<i>UIS4_sense</i>	5'- CAGAGCCAAACCAAGCGATCATA-3'
<i>UIS4_antisense</i>	5'- CCATGTTATAAACGTTATTTC-3'
<i>LSA1_sense</i>	5'- CTCTGATCCAGGGACGCCATAAGGGAG-3'
<i>LSA1_antisense</i>	5'- GTCCCCGTTTCTACTGAT-3'
<i>UAP1_sense</i>	5'- AGGATAGCAAAAATCTTCTAAAGG-3'
<i>UAP1_antisense</i>	5'- GCTCCCTGTCAAAG-3'
<i>UAP4_sense</i>	5'- GGTTTCTCTGTGTAGCCCTGG-3'
<i>UAP4_antisense</i>	5'- CATATTCAACAACCCTG-3'
<i>UAP7_sense</i>	5'- GCAGGTCTCTGTGTCCATACC-3'
<i>UAP7_antisense</i>	5'- GGACAGCCAGGGCTAC-3'

6.1.9 Sequencing

T7	5'-TAATACGACTCACTATAAGGG-3'
SP6	5'-ATTTAGGTGACACTATAGAA-3'

6.1.10 *PbC2CP* overexpression

<i>PbC2CPI_NdeI_for</i>	5'-GGAATTCCATATGGGGAGCAACAATTACTTTTC-3'
<i>PbC2CPI_XhoI_rev</i>	5'-CCGCTCGAGTCTTAGAAATGCTTCATTG-3'
<i>PbC2CPII_NdeI_for</i>	5'-GGAATTCCATATGCAGACCTCAAAGAAGATC-3'
<i>PbC2CPII_XhoI_rev</i>	5'-CCGCTCGAGGCCAATCCATGAGCATGGAG-3'
<i>PbC2CPIII_NdeI_for</i>	5'-GGAATTCCATATGCCATGCTCATGGATTGGC-3'
<i>PbC2CPIII_XhoI_rev</i>	5'-CCGCTCGAGTGATTGGTTACCTCACTCAGGATG-3'

6.2 Vector maps

All vector maps were generated using the XPlasMap 0.96 software. Shown are all unique restriction endonuclease recognition sites and recognition sites used for cloning.

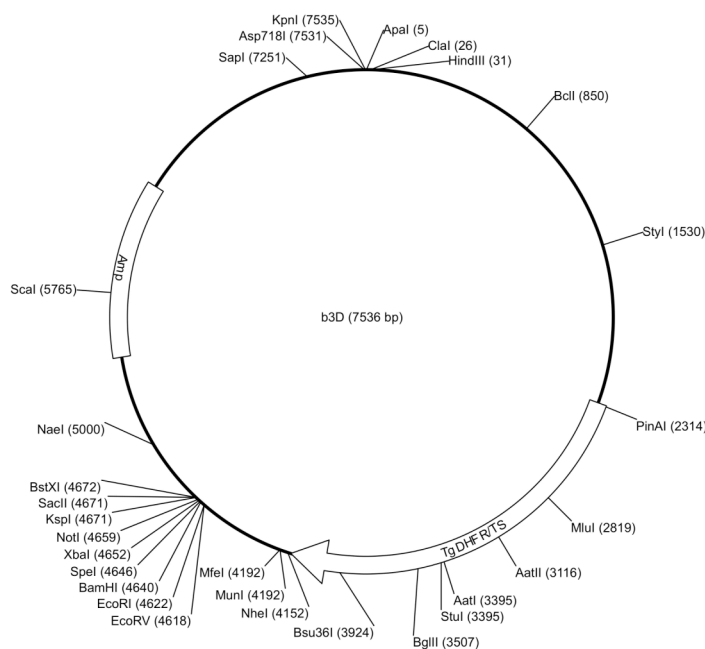


Figure 28. Vector map of the cloning vector b3D. The b3D vector contains the gene coding for the *Toxoplasma gondii* dihydrofolate reductase-thymidylate synthase (DHFR/TS) conferring to pyrimethamine resistance serving as selectable marker of transfected parasites. This marker is flanked by two multiple cloning sites. An additional gene conferring to ampicillin resistance (Amp) enables selection for resistant bacteria during cloning.

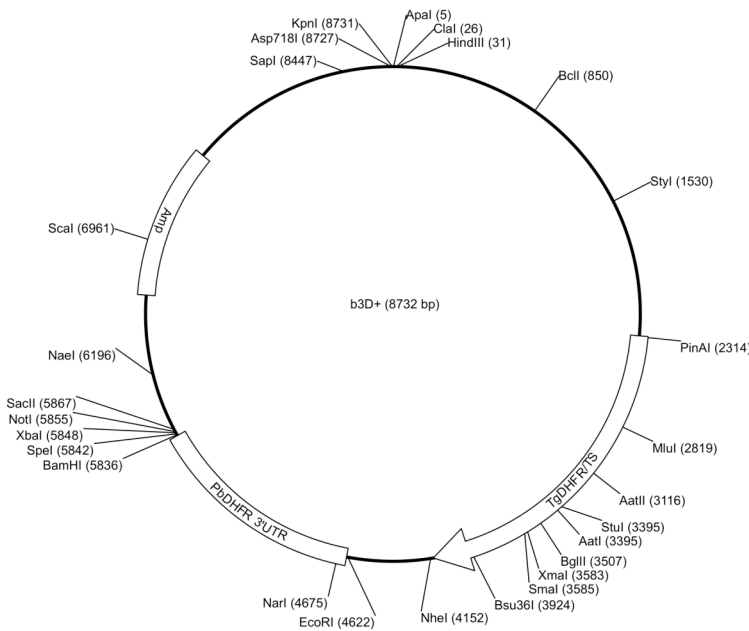


Figure 29. Vector map of the cloning vector b3D+. The cloning vector b3D+ contains in comparison to the vector b3D an additional *P. berghei* DHFR/TS 3' UTR. The respective fragment with a size of 1.2 kb was cloned using the restriction sites *BamHI* (forward) and *EcoRI* (reverse) into the b3D vector backbone.

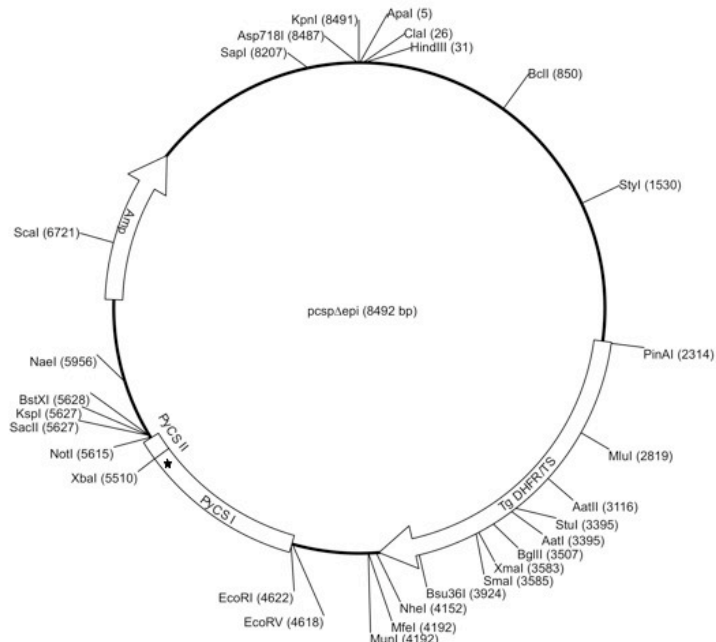


Figure 30. Vector map of the targeting construct pcspΔepi. The truncated *P. yoelii* csp ORF was cloned into the vector b3D in two parts in order to insert an unique *XbaI* restriction site for linearisation prior to parasite transfection. The *EcoRI* (forward) and *NotI* (reverse) restriction sites were used for cloning of the truncated ORF. The black star shows the position of the CD8⁺ T-cell epitope that was mutated by site-directed mutagenesis.

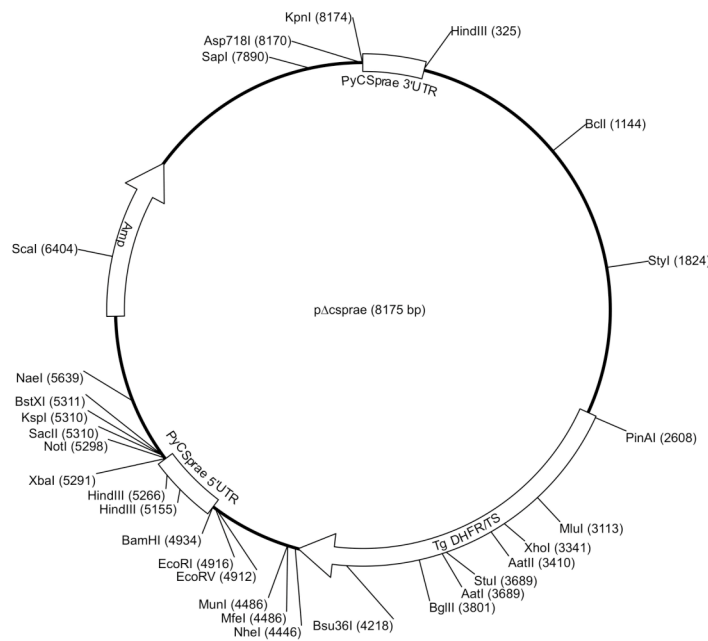


Figure 31. Vector map of the targeting construct *pΔcsprae*. Two fragments of the *P. yoelii* *csprae* gene (PY07369) were cloned into the vector b3D flanking the selectable marker using the restriction sites *Xba*I (forward) and *Bam*HI (reverse) or *Hind*III (forward) and *Kpn*I (reverse), respectively. Prior to transfection the construct was digested with *Xba*I and *Kpn*I.

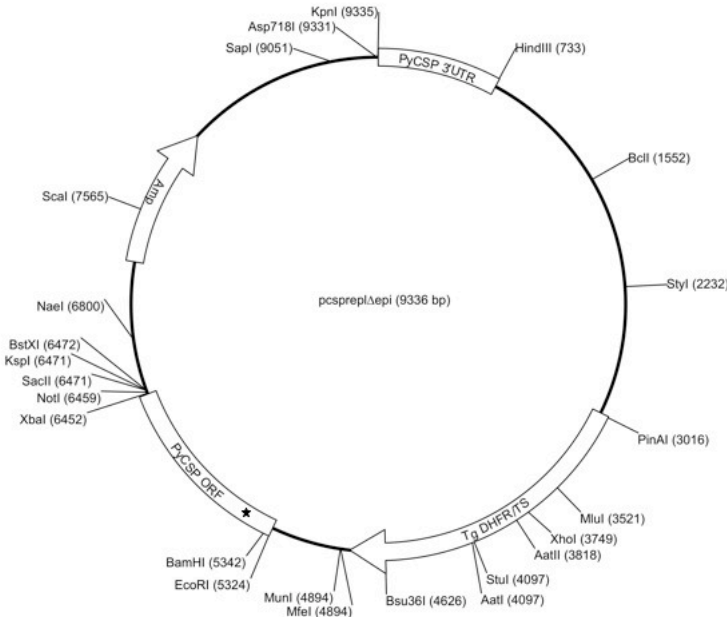


Figure 32. Vector map of the targeting construct *pcspreplΔepi*. The complete *P. yoelii* *csp* ORF and a fragment from the *Py csp* 3'UTR were cloned into the vector b3D using the restriction sites *Xba*I (forward) and *Eco*RI (reverse) or *Hind*III (forward) and *Kpn*I (reverse), respectively. The black star shows the position of the CD8+ T-cell epitope that was mutated by site-directed mutagenesis. Prior to transfection the construct was digested with *Xba*I and *Kpn*I.

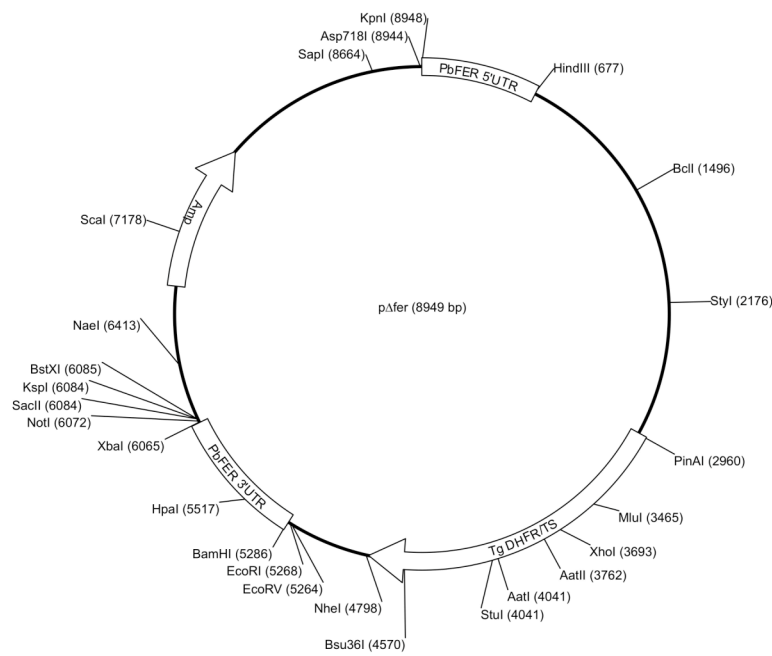


Figure 33. Vector map of the targeting construct $p\Delta fer$. Fragments of the *P. berghei* ferlin 5'UTR and 3'UTR were cloned into the cloning vector b3D flanking the selectable marker. The restriction enzymes *KpnI* (forward) and *HindIII* (reverse) and *BamHI* (forward) and *XbaI* (reverse) were used for construction, respectively. Prior to transfection the construct was digested with *KpnI* and *XbaI*.

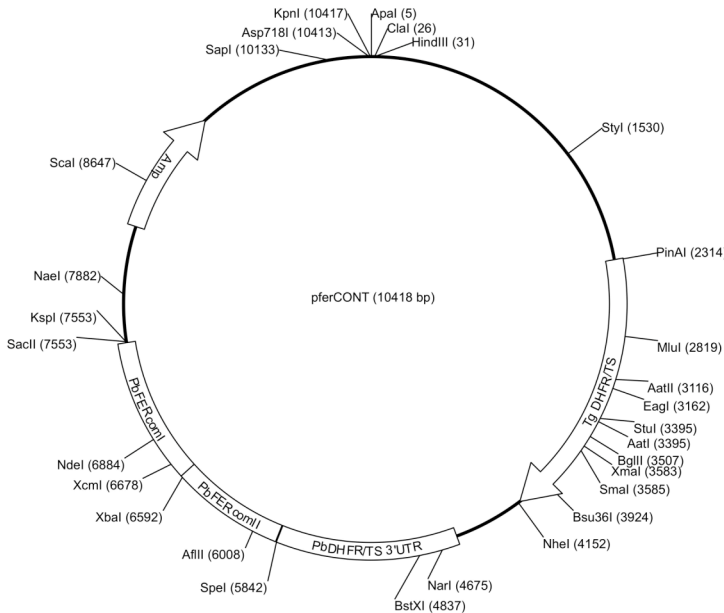


Figure 34. Vector map of the targeting construct $pferCONT$. Two fragments coding for the C-terminal part of the *P. berghei* ferlin were cloned into the vector b3D+ upstream of the *Pb DHFR/TS 3'UTR*. The restriction sites for *SacII* (forward) and *XbaI* (reverse) and *XbaI* (forward) and *SpeI* (reverse) were used for cloning. The construct was linearised with *XbaI* prior to transfection.



Figure 35. Vector map of the targeting construct $p\Delta c2cp$. Fragments of the $P. berghei$ $c2cp$ 5'UTR and 3'UTR were cloned into the cloning vector $b3D$ flanking the selectable marker. The restriction enzymes *KpnI* (forward) and *HindIII* (reverse) and *BamHI* (forward) and *XbaI* (reverse) were used for construction, respectively. Prior to transfection the construct was digested with *KpnI* and *XbaI*.

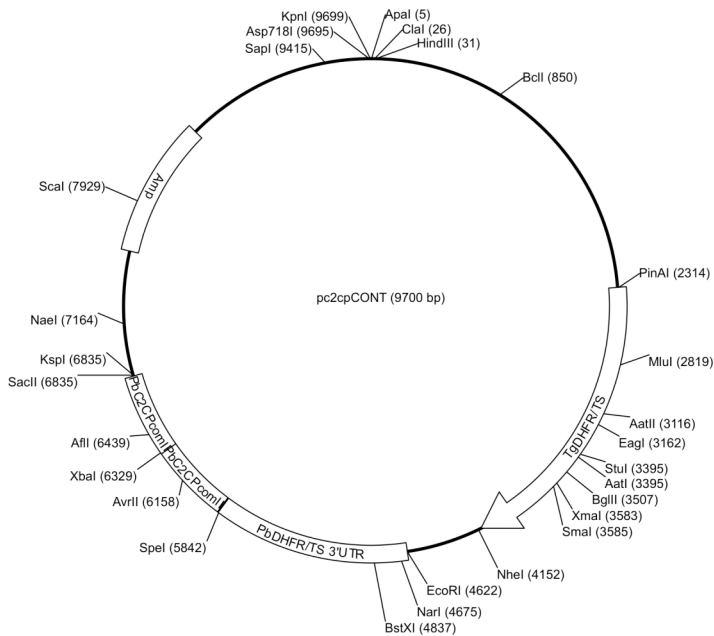


Figure 36. Vector map of the targeting construct $pc2cpCONT$. Two fragments coding for the C-terminal part of the $P. berghei$ C2CP were cloned into the vector $b3D+$ upstream of the Pb DHFR/TS 3'UTR. The restriction sites for *SacII* (forward) and *XbaI* (reverse) and *XbaI* (forward) and *SpeI* (reverse) were used for cloning. The construct was linearised with *XbaI* prior to transfection.

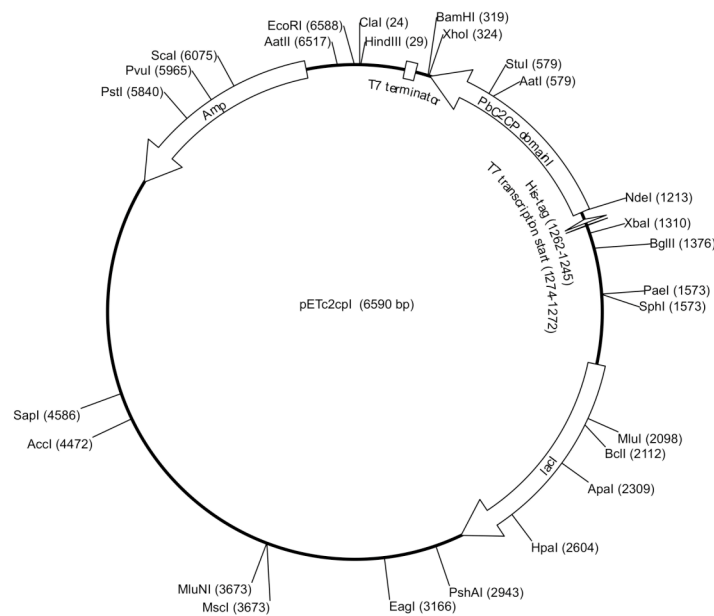


Figure 37. Vector map of the expression vector pETc2cpI. A fragment coding for the N-terminal part of the *P. berghei* C2CP (C2CPI) was cloned into the expression vector pET-15b (Novagen) using the restriction sites *NdeI* (forward) and *XhoI* (reverse). By that C2CPI is expressed as fusion protein with a N-terminal His-tag under control of the T7 promotor. The *lacI* coding sequence and the *bla* gene (Amp) serve as selection marker.

6.3 Sequence analysis of the *Py* CSP mutant clone I-2

T7 →

```

GGACGAATCCAGATGGAGATGGCTGTAGCGGAAATAAGAAGTAGCTTGATCCGGTTTTCTTAATTATATTATAACCAATTGA
TTGATTTATAACTGAAAAATGTATGTTGTCATATTTTTTGTCATGCACATGCATGTAAGCTAAATTATGAACATT
TTATTTTTGTCAGAAAAAAAAACTTACACACATAAAATGGCTAGTATGAATAGCCATATTATAAAATTAAATGCTATGAATT
TATGACGATATTAAAAATTAGATATTATGAAACATAATATGTTGAAACAATAAGACAAAATTATTATTATTATTATTATTATTAA
GTTATAATTATGTTGTCATGATTCAATAAATAGTTGACTTGATTTTAAATGTTATAATATGATTAGCATAGTTAAATAAA
AAAAAGTTGAAAAATTAAAAACATATAAACACAAATGATGTTTTCATTCATTCATTCATTCATTCATTCATTCATTCATTCATTC
TTTAACTGTTAGCGTCACTTTATTAGTTGATTCTACTTC.....
```

.....GAGCACCCACAGGGTOCAGGAGCACCA

```

CAAGGACCAAGGAGGACCACACAGGGCGAGGAGCACCACAGGACCAAGGACCAAGGAGGAGGACACAGGACCAAGGGCGAGGAGCAG
CACAAGGGCGAGGAGCACCACAAAGAACCCACCCACAAACCCACCCACAAACCCACACAGGCCACAAACAGGCCACCAACAGCCA
CCACAAACAGGCCACCAACAAACCCACGCCACAGCCAGATGGTAATAACAACAATAATAATGTAATAATAATGAAGATTCTT
ATGTCCTAACGGCGGAAACAATACTAGAATTGTTAACAGTCTAGAATAAGTAGTCACAGAGGAATGGTCATGTAAGTG
TAACCTGTTCTGGTGTAAAGAGTTAGAAAACGAAAAAATGTAACAAAGCAAGGAAAGAAAATTGACCTAGAGGATATTGATACTGA
PyCSP_complII_NotI_rev
AATTGTAATAACATTACACATTATAAAATTTATATATAAAATTTATACATATAATGTTGTTAGACTTTATTTATGTTGTTAGTATTCTTA
ATTGTGAACCTTCCTCATTTATTACGATTATTTATATACATATTTAATATGTAACAAATTAAAGAAAAAGAAATAATAGAAATC
TTATTATTTATGATATAAAATTAAAAAATAAATATACATTACAAATTACTTTTTAGTTATTCTCGTGTATTATT
ATATGTAATTAACTTGTATGAC ← SP6
```

Figure 38. Sequence of the CD8⁺ T-cell epitope mutant *Py* CSP me01 clone I-2. Shown is the combined sequence of the amplified integration-specific DNA fragment of the *Py* CSP me01 clone I-2 (see also figure 5; test fragment). Sequencing was performed using the oligonucleotides T7, SP6 and *PyCSP_complII_NotI_rev*. The respective oligonucleotide binding sites are indicated with an arrow. The *EcoRI* and *XbaI* restriction recognition sites are highlighted bold. The red nucleotides indicate the wild-type (non-mutated) sequence coding for the CD8⁺ T-cell epitope in a complete *csp* ORF (including start and stop codon). Light grey nucleotides derive from the b3D cloning vector.

Danksagung

Am Ende dieser Arbeit möchte ich mich bei den Menschen bedanken, die dazu beigetragen haben, dass diese Arbeit entstehen konnte. Freunde, Kollegen und meine Familie haben mich in verschiedenster Weise unterstützt. Danke!

Allen voran möchte ich mich bei dir bedanken, Ann-Kristin. Danke, dass du mir ganz zu Beginn deiner eigenen Arbeitsgruppe die Chance gegeben hast, mit dir zu arbeiten. Diese Zeit werde ich nie vergessen. Ich habe nicht nur fachlich und methodisch, sondern auch persönlich, unglaublich viel gelernt. Danke für deinen Optimismus, deine freundlichen und freundschaftlichen Worte, wenn diese angebracht waren, aber auch deine Anleitung und Unterstützung im Labor.

Bei Prof. Michael Lanzer möchte ich mich ganz herzlich bedanken, dass er dazu bereit war das Erstgutachten dieser Arbeit zu übernehmen. Außerdem danke ich Alexander Dalpke dafür, dass er als Prüfer an meiner Disputation teilnimmt. Ihnen beiden möchte ich ganz herzlich für die konstruktiven Treffen im Rahmen der "TAC meetings" danken und, dass Sie beide es zu guter Letzt unterstützt haben, dass diese Arbeit nach langer Unterbrechung abgeschlossen wurde.

Ein herzliches Danke gilt dir, liebe Kirsten. Du hast mich vor allem mit den immunologischen Experimenten enorm unterstützt. Ach was sag ich, ohne dich wären die harvests einfach nicht möglich gewesen. Danke für deine Hilfe, deine Geduld und die Ruhe, die du immer ausstrahlst.

Liebe Beatrix, ich möchte auch dir für die unglaublich große Unterstützung danken. Danke, dass du mir vor allem in der Immunologie mit deiner Erfahrung zur Seite standest. Du hast uns nicht nur mit Protokollen und Materialien versorgt, sondern warst auch immer zur Stelle, wenn ich dich gebraucht habe. Danke für deine Hilfe.

I want to thank Eleanor Riley and her group for the fantastic time at the London School of Hygiene and Tropical Medicine. My particular thanks goes to Julius, your supervision in the lab was special and it was a great experience to work with you. You introduced me to a new labculture. I think, I learned for life.

This visit at the LSHTM would not have been possible without financial support. I want to thank EMBO for funding me with a Short-Term Fellowship and the Disease Models and Mechanisms Journal (DMM) for awarding me the travel grant.

Ein ganz besonderer Dank gilt dir, liebe Chrissi. Die Zugfahrten mit dir waren immer schön und vor allem trotz der Regelmäßigkeit nie langweilig. Danke, außerdem für die Unterstützung im Labor und die gemeinsamen Wege zum Tierstall. Ich konnte mich immer auf dich verlassen, bleib so gewissenhaft. Ich danke dir auch im Speziellen ganz herzlich für jede Arbeit, vor allem für das Dissecten, die du für mich übernommen hast, als ich nicht mehr durfte. Ich bin froh, dass wir Freundinnen geworden sind und hoffentlich auch bleiben.

Auch der restlichen Mädelstruppe, liebe Britta, Sabrina und Sabine, möchte ich ganz herzlich danken. Auch wenn uns unterwegs einige verlassen mussten, hab ich die Kaffeepausen und die Cocktail-, Koch- und Backabende mit euch allen genossen. Vielen Dank für die schöne Zeit in Heidelberg!

Die Jungs, Matt, Roland und Flo, haben die tolle Arbeitsgruppe in der ich arbeiten durfte abgerundet. Danke euch dreien, dass ihr vor allem an den Wochenenden so oft ohne zu zögern Arbeiten übernommen habt und ich auch zum Ende der Arbeit, während der Schwangerschaft, auf eure Unterstützung zählen konnte. Lieber Roland, dir möchte ich speziell für die Unterstützung in den letzten Wochen im Labor danken und dafür, dass du mich in den letzten Monaten mit updates versorgt hast. Ich wünsch dir viel Erfolg für deine Arbeit.

Ein großer Dank geht an die technische Assistenz. Nadine, dir möchte ich für die unvergessliche Anfangszeit in Würzburg danken. Mit deinem Fachwissen und deiner enormen Motivation alles so schnell und perfekt wie möglich erledigen zu wollen, hast du mir den Einstieg in unsere kleine Gruppe und in ein neues Labor wirklich einfach gemacht. Du bist das größte Organisationstalent, dass ich bisher im Labor angetroffen habe.

Auch du, Jenny, hast mich wirklich immer unterstützt. Vor allem zum Ende der Arbeit im Labor und mit fortschreitender Schwangerschaft hätte ich ohne dich nicht arbeiten können. Ganz herzlichen Dank!

Ich möchte mich außerdem bei allen Kollegen und Freunden aus den Arbeitsgruppen Lanz und Frischknecht für die Hilfsbereitschaft in allen Fragen und Anliegen bedanken.

Zu guter Letzt danke ich meiner Familie. Liebe Mama, lieber Papa, danke, dass ihr mir mein Studium ermöglicht habt und meine Entscheidungen so bedingungslos akzeptiert habt. Ich konnte meinen Weg nur so weit gehen, weil ihr mich immer unterstützt habt. Danke, dass ihr so hinter mir steht.

Mein allergrößter Dank geht an meine eigene kleine Familie, Johannes und Helena. Ihr seid die wichtigsten Menschen in meinem Leben. Danke, Johannes, dass du mich in den letzten Monaten und Jahren ertragen und meine Arbeit immer unterstützt hast. Meine kleine Helena, du bist das Beste, was mir je passiert ist. Danke, dass du mir immer wieder zeigst, was wirklich wichtig ist im Leben. Ich liebe euch!